Gizem Ceren TÜRKMEN

SEISMIC BEHAVIOR OF AN ORDINARY RC STRUCTURE EXPOSED TO CORROSION

Gizem Ceren TÜRKMEN

IŞIK UNIVERSITY
2019

Gizem Ceren TÜRKMEN M.S. Thesis 2019

SEISMIC BEHAVIOR OF AN ORDINARY RC STRUCTURE EXPOSED TO CORROSION

Gizem Ceren TÜRKMEN
B.S., Civil Engineering, IŞIK UNIVERSITY, 2016
M.S., Civil Engineering, IŞIK UNIVERSITY, 2019

Submitted to the Graduate School of Science and Engineering
in partial fulfillment of the requirements for the degree of
Master of Science
in
Civil Engineering

IŞIK UNIVERSITY
2019

IŞIK UNIVERSITY
GRADUATE SCHOOL OF SCIENCE AND ENGINEERING

SEISMIC BEHAVIOR OF AN ORDINARY RC STRUCTURE EXPOSED TO CORROSION

Gizem Ceren TÜRKMEN

APPROVED BY:

Prof. Dr. Faruk KARADOĞAN Işık University
(Thesis Supervisor)

Prof. Dr. Esin INAN Işık University

Prof. Dr. Oğuz Cem ÇELİK Istanbul Tech. University

APPROVAL DATE: 18/01/2019

SEISMIC BEHAVIOR OF AN ORDINARY RC STRUCTURE EXPOSED TO CORROSION

Abstract

Within the scope of this thesis, seismic behavior of a 15 years old, approximately $\frac{1}{2}$scale, one storey, one bay frame which has concrete made of sea sand, mild reinforcing steel, and which was exposed to outdoor conditions for 15 years that resulted in a certain amount of corrosion of reinforcement, subjected to constant axial load and displacement reversals was examined analytically and experimentally. This frame represents the building stock with insufficient seismic details in Turkey which is built without conforming the existing design codes. Analytical part of the study consists of two approaches; distributed plasticity approach and concentrated plasticity approach. Parameters such as unit deformation and strength of materials were obtained by the axial tension and compression tests for the steel and concrete, respectively.

A reference frame having same dimensions and characteristics with the corroded frame except for compressive strength of concrete, was tested 9 years ago with the same experimental procedure also takes a part of this study for comparisons. Experimental results of corroded frame were compared with analytical results which are obtained by nonlinear static time history analysis and pushover analysis. Besides, a retrofitting technique that is RC jacketing is assumed to be applied on the columns of the frame and influence of this technique on the seismic behavior of the frame was examined for several assumptions with static pushover analysis and the obtaining the capacity curves for each assumption, comparisons were done. Moreover, a parametric study which involves the increase in the amount of corrosion of the specimen tested, was performed to have the insight about the effect of diameter loss of reinforcement due to corrosion on the lateral load carrying capacity and deformation capacity of the structure.

The experiment was ended at %3 drift ratio and bending and shear cracks were observed at the ends of columns. Structure elements underwent excessive loading which is beyond their load carrying capacity and had plastic deformation at the column ends which refers to strong beam weak column analogy. Furthermore, implementation of RC jacketing as a retrofitting technique analytically, led the

plastic deformation to occur at the beam ends instead of column top end which complies with the proposal of TEC known as strong column-weak beam situation.

According to the experimental and analytical studies, seismic behavior of the frame which is presented by capacity curve is modeled better with concentrated plasticity approach. Secondly, load carrying capacity, energy dissipation, cumulative energy dissipation of recently tested frame is higher than the reference frame which has lower compressive strength of concrete. Also, when comparing capacity curves,the frame has quite similar behavior when the concrete is 32 days old. Furthermore increasing corrosion rates of column reinforcements leads lower lateral load carrying capacity and ductility under lateral loading.

As it is expected, it was observed that retrofitting of the columns by RC thin jacketing like 4-6 cm thickness is an effective and useful method to increase sectional and hence the displacement ductility and the lateral strength of the frame. Self-leveling and self-compact special concrete can be used for those thin jackets.

Keywords: corrosion, seismic behavior, cyclic loading, pushover analysis, 15 years old frame, nonlinear behavior.

KOROZYONA UĞRAMIŞ BETONARME YAPININ SİSMİK DAVRANIŞI

Özet

Bu çalışmada, beton birleşiminde deniz kumu bulunan ve 15 yıl boyunca açık hava koşullarına maruz bırakıldığı için bir miktar doğal korozyona uğramış nervürsüz yumuşak donatı bulunduran yaklaşık $\frac{1}{2}$ölçekli betonarme çerçevenin sabit eksenel yük ve tersinir yatay yükler altındaki davranışı deneysel ve analitik olarak incelenmiştir. Bu numune Türkiye'de ilgili yönetmeliklere uygun olmayarak yapılan deprem güvenliği yetersiz yapı stoğunu temsil etmektedir. Kuramsal inceleme plastikleşmenin yayılı ve yığılı olduğu durumları gözönüne alan iki farklı program ile gerçekleştirilmiş ve malzeme mekanik özellikleri, çerçeveden elde edilen karot ve donatı numunelerinin sırasıyla basınç ve çekme deneylerine tabi tutulmasıyla elde edilmiştir.

15 yıl önce denenmiş, daha düşük dayanımlı, ilgili çerçeve ile birebir aynı özelliklere sahip ve aynı deney prosedüründen geçmiş bir çerçevenin deprem yükleri altındaki davranışı referans alınarak karşılaştırılmalar yapılmıştır. Korozyona uğramış çerçevenin deneysel sonuçları, şekil değiştirmenin yayılı olduğu varsayımıyla zaman tanım alanında doğrusal olmayan analiz ve şekil değiştirmenin yığılı olduğu varsayımıyla yatay itme analizi sonuçları ile karşılaştırılarak değerlendirilmiştir. Bununla birlikte, bir güçlendirme tekniği olan betonarme mantolama yönteminin kolonlara uygulanması kabulünün, ilgili çerçevenin deprem davranışı üzerindeki etkileri, yatay itme analizi ile kuramsal olarak incelenerek, farklı varsayımlar için kapasite eğrileri elde edilmiş karşılaştırmalar yapılmıştır. Güçlendirme amacıyla yapılan kabullerin kesit sünekliliğine etkisi de karşılaştırmalarla belirtilmiştir. Ayrıca mevcut çerçeve için belirli kesitlerde korozyon miktarının değişmesi ve bu durumun çerçevenin yatay yük taşıma kapasitesine olan etkisi parametrik olarak incelenmiştir.

Deney %3 öteleme oranında sonlandırılmış, kolonların uç kısımlarında, kesme ve eğilme çatlakları gözlemlenmiştir. Zayıf kolon güçlü kiriş durumunun oluştuğu ve yapı elemanlarının yatay yük taşıma kapasitelerini aşarak plastikleştiği görülmüştür. Ayrıca, analitik çalışma ile yapının yatay yükler altındaki davranışına, plastikleşmenin yığılı olduğu varsayımıyla daha yakın bir sonuç elde edilmiştir.

Bununla birlikte, betonarme mantolama tekniğinin kuramsal olarak uygulanması ile plastik mafsalların yatay yükler altında, kiriş uçlarında oluşmaya başlaması durumu, Deprem Yönetmeliği'nin önerisi olan güçlü kolon zayıf kiriş prensibine uygundur.

Deneysel ve kuramsal çalışmalar sonucunda bir miktar korozyona uğramış ve daha yüksek beton dayanımına sahip çerçevenin deprem yükleri altındaki davranışının 9 yıl önce test edilmiş ve korozyona uğramamış bir çerçeveyle karşılaştırılması sonucunda yatay yük taşıma kapasitesinin ve sönümlenen enerji miktarının daha yüksek olduğu görülmüştür. Ayrıca, güçlendirme işleminin yapının sünekliliğini ve dayanımını önemli ölçüde arttırdığı ve bu yöntemin yapıların depreme karşı güçlendirilmesinde etkili ve uygun bir teknik olacağı düşünülmektedir.

Anahtar kelimeler: korozyon, sismik davranış, çevrimsel yükleme, itme analizi, 15 yıllık çerçeve, nonlineer davranış.

Acknowledgements

I would like to express my special and deep gratitude to my thesis advisor Prof. Dr. Huseyin Faruk Karadogan for his valuable inputs,encouragement, patience, and valuable guidance. I would like to acknowledge Prof Dr. Esin Inan for her valuable support.

I would like to thank Prof Dr. Ercan Yuksel for his valuable guidance during experiments.I also would like to thanks Hakan Saruhan,C.E.,MSc, Mahmut Samli and Arasto Khajehdehi for their help with my experiments.

I would like to express my special gratitude to Safak Arslan I.E.,MSc for his endless support, help and encouragement during that period and to my family for their morale support and assistance during my difficult times.

To my loved ones...

Table of Contents

List of Tables

List of Figures

List of Abbreviations

RC	**R**einforced **C**oncrete
ITU	**I**stanbul **T**echnical **U**niversity
cm	**c**enti **m**eter
mm	**m**illi **m**eter
N	**N**ewton
kN	**k**ilo **N**ewton
Pa	**Pa**scal
LVDT	**L**inear **V**ariable **D**isplacement **T**ransducers

Chapter 1

INTRODUCTION

Due to rapid industrialization and rapid urbanization, low rise structural stock that is not served well from the point of engineering view, is considerable. Adding stories or modifying structural properties of columns and beams of these structure, it was aimed to meet the needs in the regions with high seismocity. This structural stock is exposed to seismic actions with different degree and other external effects, therefore it can be damaged by future earthquakes. In most of them, while preparing the granulometry, sea sand was used and also mild steel which is allowed at that time period were used. Turkish Earthquake Code is requiring performance analysis to assess the structures' earthquake resistance, so that they can be retrofitted when they are not providing the safety requirements. The application of this analysis that is based on material nonlinearity, necessitates, the stress strain relationship of the concrete of these old structures and the stress strain relationship of the mild still which is hard to find in market anymore, to be known.

It is obvious that the question "at what rate do the Code's regulations match up with the real situations?" has to be answered from the engineering point of view. During site observations it was detected that corroded reinforcements that are not protected well against external effect, expanding in volume causes vertical concrete cracks. Existent studies examine the loss of cross sectional area of reinforcements because of accelerated corrosion and the effect of corrosion on

the reinforced concrete's section properties, however, it has to be evaluated that in what extent these studies present the effect of natural corrosion on structural behavior.

Methods to retrofit this kind of structures in order to increase earthquake resistance to adequate degree, are determined according to performance analysis. It is important to find out how to present loss of adherence of reinforcing bar because of corrosion in calculations and structural models.

Performance analysis is based on nonlinear incremental lateral load analysis and its aim is to monitor the behavior of the structure up to collapse under seismic loading. It is still discussed whether the incremental lateral load analysis presents the reversed (bilateral) effect of earthquake.

Being aware of the difficulty of a research which includes all these study fields, the aim of this study is conducting an experimental and theoretical work whose details given below, to achieve some assessments by comparisons.

Chapter 2

LITERATURE REVIEW

Due to the fact that corrosion is the main and continuing issue of the steel bars in reinforced concrete structure, studying the effects of the corrosion on the reinforced concrete structures has received increasing attention in last years. To have ability to understand process and assessing the thesis study's results, the literature investigations are given in this chapter. Studies, generalizations and the comparisons related to corrosive effects on reinforced concrete structures in literature are summarized below.

2.1 Corrosion in Reinforced Concrete Structures

Reinforced concrete and steel structures are designed by considering the loads such as; dead, earthquake and service loads. Structures may experience the failure both due to these loads or the corrosion of the reinforcement. Corrosion is the deterioration of a metal due to chemical and electrochemical reactions between it and surrounding environment and it causes metals to lose their metallic properties. As it is defined in study Ahmad (2003) [1] generally there are two main factors that result in reinforcement corrosion in concrete: carbonation and chloride penetration that commonly cause uniform and localized attacks respectively.

2.1.1 Chloride Induced Corrosion

According to Dogan (2015) [2] study, both construction stage and service life affect corrosion of reinforcing bars. Chloride amount which penetrates to the concrete is in direct proportion to permeability and porosity of concrete. Due to the fact that structures experience earthquakes, mechanical fatigue, vibration and other environmental conditions, firstly micro cracks than macro cracks occur in the structure. These cracks and pores allow humidity, CO_2, sulfur nitrogen oxides in air leak into the concrete. Presence of oxygen, humidity and electrolyte are main causes of corrosion. Salt and chloride in connection with the usage of sea sand also cause the corrosion of reinforcing bars in concrete providing an electrolyte. Chloride ions permeate from outside to concrete through micro cracks results in deterioration of the passive layer of the reinforcement. Chloride ions pass through passive layer of steel bars and absorbed by the bar's surface, this absorption results in enhancement in negative direction with the potential of steel bar. Therefore, reinforcing bar which is closer to the surface acts like anode and reinforcing bar that chlorides can't reach behaves like cathode, then electron flow starts due to metallic bound. Then as a result of these reactions rust forms and starts to expand in the volume. This expansion causes concrete crack and spall at the end. Formation of the corrosion of reinforcement in concrete is given below:

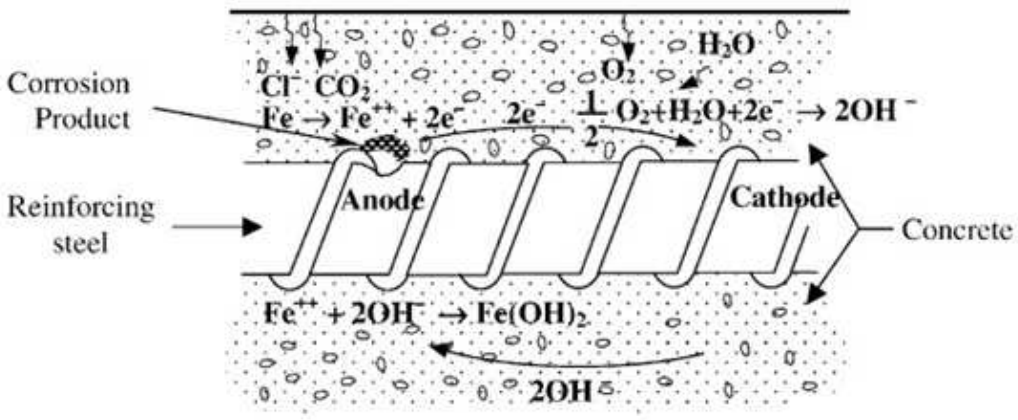

Figure 2.1: Formation of corrosion [3]

2.1.2 Carbonation Induced Corrosion

Normally, concrete provides high alkalinity to the reinforcing steel bars and concrete carbonation that is chemical deterioration of the concrete surface is the most critical agent that reduces pH value of the concrete. Ingress of carbon dioxide from the atmosphere may decrease pH value to 9 and passivation feature of concrete on steel bar can be lost and depending on the factors such as humidity and oxygen, corrosion may occur (Dogan (2015) [2]).

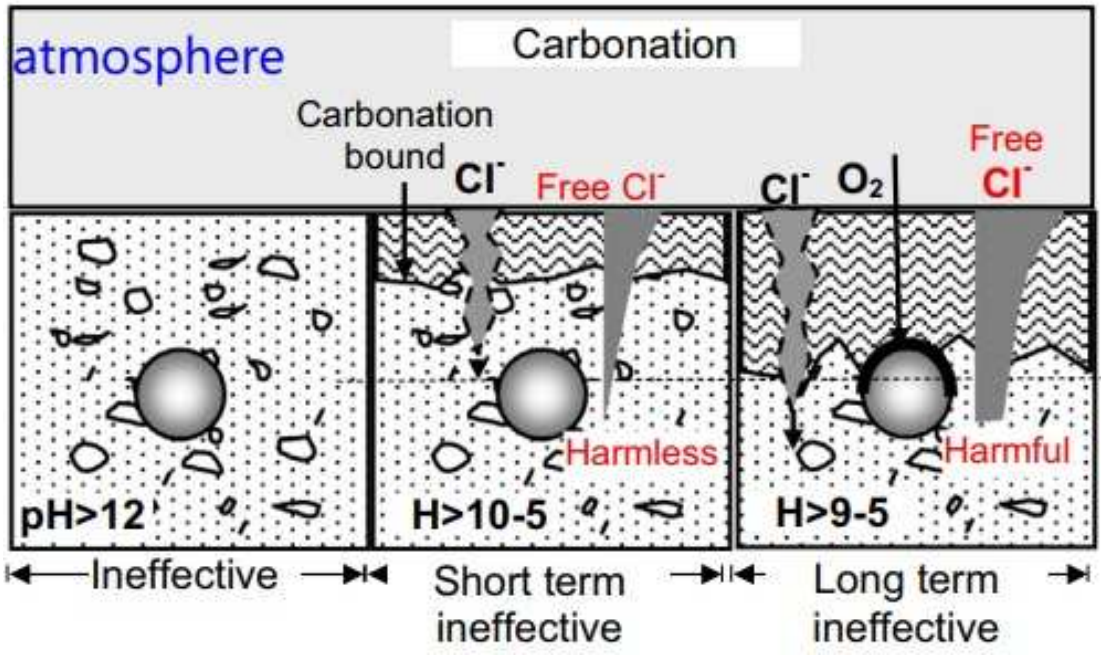

Figure 2.2: Carbonation (Dogan (2015) [2])

2.1.3 Studies on the Influence of Corrosion on Mechanical Characteristics of Reinforcement

In Almusallam (2001) [4]'s Study longitudinal reinforcements 6 and 12 mm in diameter, which were corroded in concrete specimens were removed and then subjected to tension test. After casting and curing for 28 days the corrosion of reinforcements was accelerated by inducing with anodic current of 2 $mA/cm2$. Attaining desired degree of reinforcement steel corrosion, concrete specimens were split along the line of the steel bars. The amount of corrosion of bars was evaluated as gravimetric loss in weight of the steel reinforcements. After investigating weight loss, steel reinforcements were subjected to tensional forces to analyze the mechanical properties. To obtain the elongation of the bars an extensometer was used. Loading and elongation output was recorded by a computerized system till specimens failed. These data was utilized to obtain stress-strain relation for each tested specimen. These stress-strain relationships were used to define the yielding and tensile strength of the reinforcements. The unit deformation of the

bars was obtained at the end of tension test. To evaluate the influence of the corrosion, tension tests were applied to both uncorroded and corroded reinforcements. Results have shown that the amount of reinforcement corrosion is not effective on the tensile strength of reinforcements. But, as the nominal diameter is taken into consideration, the tension strength is less than the ASTM A 615 proposal of 600 MPa for the corrosion amounts 11 and 24% for 6 mm and 12 mm diameter reinforcements, respectively. Additionally, reinforcement that has more than 12% corrosion represents brittle failure.

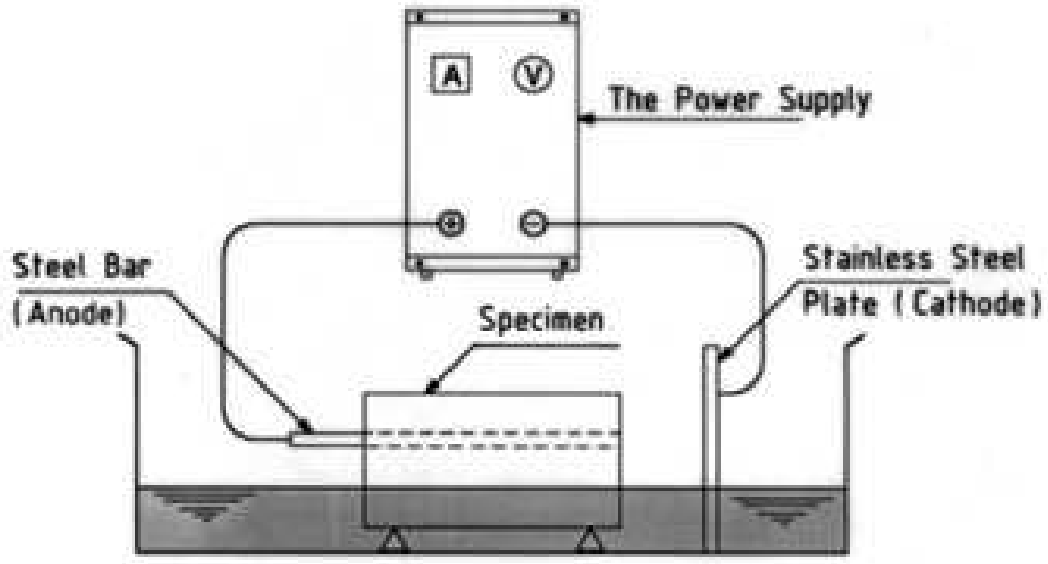

Figure 2.3: Test set up of accelerated corrosion (Almusallam (2001) [4])

Andrade et al.(1994) [5] performed an accelerated test concerning ductility and results indicated decrease in the elongation at maximum load of 50% and 30% correspond 28% and 15% cross section loss respectively. The similar conclusions were also arrived by Yang at al (2016) [6]. Performing cyclic lateral loading test of corroded reinforced concrete columns and tensile test for corroded reinforcing steel bars, they conclude that flexural strength ,the energy absorption and ductility of RC column elements which are correded, decreased as the amount of corrosion of the steel reinforcement increases.

Malumbela et al. (2009)[7] conducted a study concerning mechanical behavior of corroded reinforced concrete beams exposed to constant sustained service loads. Accelerated corrosion procedure was implemented for the corrosion of tensile steel bars. The number of tested beams was 4. They have a width of 153 mm, a depth of 254 mm and a length of 3000 mm. 1%, 8% and 12% of the ultimate load were taken as the load applied to specimens. Experimental results have indicated that with the increase in the amount of corrosion, the deflections of corroded specimens under load increase. Moreover, they conclude that degree of sustained load throughout corrosive period does not have an important influence on maximum mass loss of reinforcing bars. Also corroded specimens'load carrying capacity reduces while loss of mass of reinforcement increases.

Dang et al. (2013)[8] evaluated the performance of 27 years old beam by implementing 3 point bending test. The specimen is corroded by chloride induction. As a result of tests they claim that decrease in cross sectional area of reinforcement at the location where failure occurs, causes reduction in both yielding moment and ultimate moment and due to decrease in maximum elongation of reinforcement in tension. Because of the corrosion, ultimate elongation of corroded reinforcement does not meet the minimal requirement of design codes like Europe.

Similarly, the effect of corrosion on loss of mass, low and high cycle fatigue features of Bst500s reinforcement that is used commonly in Greece between the years 1990 and 2005 was studied by Apostolopoulos et al. (2006)[9]. Reinforcements which have 12 mm diameter were exposed to accelerated corrosion procedure and experiments were carried out low and high cycle fatigue ranges. Experimental results have shown that with the increase of corrosion degree, yield and failure strengths and the ductility reduce.

2.1.4 Studies on the Influence of Corroded Reinforcements on Flexural Behavior of the Structure

In Zhang et al. (2010)[10] study, 14 and 23 years, two corroded beams(named as B1CL1,B2CL1 respectively) that were exposed to chloride environment were exposed to chloride environment and loaded in 3-point bending. They observed and recorded the corrosion activities from the beginning of the experiment .At the end of 14 and 23 years of exposure, a lot of longitudinal cracks because of the corrosion of reinforcing bars could be seen all around the specimens. In order to evaluate damage due to corrosion, removing reinforcement from the concrete, loss in diameter was obtained from the mass loss of the reinforcing bars. In this study it is indicated that reinforcements of B2CL1 had more corrosion than B1CL1's reinforcements. Moreover, they conclude that because of ingress of chloride, localized corrosion is the prominent pattern of corrosion. Also the pitting type corrosion is the principal factor which affects corrosion process at crack formation stage. When corrosion cracks increase, general corrosion forms immediately and progressively becomes dominant in the second level of cracking propagation. Comparing with existing Vidal et al. (2004)[11], Vidal et al. (2007)[12] model and experimental results, it can be said that their model is not appropriate to estimate beam B2CL1 under general corrosion however it can be used to estimate the reinforcement corrosion of specimen B1CL1 when localized corrosion is dominant. Also Rodriguez's model, derived from general corrosion formed by artificial corrosion tests is not in good agreement with the natural corrosion. Therefore, a new model is obtained based on the average cross sectional loss of reinforcing bars for natural general corrosion.

Ali (2014)[13] researched the influence of pre-corrosion of steel bars of reinforced concrete beams on the flexural behavior. Rebars were corroded artificially by two methods before using them as reinforcement. First method was putting rebars in water with 8% salt concentration inside lab and the other method was surrounding the rebars by salt outside the lab leaving them changing weather

conditions. Beams were tested under increasing two point loads at mid one-third span until the failure occurred. They observed more corrosion rate with second method when compared to first method. Results revealed that for the early ages, noncorroded rebar beams gave maximum load, displacement, moment, curvature however, situation changed at late age. Moreover, highly corroded rebars gave better results compared to beams with lower degree of corroded rebars and highly corroded rebars of 10 mm gave better results than same amount of corrosion of 12 mm rebars, this situation can be explained with improved bond characteristics at steel concrete interface for high amount of corrosion where degradation layers of these bars were not removed when using them in beams. They also conclude that failure condition is determined by concrete and the reduction of steel section increase the ductility of beam. Unlike the other researchers, they claim that using the corroded steel rebar at beams is useful but these results need more investigation on different size and different structural elements.

The studies of Lee et al. (2003)[14] and Meda et al. (2014)[15] indicated results such as decrease in flexural strength and ductility with the increase of amount of corrosion of steel reinforcements concerning hysteretic loaded corroded RC columns.

Dekoster et al. (2003)[16] presented a finite element study related to flexural behavior of corroded beam conducting four point bending load test. Using CASTEM 2000 computation software, results compared with two experimental studies, one of them is about beams which have uniform corrosion and the other one is about a long term experimental progress that contains inducing localized corrosion of beam specimens. The interface between concrete and steel which is named as rust is represented as special elements using different sizes of it. According to this study, to obtain the model of the flexural behavior of corroded beams two parameters are significant: cross sectional loss of reinforcement and deterioration of steel-concrete interface which can be considered as rust elements. Results indicated good correlation between experimental studies and finite element method.

Additionally in case of localized corrosion, load deflection curves match with experimental results as a flexural failure occurs and incase of uniform corrosion a bond failure occurs especially for higher levels of corrosion. As a result damage model for concrete combined with the change in reinforcement section and considering rust effect, allow the ability of evaluation of flexural behavior of corroded specimens.

2.1.5 Studies on the Effect of the Corroded Reinforcement on Bond Behavior

Fang et al. (2006)[17] conducted tests concerning bond behavior of corroded reinforced concrete under cyclic loading. The results indicated that bond behavior decreased under cyclic loading. For deformed bars, degradation in bond was less than for plain bars at the first loading cycle however the difference was reduced with loading. For unconfined steel reinforcement bond decrease was more significant than for confined bars. Degradation caused by great amount of corrosion in first five cycles and the influence of the corrosion diminished with loading. It has been concluded concluded that cyclic bond stress-slip curves depended on loading history.

Carbone et al. (2008)[18] performed an analysis on a portion of a beam subjected shear and under 85% of the limit bending moment using a numerical model that is able to consider corrosion effects of a uniform corrosion of reinforcement. They claim that existence and amount of shear is important since it determines the macro-slip effect on concrete block and the final configuration in terms of equilibrium. So, the solution exactly depends on the loading conditions. For full bond strength increment of deformation in compressed concrete at top section is about 6% but when it reaches 10%, bond strength is diminished of the half. Therefore, when the loss of bond takes place because of corrosion and the strain pattern is modified all over the affected zone corrosion causes significant effects on the entire structure such as loss of ductility and presenting brittle failure.

2.2 Seismic Retrofit of Reinforced Concrete Structures

According to inspection of concrete buildings, especially building stock of Turkey constructed before 1998 Turkish Earthquake Code, having large spacing of hoops, no use of 135° seismic hooks, concrete with a low compressive strength cause decrease in flexural capacity, shear capacity and the deformation abililty of the structures. For that reason, structures and structural members having inadequate seismic details must be retrofitted to perform reliable seismic performance as specified in the current seismic design codes. There are codes widely accepted, like the EUROCODES, has an entire volume (EC 8) to seismic design, and its part 1998-3 "Assessment and Retrofitting of Buildings", FEMA 237-Development of Guidelines for Seismic Rehabilitation of Buildings, FEMA 275-Planning for Seismic Rehabilitation are the codes that guide rehabilitation of the structures. This shows the important role of retrofitting existing vulnerable structures in structural engineering.

Retrofit strategies for strengthening can be divided into two approaches. The first approach is the global strengthening which is addition of new elements to the system to achieve increase in its global strength. The second approach is local (element) strengthening. The local strengthening of structural members aims to improve the deformation capacity of vulnerable structural elements so that they will not reach their limit state as the structure responds at the required level. Local retrofitting techniques can be applied to more than one member of a structure that suffer from structural imperfections.The influence of global retrofitting and the influence of local retrofitting on overall behavior of structure are summarized in Figure 2.4 and Figure 2.5 ,respectively.

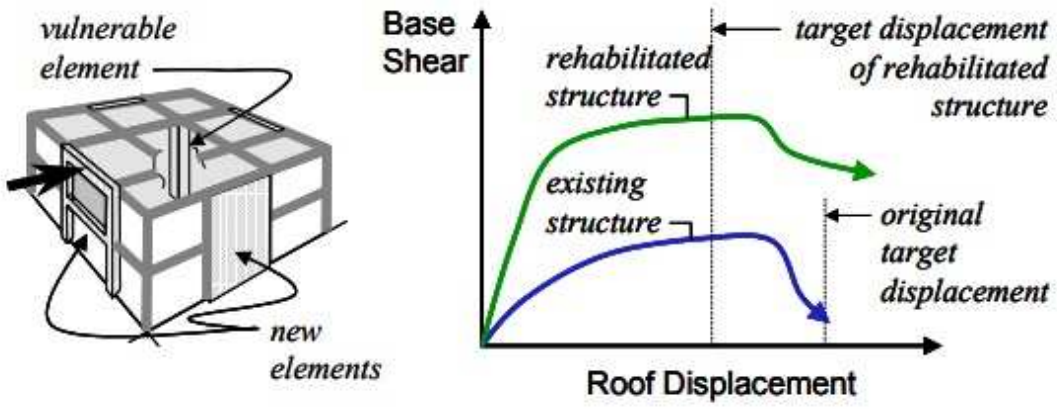

Figure 2.4: Global retrofitting of the structural system [19]

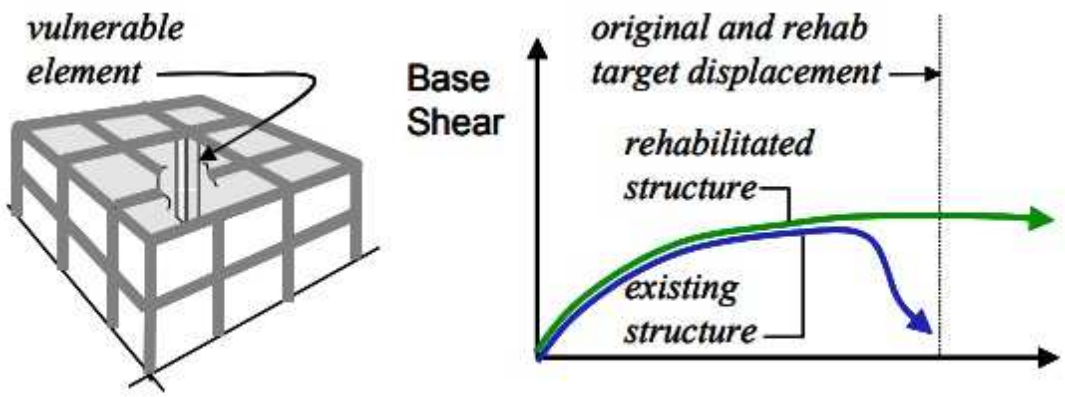

Figure 2.5: Local retrofitting of the structural system [19]

2.2.1 Global Retrofit Methods

Global retrofit methods are applied to improve seismic resistance of vulnerable structures to desired level by elimination or decreasing the unfavorable effects of design or construction. In the following subsection, common global retrofit methods and their effects on overall behavior of structure are summarized.

2.2.1.1 Addition of Walls or Braces

Addition of shear walls and steel bracings to systems are commonly used methods to provide strength, stiffness, energy dissipation of existing structures required to

resist lateral earthquake loads. Many studies conducted on the placing of shear walls and the studies revealed that shear wall can highly improve the lateral load capacity and lateral stiffness of the structures.

Retrofitting a system by addition of shear wall increase structures' lateral rigidity, thus the natural period of the structure decreases [20]. In the study of Kaplan et al. (2012)[21], existing partition walls of a structure were removed and shear walls were placed instead. This kind of application leads shear walls bearing most of the lateral loads and decreasing the displacement of the structure. In other words, due to frame-shear wall interaction RC frame resist very low amount lateral load and shares it with the shear wall.

Alashkar et al. (2015)[22], analytically studied an existing eight story RC frame structure retrofitted by concrete shear wall and steel bracing placed at the boundary and core of the building .They conclude that, addition of shear wall provides effective control of global lateral drifts and reduces damage of the structure and decreases important amount of lateral displacement, bending moment and lateral forces in structural members when comparing to other retrofit methods.

Alashkar et al. (2015)[22] also conclude that X-bracing system reveals minimum moment when comparing to other types of bracings and V-type bracing causes some additional flexural moment in beams and columns.

As it is stated in [23] another retrofitting technique, addition of infill walls, enhance structures' lateral load carrying capacity and lateral rigidity.

Benavent-Climent et al. (2018)[24] conducted a study which includes strengthening a RC frame structure with the addition of two masonry infill walls and the RC frame structure retrofitted with infill walls was tested under four seismic simulations on a shaking table up to large drift ratios. They concluded that infill walls increased the initial stiffness and the lateral strength of the bare frame by about 25 and 5 times, respectively.

An experimental investigation was conducted by Dautaj et al. (2018)[25]. They researched the behavior of masonry-infilled (RC) frames with various lateral strengths. Firstly, RC frame was cast,then masonry walls were placed. 2/3 scale, single-bay, single-story, eight RC frame specimens were tested. They investigated that the type, dimensions, shape and shear strength of the masonry affects the strength and failure mechanism of the RC frame when it is infilled.Besides,it dramatically enhances lateral strength and stiffness of the structure.

2.2.1.2 Reduction of Irregularities

Non-uniform distribution of material properties on structural components causes irregularities in the seismic behavior of structures. Thereby, material irregularities result in strength irregularities. As a solution equivalent "material eccentricity " was proposed by Sassu et al. (2017)[26], performing pushover analysis applied to an existing building located in Italy. The analysis revealed how the structure is influenced due to variability of compressive strength of the concrete.

2.2.1.3 Reduction of Mass

Reduction of mass can be an efficient retrofitting method for some existing buildings. Reduction of effective mass leads to shorter vibration period of the structure, decrease in inertial forces and displacement demand. To achieve mass reduction, heavy nonstructural elements (such as water tanks, heavy contents such as equipment and storage, cladding and soil used as part of landscape architectural features) can be removed. In the extreme, it can be also done by removal of one or more storeys in the existing building. Even though mass reduction can be a very effective technique in some cases, in most cases it is of marginal value [27].

2.2.1.4 Introduction of Energy Dissipation Devices

As another retrofitting technique, to reduce dynamic response through increased damping energy dissipators can be used in structures. Visco-elastic fluid dampers, visco-elastic solid dampers, friction dampers, hysteretic energy dissipating dampers can be used in seismic- retrofitting. The devices usually are mounted on supplementary vertical braced frames, which cause also an enhancement in stiffness of the structure. However, in the case of failing in brittle modes of existing members at small deformation, such energy dissipation devices may be insufficient [27].

2.2.1.5 Base Isolation

In order to achieve enhanced performance base isolation technique also can be used. Base isolation basically requires a double foundation system, for instance, one foundation for the superstructure above the isolation devices and another for the entire structure below the isolation system. Nonetheless, base isolation can provide safety of the building and its occupants in the case of very strong and rare earthquakes, and also protects building contents under any seismic circumstance.

Ferraioli et al. (2017)[28] carried out the seismic assessment of existing multiple story building which is retrofitted by base isolation. They conclude that, even if, conventional retrofitting techniques are based on increasing ductility, stiffness and strength, with the addition of new elements and modifications causes loss of functionality. However, reducing the seismic force demand on the superstructures, base isolation provides great protection above its plane without wide strengthening applications.

2.2.2 Local Retrofit Methods

Vulnerable components of a structure can be retrofitted to increase deformation capacities and strength. In the following subsection, common local retrofit methods and their effects on overall behavior of structure are summarized.

2.2.2.1 RC Jacketing

One of the popular retrofitting technique is RC jacketing due to its ease of application and comparatively low cost. RC jacketing has many advantages due to uniform distribution of lateral load capacity through the structure. It results in elimination of concentrated lateral load resistance that occur if only some shear walls added(Thermou et al. (2006)[29]).

Valente et al. (2017)[30] analyzed a four storey RC frame with insufficient seismic resistance by nonlinear static analysis and obtained that RC jacketing is effective in reduction the sudden change in the flexural rigidity of the column at the third story and also avoids the soft story collapse mechanism. They conclude that application of RC jacketing on vulnerable columns can eliminate unfavorable torsional effects.

Baciu et al. (2015)[31] conducted an analytical study of retrofitting a single storey,RC industrial building's columns, using variable rehabilitation options. They investigated that the highest values for safety factor is obtained by classic RC jacketing retrofitting method, however it causes considerable work process with considerable costs.

Elbakry et al. (2016)[32] studied the effect of surface preparation and concluded that, as the surface roughness of the substrate concrete increases, shear friction increases, then it results in enhancement on the overall bond strength.

Also Sheikh et al. (2017)[33] and Rawat et al. (2017)[34] reported that, RC jacketing leads enhancement in member stiffness and strength and provides better solution to avoid buckling problems.

2.2.2.2 FRP Jacketing

Externally bonded fibre reinforced polymers (FRPs) can be in the form of carbon (C), glass (G) or aramid (A) fibres. It has being utilized widely all over the world

to retrofit RC structures. The shear capacity of deficient structural elements can be increased by providing externally bonded FRP with the fibres in the direction of hoop. Ductility of flexural plastic hinges at beam or column ends and joints can be provided by applying FRP jackets which is another form of confinement with the fibres placed across the column or beam element circumference [27].

This material also resists corrosion in chloride environments that can possibly leads to reduction in maintenance cost. The rehabilitation of vulnerable RC columns with CFRP provides more ductility and increase energy dissipation capacities, thus, improvement in terms of total seismic resistance [35].

Hemy (2016)[36] conducted a test to obtain behavior of RC columns under uniaxial compressive stresses. Specimens were divided two groups according to techniques used, such as: Vacuum Assisted Resin Transform Technique and hand lay-up technique and each group consist of one control column and three retrofitting columns using GFRP wraps. Columns were retrofitted using single, double and treble layers of bi-directional GFRP wraps.

According to test results, they concluded that, for a considerable increase in the strength more than one layer of GFRP should be used. Also confining the specimen with GFRP leads higher load carrying capacities and higher ductility when compared to control specimens and VARTM technique produces greater ductility and load carrying capacity when compared to hand lay-up technique.

2.2.2.3 Steel Jacketing

Steel jacketing is another effective retrofitting method It is not only a fast method but also effective when there is need for immediate use of the building after a damaging earthquake, or where there is a danger of collapse of the structure. It can be applied beam and column elements to increase shear strength and ductility and improve insufficient lap splices. Because of the fact that steel is isotropic it

has significant role to enhance strength and stiffness in longitudinal direction as well when comparing to FRP wrapping [27].

He et al. (2018)[37] presented the experimental and mathematical studies on the seismic behavior of reinforced concrete columns which includes recycled aggregate concrete and retrofitted with steel jacketing. Lateral cyclic loading is applied to columns. Comparing these retrofitted columns with reference column, they obtained that steel-jacket retrofitting method improves the initial stiffness, ultimate strength, deformation ductility and energy dissipation capability of the columns substantially. Additionally, the ultimate strength of the rehabilitated specimens were higher 1.86-3.44 times than that of the reference column, and the rehabilitated specimens demonstrated ductile post-peak load behavior with the ductility coefficients varied from 4.05 to 7.93. Also, when the steel jacket thickness increases, the ultimate strength of steel jacketed specimen enhances significantly. Therefore the influence of the thickness of steel jacket on the ultimate lateral strength of steel jacketed column is quite important.

Chapter 3

TEST PROGRAM AND MATERIAL CHARACTERIZATION

In this chapter experimental test program is described to assess the seismic performance of a structural frame exposed to corroded material properties. Test set up, description of the test specimen, implementation of experiments and material characteristic are presented here.

3.1 Test Specimens

The RC frame constructed in ITU Civil Engineering Faculty at 2003 has sea sand and low strength (mild) reinforcement. This type of structure represents the strong beam- weak column type of structure which were very common in Turkey. The RC frame exposed to weather conditions in ITU for 15 years and the physical characteristics of frame are as follows:

• 1/2 scale frame is one story and bay and it has slab on top and a foundation at the bottom.

• The cross sectional dimensions of columns of the frame are 20 cm by 25 cm, the cross sectional dimensions of the beam of the frame are 20 cm by 32,5 cm.

• The height of the frame is 152,5 cm and the width of the frame is 220 cm.

• Longitudinal reinforcing bars of the frame consists of 16 mm steel bars.

• The foundation thickness is 38 *cm* and the reinforcing bars of the columns continue to the bottom of the foundations and at the foundation level, there is no lap-splice.

• Seismic details of the frame is insufficient due to large spacing of transverse reinforcement, in beam column joint there is not transverse reinforcement and there is no use of 135° seismic hooks.

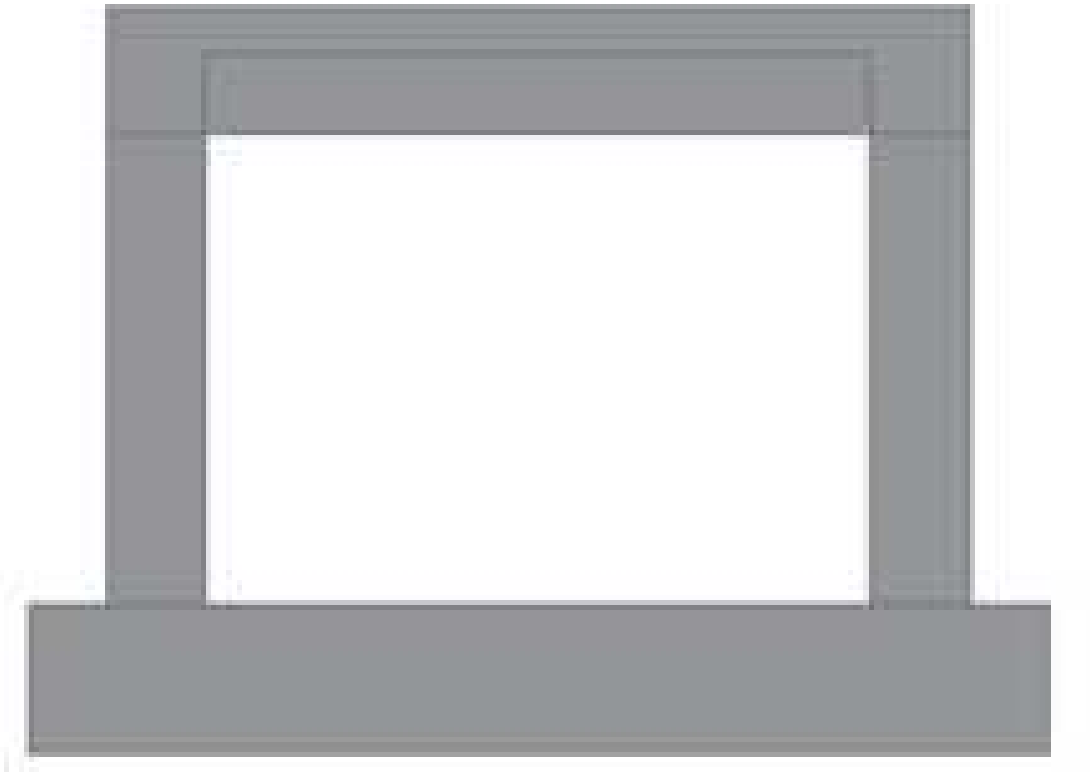

Figure 3.1: View of the 15 years old frame

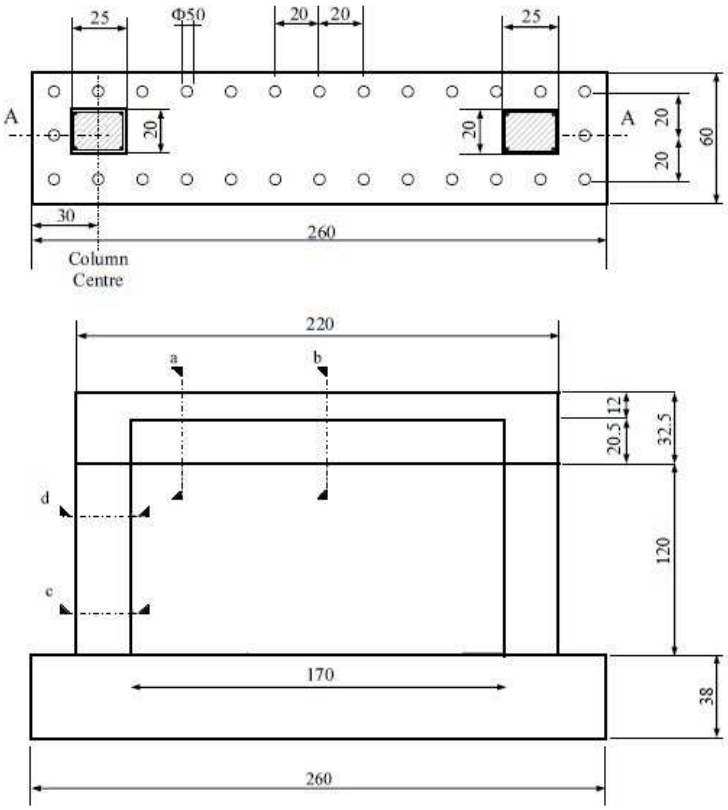

Figure 3.2: Geometry of the 15 years old frame

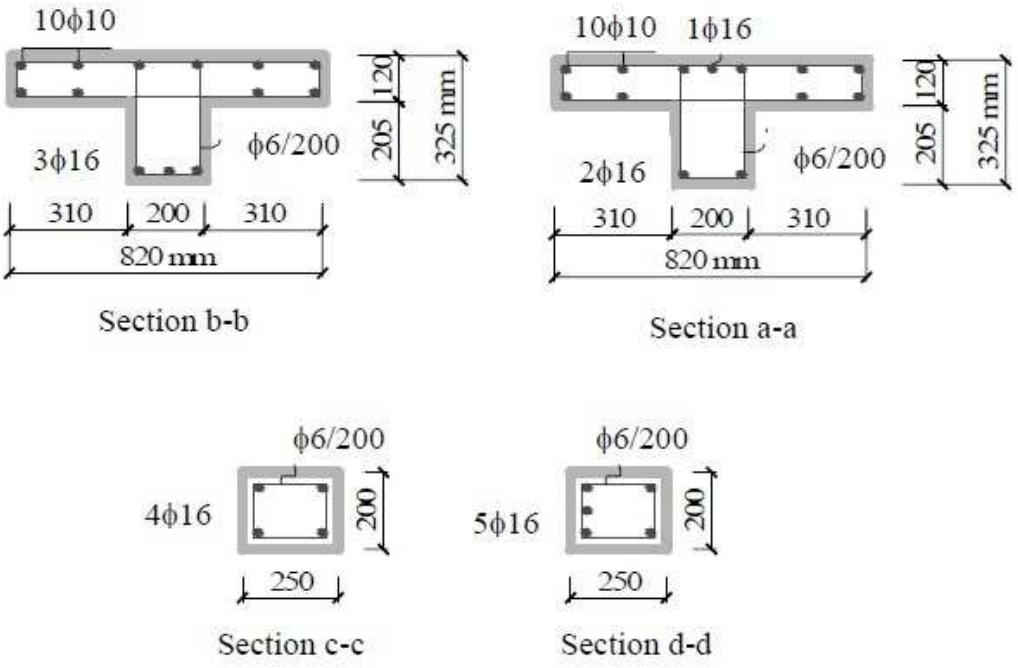

Figure 3.3: The details of frame reinforcement

Figure 3.4: The details of frame reinforcement

3.2 Experimental Procedure

This section explains experimental set up and procedure for the 15 years old frame. In detail, equipment used, data acquisition and loading systems are also presented here.

3.2.1 Test Setup, Equipment and Loading System

General view of test setup of the frame has shown in Figure 3.6. The details of test setup are as follows:

• Using enough number of anchorage bolts of $\phi 39\ mm$, foundation of specimen is fixed to the adapter foundation in order to avoid any movement or sliding at foundation level during the experiment. Therefore foundation of the specimen becomes similar to fixed support.

• The columns were subjected to constant axial load during the experiment and hydraulic jack and load cell were used for that purpose. Amount of the axial load is 167.5 kN which is 15-20% of axial load carrying capacity of the columns that is determined according to TS500.

• Displacement based load protocol was used in this experiment and lateral cycling loading applied to the 15 years old specimen as displacement reversals to simulate earthquake action. Displacement reversals are applied using 250 kN capacity actuator that placed at the beam level of the frame. The displacement capacity of the actuator is $\pm 300\ mm$ (30 cm).

• Displacements and the deformations of specimen were obtained during the test by the linear variable displacement transducers (LVDT) that are connected to various critical regions on the specimen. To attach LVDTs, small holes drilled at each predefined point and using epoxy resin dowels are fixed to these holes. Then holders of LVTDs are attached to dowels and LVDTs placed at holders. Top displacement was assigned as control displacement placing there a high sensitive

LVDT in order to measure the displacement. Types of LVDTs and their measurement purposes are given in Table 3.1. Figure 3.5 shows locations of LVDTs.

Name	**LVDT Type**	**Measurement Purpose**
T1	CDP100	Top displacement
T2	CDP10	Left column upper rotation
T3	CDP10	Right column upper rotation
T4	CDP10	Left column upper rotation
T5	CDP10	Right column upper rotation
T6	CDP25	Left column lower rotation
T7	CDP25	Right column lower rotation
T8	CDP25	Left column lower rotation
T9	CDP25	Right column lower rotation
T10	CDP50	Displacement of the whole system (foundation sliding)
T11	CDP50	Out of plane
T12	CDP50	Out of plane

Table 3.1: LVDT's used for the frame

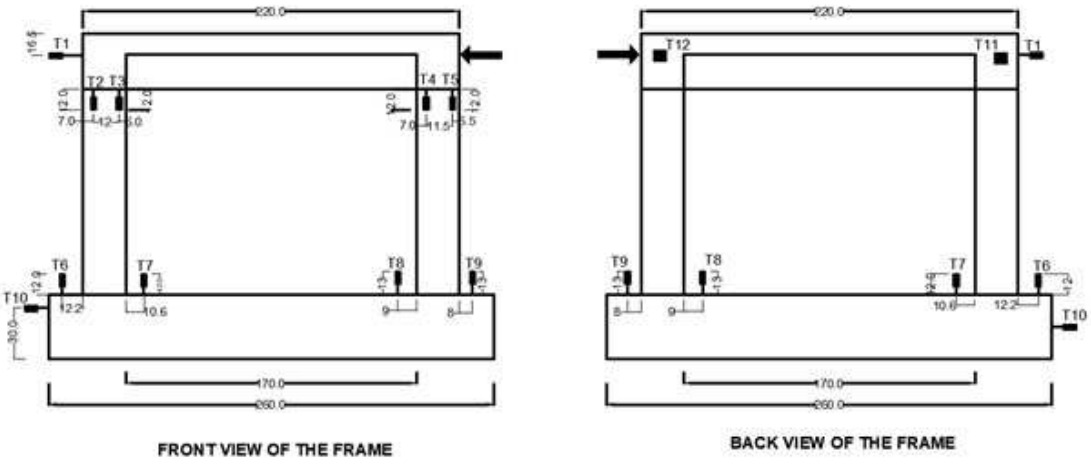

Figure 3.5: Locations of LVDTs

Figure 3.6: General view test setup

Details of the setup is given in following figure (Figure 3.7).

Figure 3.7: Details of setup

3.2.2 Load Pattern and Data Acquisition

With the constant axial load of 167.5 kN for each column, reverse-cycling loading was applied the frame to create an action similar to seismic action by actuator that arranges the increasing intensity of loading. Displacement based load protocol starting from 0.035 mm up to 42 mm target value of top displacement was applied. Each displacement cycle, repeated thrice for both pulling and pushing cycles. Data of Displacement and force of the hydraulic actuator, deformations and displacements of LVDTs were monitored and recorded by computerized system. At the end of the each specified displacement target, cracks that occurred were determined and marked on the frame by a marker. The details of displacement protocol is shown in Figure 3.8 and Figure 3.9 .

Load level	Top displacement $[mm]$	Relative Drift δ/H
1	0.035	0.000025
2	0.070	0.000050
3	0.140	0.000100
4	0.280	0.000200
5	0.350	0.000250
6	0.467	0.000300
7	0.700	0.000500
8	1.400	0.001000
9	2.800	0.002000
10	3.500	0.002500
11	4.200	0.003000
12	4.900	0.003500
13	5.600	0.004000
14	7.000	0.005000
15	10.500	0.007500
16	14.000	0.010000
17	28.000	0.020000
18	42.000	0.030000

Figure 3.8: Steps of the displacement protocol

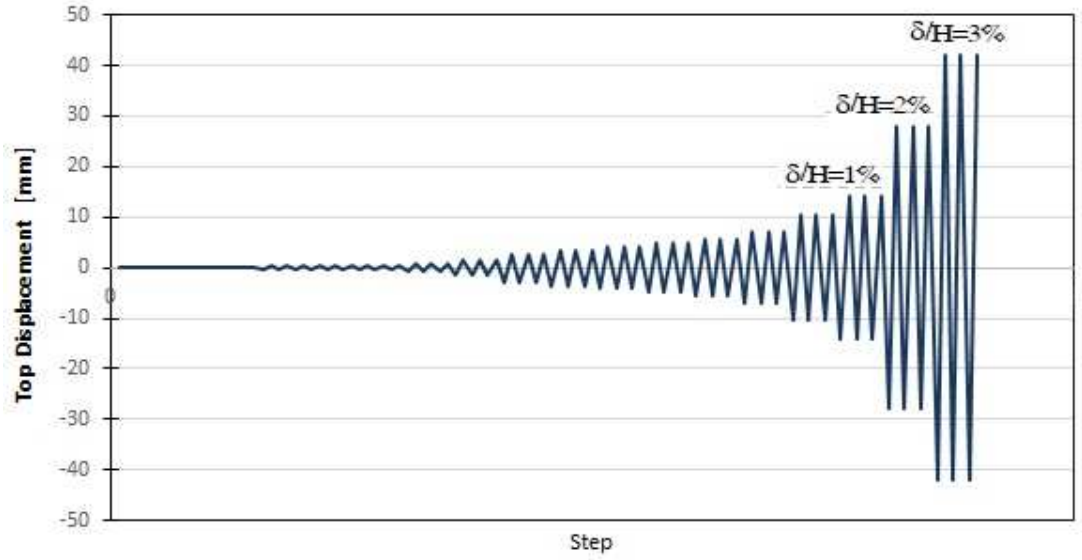

Figure 3.9: Displacement protocol

3.3 Material Test

3.3.1 Concrete Tests

3.3.1.1 Standard Cylinder Specimens

Displacement controlled compression test was conducted to obtain the pre-peak and post-peak response of 15 years old standard cylindrical concrete specimens at Construction Materials Laboratory of ITU Civil Engineering Faculty. Cylinders of 150 mm diameter and length of 300 mm were used for the test. Cylindrical concrete specimens that have same concrete mix proportions with the tested frame specimen which is called 34 numerically

To measure the vertical deformation totally four LVDTs were used; two LVDTs at the middle part of the specimen (between two clamps) to obtain the deformation of the middle part of the specimen and between loading platens other two LVDTs, to obtain the total vertical deformation, were placed. To measure the horizontal deformation 3 LVDTs mounted at 120 degree intervals along the circumference of the specimen. Before the tests making sure that the specimen's lower and upper

surfaces are flat, a friction reducing pad placed between the loading platen and specimen. Then the test was conducted using 5000 kN capacity Instron Testing Machine.

Identical test procedure was carried out for each specimen. Stress-Strain diagrams were obtained for each specimen. The axial stress is computed dividing the load by the net cross sectional area. The axial and horizontal strains are the average of axial and horizontal deformations respectively divided by the specimen length. The compressive test configuration and the deformed view of a specimen are given below (Figure 3.10).

Figure 3.10: Compression test

The compressive strengths of cylinder specimens casted and tested 15 years ago called 34_1, 34_2, 34_3 and compressive strengths of cylinder specimens tested after 15 years called 34U_1, 34U_2, 34U_3 are given in below (Table 3.2) according to compressive test results.

Specimen No	**Number of Cylinders**	**Compressive Strengths (Test Results) [MPa]**	**Average Cylinder Compressive Strength [MPa]**	**Cylinder Compressive Strength [MPa]**
Specimens (34_1,2,3,4 (32.days))	4	21.52 21.80 23.36 21.38	22.02	20.85 (Standard Deviation: 0.91)
Specimens (34U_1,2,3 (5250-5271- -5298.days))	3	21.52 21.80 23.36 21.38	25.66	21.29 (Standard Deviation: 3.41)

Table 3.2: Compressive strengths of cylinder specimens

Average state of stress strain relationship of concrete which is obtained by cylinder specimens' compressive tests is given in Figure **??**.

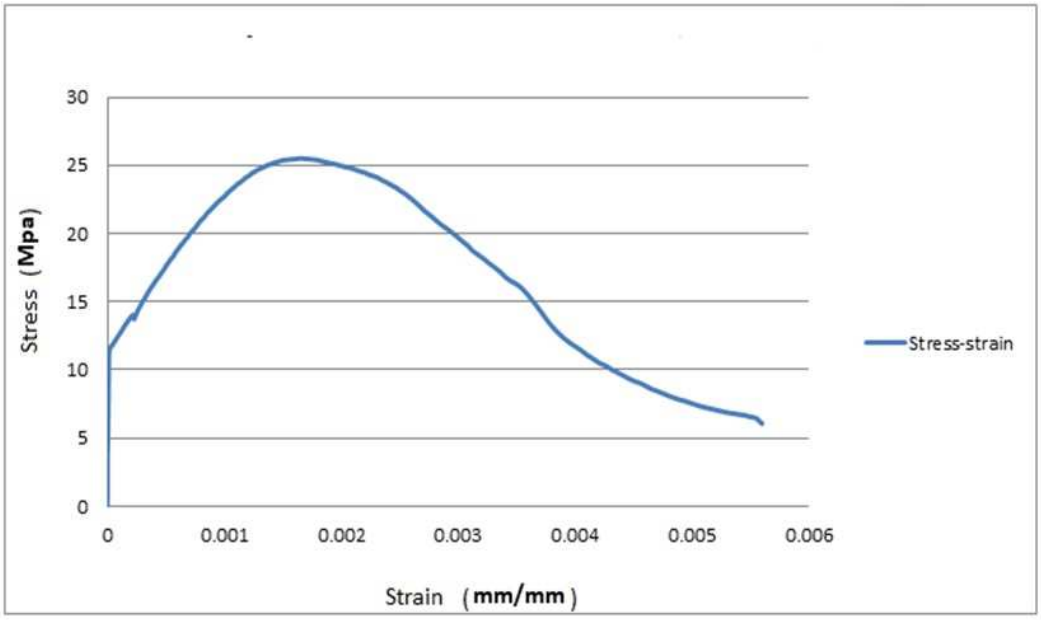

Figure 3.11: Stress-strain relationship of concrete with sea sand

3.3.1.2 Core Specimens

In order to define the mechanical properties of concrete accurately, cylindrical core specimens were taken from columns, beam and slab of the frame. Drilling and testing of the core specimens were performed according to TS EN- 13791 code which specifies the technics for drilling core specimens from hardened concrete, their examination, preparation for compressive test and specification of compressive strength of concrete. After coring, the specimens were tested under compressive force till failure at Construction Materials Laboratory of ITU Civil Engineering Faculty. Details for each core specimen, their compressive strengths and the obtained compressive strength for frame as a result of correlation between compressive test results of core sampling and compressive test results for 15 years old cylinders are given in Figure 3.13. The Figure 3.12 below shows the drilling and testing of core specimen.

Figure 3.12: Drilling and testing of core specimens

Core Specimen No	Coring Place	D (Diameter)	h (Height)	slenderness ofcore specimens not considered		NEVILLE	
				Fracture Force	Core Specimen Comp. Strentgh	Cube (150x150x150) Comp. Strentgh	Cylinder(150x300) Comp. Strentgh
		[mm]	[mm]	[kN]	[MPa]	[MPa]	[MPa]
GK1	LEFT COLUMN -1	93	98	210,4	30,99	30,58	25,99
GK1 K1	LEFT COLUMN -11	93	105	179,9	26,50	26,70	22,70
GK2	RIGHT COLUMN -2	93	96	213,8	31,49	30,88	26,25
GK2 -K2	RIGHT COLUMN -22	93	104	201,6	29,69	29,84	25,36
K7-1	BEAM	93	101	182,4	26,87	26,76	22,74
K7-2	BEAM	93	103	175,7	25,88	25,93	22,04
K16- D2	SLAB	93	99	199	29,31	29,01	24,66
K17-D3	SLAB	93	101	192,3	28,32	28,21	23,98
K18-D1	SLAB	93	102	184,7	27,20	27,18	23,10
	34_U1						29,16
	34_U2						22,35
	34_U3						25,46
Average					28,47	28,34	24,48
Standart Deviation					*2,01*	*1,82*	*2,09*
$f_{c,recovered} = f_{c,aver} - 1.28$ x St.Deviaton					25,89	26,01	21,81

Figure 3.13: Correlation of concrete compressive strengths

For more accurate analysis compressive strength of concrete is found by the formula where ± standard deviation is used and also directly taking mean value of the material compressive strength test results. Elasticity modulus for each compressive strength was found according to TS500. These obtained values are given in Table 3.3. Additionally the elasticity modulus which is obtained from stress

strain curve of concrete, 12500 MPa is also considered for the analysis for more accurate results.

F_c **(MPa)**	**E (MPa)**
21.81	29177.88
27.16	30935.96
24.48	30080.11

Table 3.3: Elasticity modulus according to compressive strength

3.3.2 Steel Reinforcement Tests

In order to determine the mechanical characteristics of mild steel reinforcements with a little amount corrosion, tensile test carried out at the Material Testing Laboratory of ITU Civil Engineering Faculty using MTS Testing Machine of 300 kN tension capacity. The steel reinforcements have small amount of corrosion and taken from one column of the 15 years old frame are given in Figure 3.14. ϕ16 bars are used for longitudinal reinforcement for columns and beam, ϕ6 bars used as stirrups, ϕ10 bars are used as longitudinal reinforcement of slab bars of the frame. The mechanical properties of the rebars that were obtained 15 years ago are given Figure 3.15.

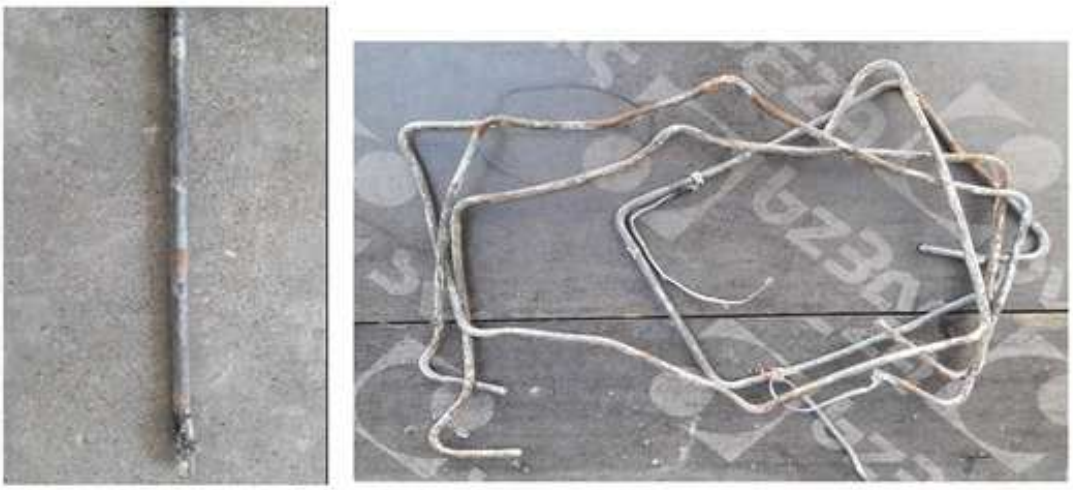

Figure 3.14: a.)One of the corroded longitudinal reinforcement - b.)Corroded transverse reinforcement

Diameter [mm]	ϕ16	ϕ10	ϕ6
σ_y [MPa]	270	290	325
σ_{max} [MPa]	420	450	481
ε_{su} [mm/mm]	0.25	0.30	0.35

Figure 3.15: Mechanical properties of steel bars

Five longitudinal reinforcing bars that were taken from one column of the frame were cut into eight part totally. Each specimen was tested under increasing tensile force till failure. An extensometer was utilized to obtain the vertical deformation during the tests. The data was recorded using a computerized system of the testing machine. Test set up is given in Figure 3.16 and Figure 3.17. After tests, stress-strain relationship of each specimen derived from the data obtained. Properties of specimens are given in Table 3.4. Tensile properties of the specimens after 15 years given in Table 3.5.

Figure 3.16: Test setup for longitudinal reinforcement

Figure 3.17: Configuration of the steel rebars after tensile test

Specimen No	**Weight (gr)**	**Lengt (mm)**	**Diameter (mm)**	**Initial Lenght (mm)**	**Measured Diameter (mm)**
1	729.6	449	16	80	16.2
2	651.3	411	16	80	16.0
3	788.2	483	16	80	16.3
4	790.4	487	16	80	16.2
5	616.7	395	16	80	15.9
6	579.3	357	16	80	16.2
7	617.8	394	16	80	16.0
8	591.9	366	16	80	16.2

Table 3.4: Reinforcement specimen characteristics

Specimen No	Yielding Limit (Re)		Tensile Strength (Rm)		Ultimate Strain %
	kN	**Mpa**	**kN**	**Mpa**	
1	66.2	329	88.1	438	41%
2	58.5	291	85.0	423	43%
3	63.7	317	88.0	438	44%
4	60.3	300	87.3	434	40%
5	60.3	300	81.4	405	40%
6	58.4	290	84.1	418	40%
7	59.4	295	81.4	405	41%
8	57.6	286	84.1	418	42%

Table 3.5: Reinforcement specimen characteristics

Since the data of three specimens are not clear and proper they were ignored while obtaining the stress-strain relationships. The stress-strain relationships of the five longitudinal reinforcement are given in Figure 3.18:

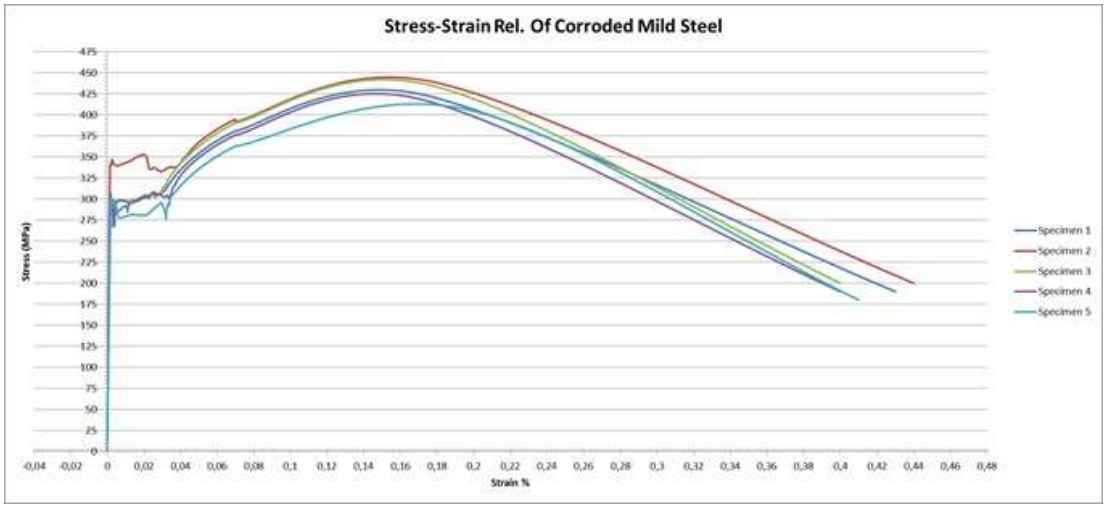

Figure 3.18: a)Stress-strain rel. of corroded mild steel

In order to check and control the accuracy stress strain relationship of average of five specimen and the proposal of Turkish Earthquake Code for stress strain relationship of S220 are included in the chart below (Figure 3.19).

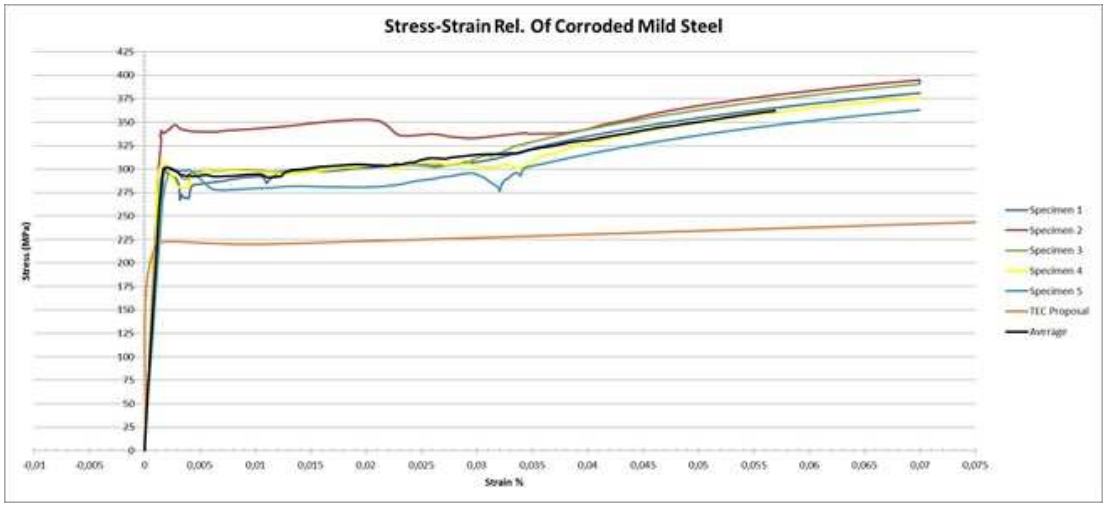

Figure 3.19: b)Stress-strain rel. of corroded mild steel

If we ignore also specimen number 2's data, since it is not that correlated with the other four specimens', we get the below graph (Figure 3.20) for the average of all specimens' stress-strain relationship.

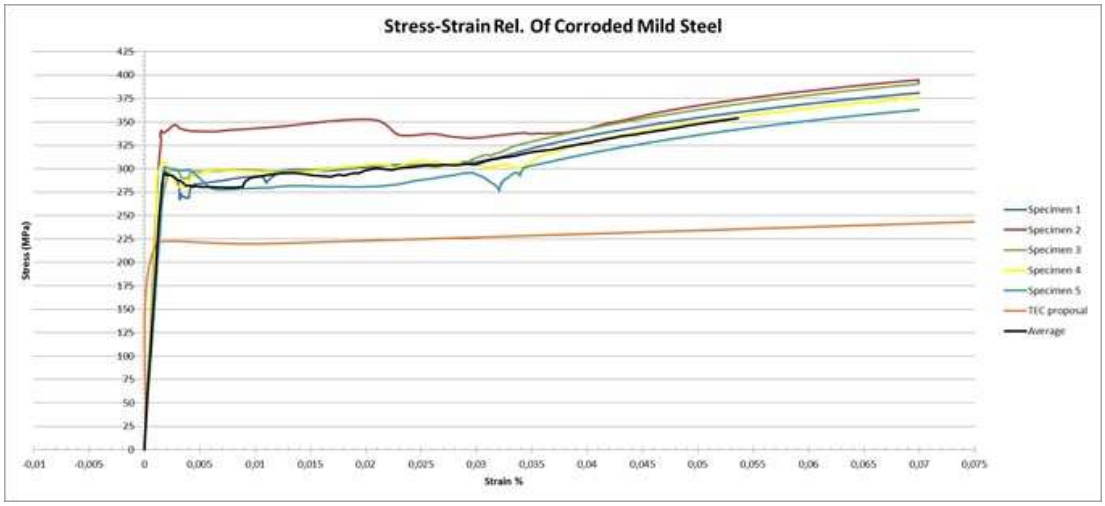

Figure 3.20: c)Stress-strain rel. of corroded mild steel

Evaluating specimen's test results the basic properties of steel reinforcement are as follows (Table 3.6):

Longitudinal Steel	**Transverse**
E_s=210000 MPA (modulus of elasticity of steel)	E_s=210000 MPA
f_{sy}=295 MPA (yield stress of steel)	f_{sy}=325 MPA
f_{su}=425 MPA	f_{su}=481 MPA
ε_{su}=0.16	ε_{su}=0.35

Table 3.6: Reinforcement properties

Chapter 4

EXPERIMENTAL RESULTS

4.1 Test Results of The Specimen

The largest target displacement value applied to specimen was 42 mm which corresponds to 4% drift for both pulling and pushing cycles. Base shear force-top displacement curve of the specimen under cyclic loading is presented in Figure 4.1. The ultimate strengths in pushing and pulling are 133.65 kN and 128.65 kN respectively, which obtained at 3% story drift. The data of envelope curve is calculated as the average of three cycle at each target displacement levels given in Figure 3.8. The envelope curve of base shear top displacement of the 15 years old specimen is given in Figure 4.2.

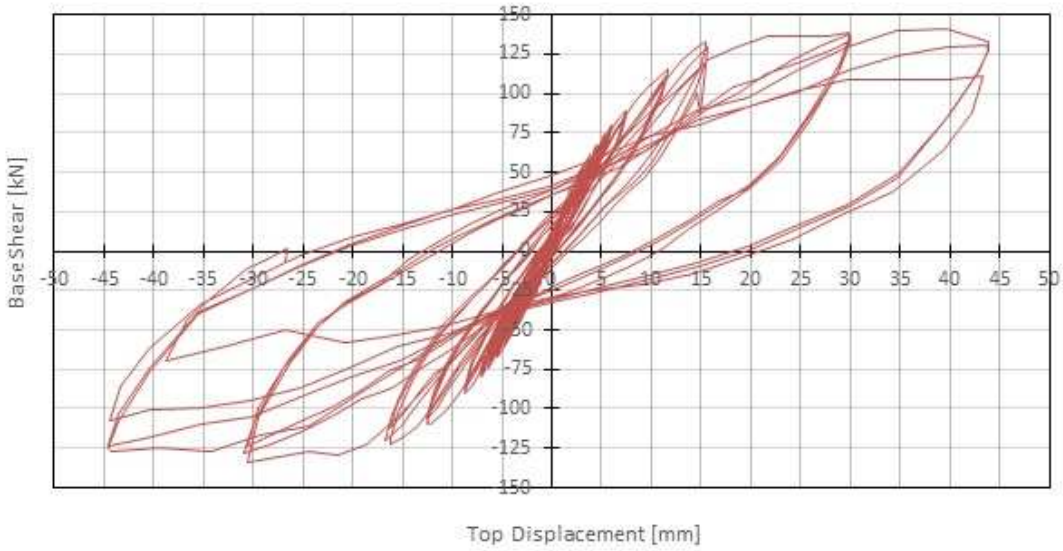

Figure 4.1: Base shear-top displacement curve of the 15 years old specimen

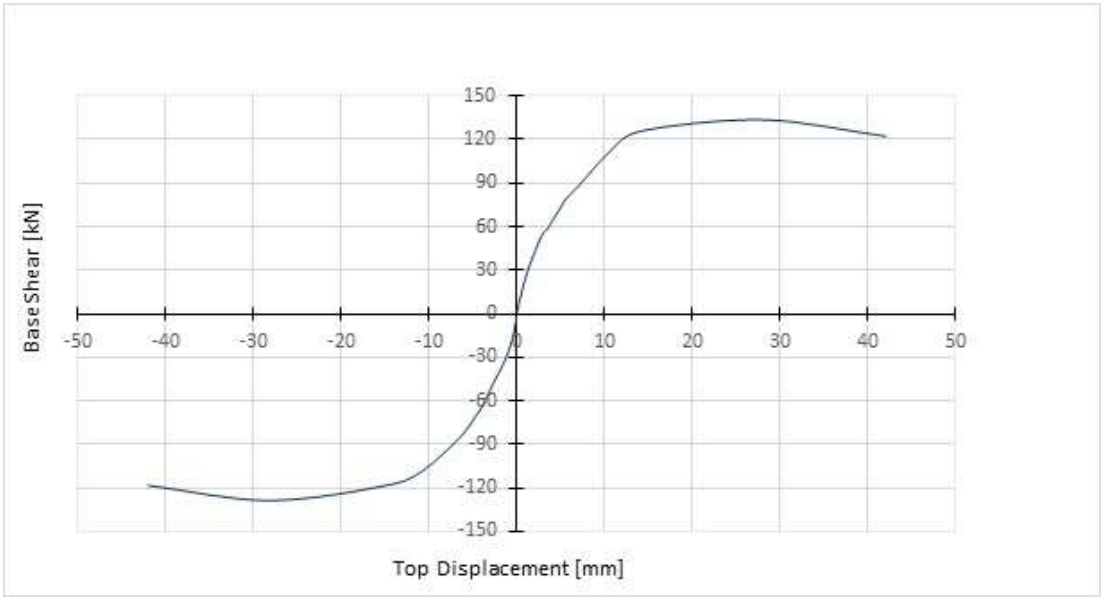

Figure 4.2: Envelop curve of the 15 years old specimen

Crack pattern on front view and back view of the specimen are given in Figure 4.3 and Figure 4.4 respectively. Cracks named A1, A2, A3 and A4 are the cracks that are observed before the experiment.

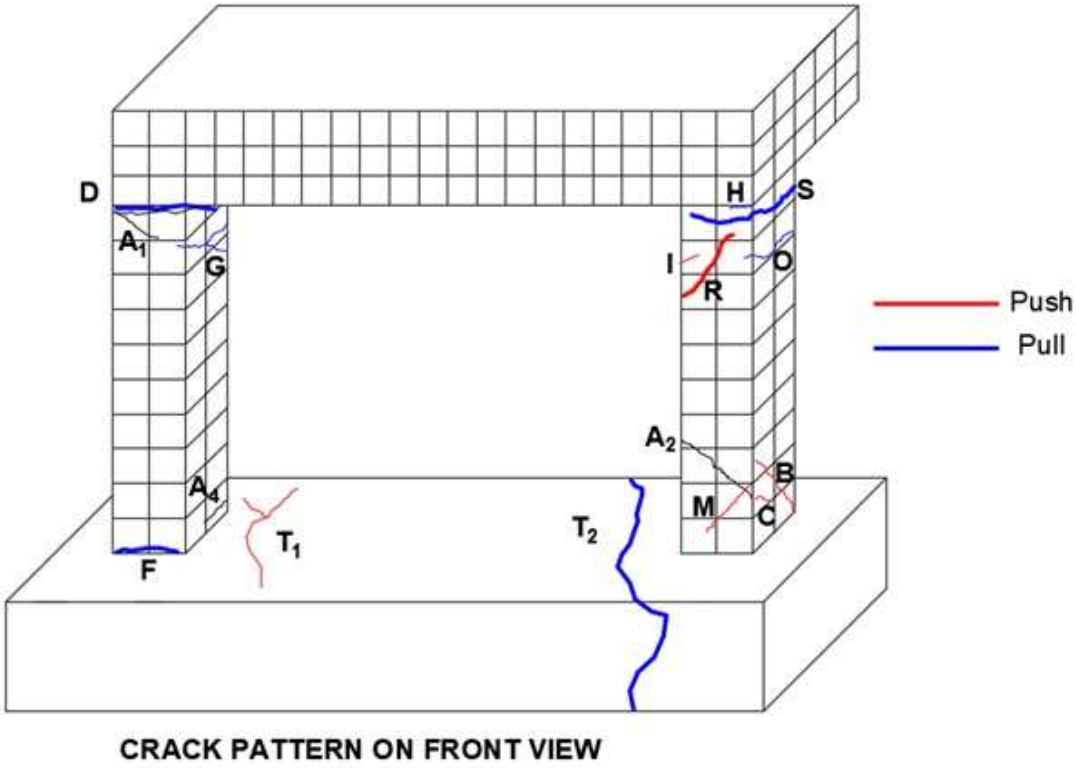

Figure 4.3: Crack pattern on front view of the specimen at the end of the experiment

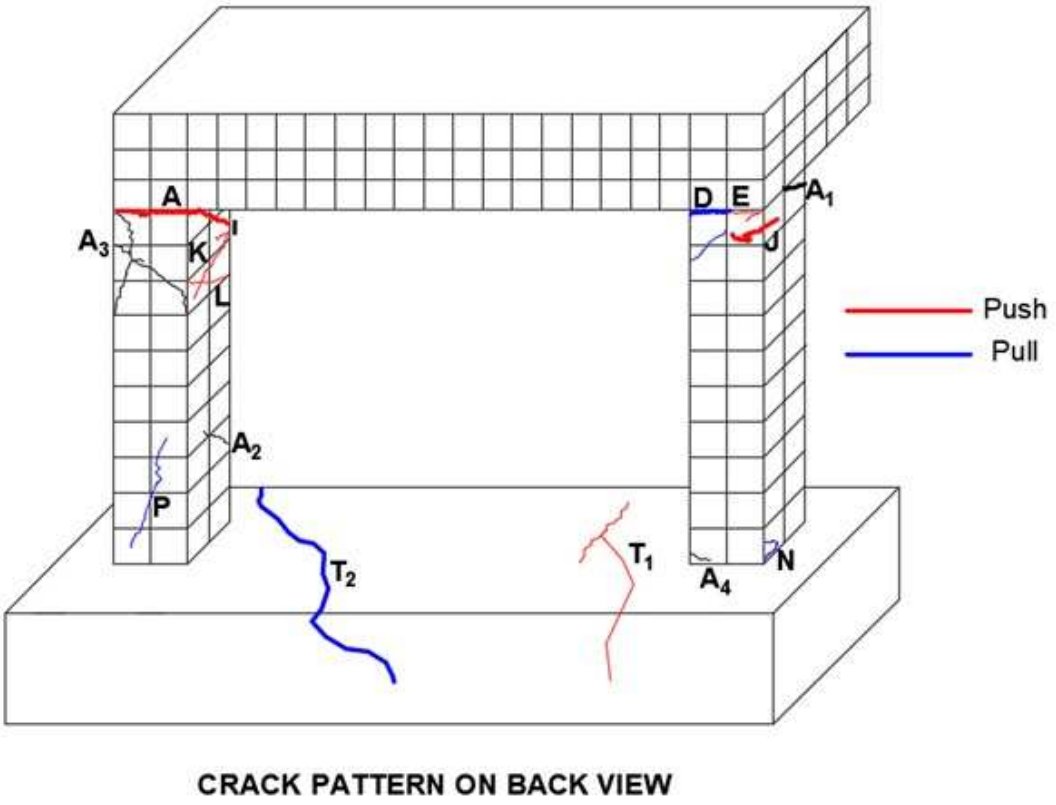

Figure 4.4: Crack pattern on back view of the specimen at the end of the experiment

Width of the cracks with respect to specific drift levels are listed below in Table 4.1.

Crack	**1% Drift**	**2% Drift**
A	1.2	-
B	0.6	0.4
C	0.3	0.2
D	1.1	-
E	0.4	0.9
F	0.8	1.2
G	0.7	0.7
H	0.7	0.7
I	0.3	0.3
J	0.4	1.6
K	0.2	0.2
L	0.1	0.2
M	0.3	0.4
N	0.1	0.1
O	0.1	0.1
P	0.1	0.7
R	-	0.1
S	-	1.7
T1	0.6	0.6
T2	1	1.2

Table 4.1: Crack width in mm for specific drift ratios

4.2 Comparison of the Test Results with Reference Specimen's Results

In this section, test results of reinforced concrete frame is evaluated. Failure modes, initial stiffness, cumulative energy dissipation, equivalent damping characteristics of the tested RC frame is discussed here. Besides, comparison of the test results with a reference frame's test results which was tested nine years ago

was done. This reference frame has same dimensions and cross sectional characteristics with the fifteen years old frame, the differences are compressive strength of concrete of the frames and the reinforcement characteristics due to slightly corroded reinforcement of fifteen years old frame. Compressive strength of concrete of the reference frame is 16 MPa. Reference frame is named as "specimen-R" (reference) and the fifteen years old frame is named as "specimen-A" (actual) while doing comparisons.

4.2.1 Failure Modes

Table 4.2 shows the summary of the hysteretic behavior of the specimen during the experiment. All the data are taken from experimental study. Due to the fact that specimen-A has low shear strength properties having mild steel and sea sand, bending and shear failures at column ends occurred in the frame as it can be seen in Figure 4.5. Last situation of the specimen-A is presented in Figure 4.6.

Drift Ratio (%)	δ **(mm)**	**P(kN)**	**Observations**
0.05	0.7	18.57 /21.3	First flexural crack at left beam column joint was observed.
0.1	1.4	32.46/-32.9	First shear crack at column-footing joint and flexural crack at right beam column joint were observed.
0.2	2.8	53.41/-49.45	Additional flexural crack at right beam column joint was observed.

Table 4.2 – *Continued on next page*

Table 4.2 – *Continued from previous page*

Drift Ratio (%)	δ **(mm)**	**P(kN)**	**Observations**
0.25	3.5	58.67/-58.66	Flexural cracks became wider and flexural crack at left column-footing joint was observed.
0.3	4.2	65.47/-66.49	Shear cracks at top end of left column and flexural crack at right beam column joint were observed.
0.35	4.9	72.47/-72.45	Flexural cracks became wider at left column-footing joint and left beam column joint.
0.4	5.6	79.15/-78.96	Shear crack at right column bottom end became longer.
0.5	7	87.86/-88.44	Flexural crack formed at right column top end. Cracks are formed at footing. Cracks observed before the experiment became longer and spalling of concrete at column-footing interface was observed.
1	10.5	111.11/-107.23	Flexural and shear cracks were formed.
2	14	125.68/-117.23	A long shear crack was formed at left column. Crushing and spalling of concrete at column bottom ends were observed.

Table 4.2 – *Continued on next page*

Table 4.2 – *Continued from previous page*

Drift Ratio (%)	δ **(mm)**	**P(kN)**	**Observations**
3	28	133.65/-128.65	Concrete cover spalled completely.
4	42	122.25/-118.27	Specimen underwent excessive lateral displacement out of its axis and experiment was ended.

TABLE 4.2: Summary of seismic behavior of specimen

Figure 4.5: Bending and shear failure at right column top end

Figure 4.6: Front view and back view of the specimen-A, respectively, at the end of the test

R-specimen which was tested in the same experimental procedure had 165 kN constant axial force. The largest displacement applied to R-specimen was also 42 mm in both pulling and pushing cycles.

The maximum strengths in pushing and pulling for the specimen-R are 133 kN and 123 kN respectively and for the specimen-A, strengths in pushing and pulling are 133.65 kN and 128.65 kN respectively. Comparison of base shear-top displacement curves of reference frame and actual frame is given in Figure 4.7.

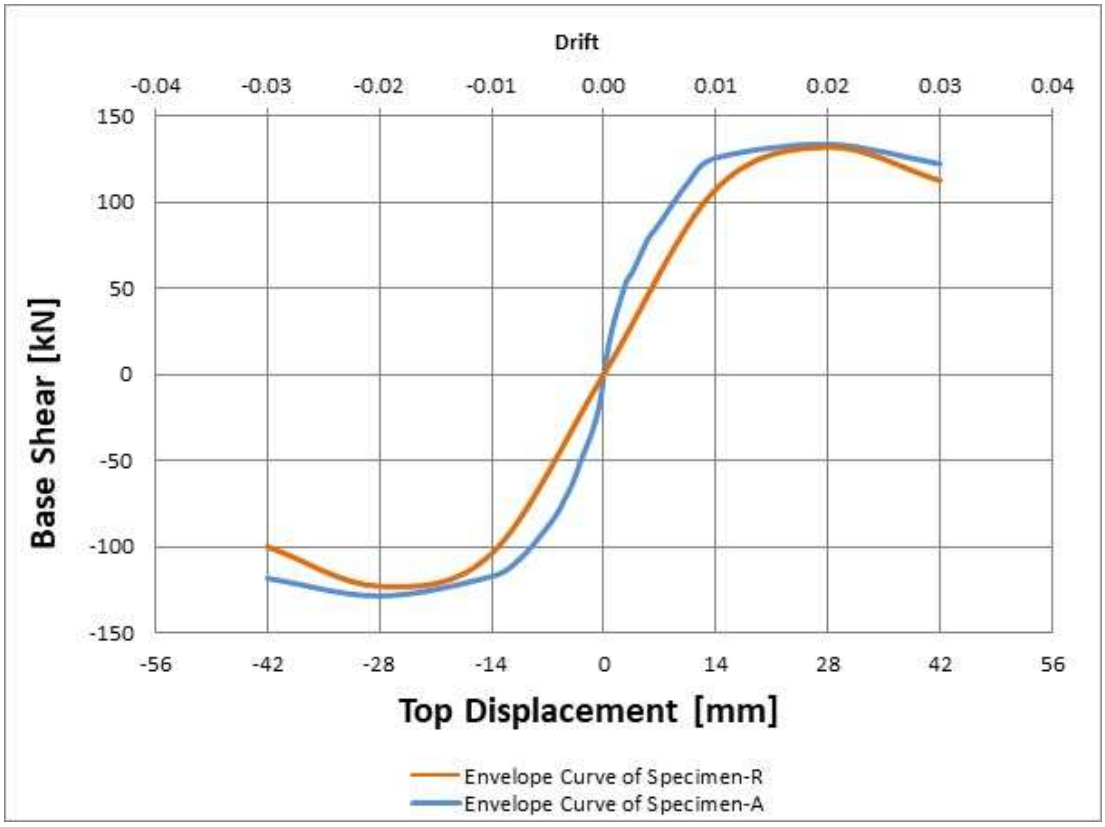

Figure 4.7: The comparison of envelope curves of specimen-A and specimen-R

The failure mode of reference specimen is similar to actual frame. Both tests ended with bending and shear failure at column ends. Figure 4.7 indicates that the strength of specimen-A is bigger than strength of the specimen-R.As it is given in PhD. Thesis of Teymur [38] crack patterns are also quite similar.

4.2.2 Cumulative Energy Dissipations

As it is presented in Figure 4.8, the cumulative energy dissipation of the specimen which is the frame tested recently is 2 times higher for 1% drift value than the frame which was tested fifteen years ago. Since Specimen-A has bigger lateral strength and deformation capacity, for 2% and 3% drift, it is almost 1.5 times and 2 times higher respectively.

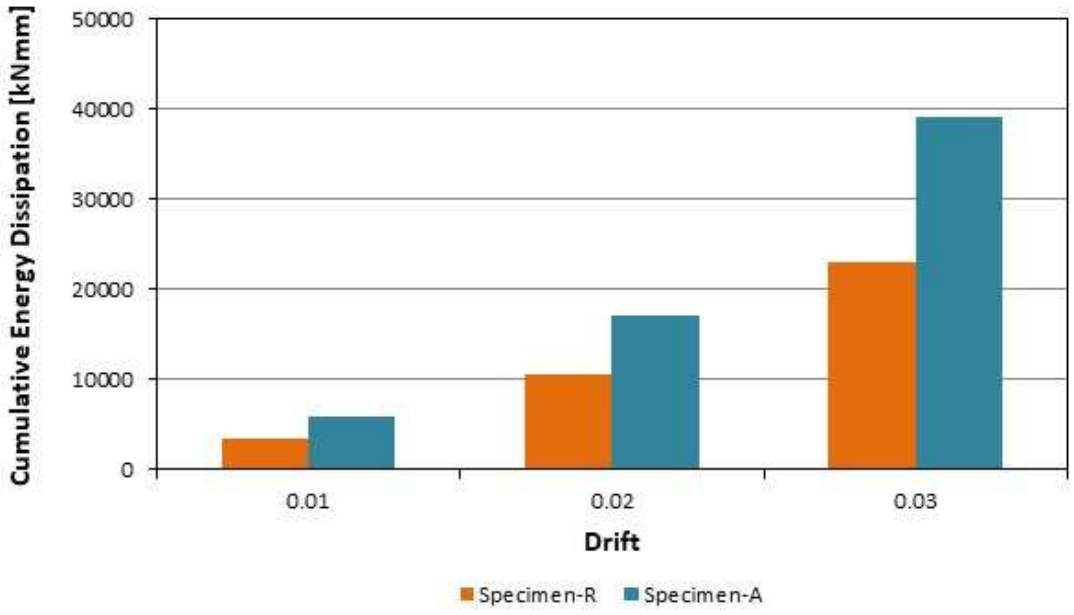

Figure 4.8: Cumulative energy dissipation capacities at specific story drifts

The comparison of the energy dissipation capacities of two frames is given in Figure 4.9 with another representation.

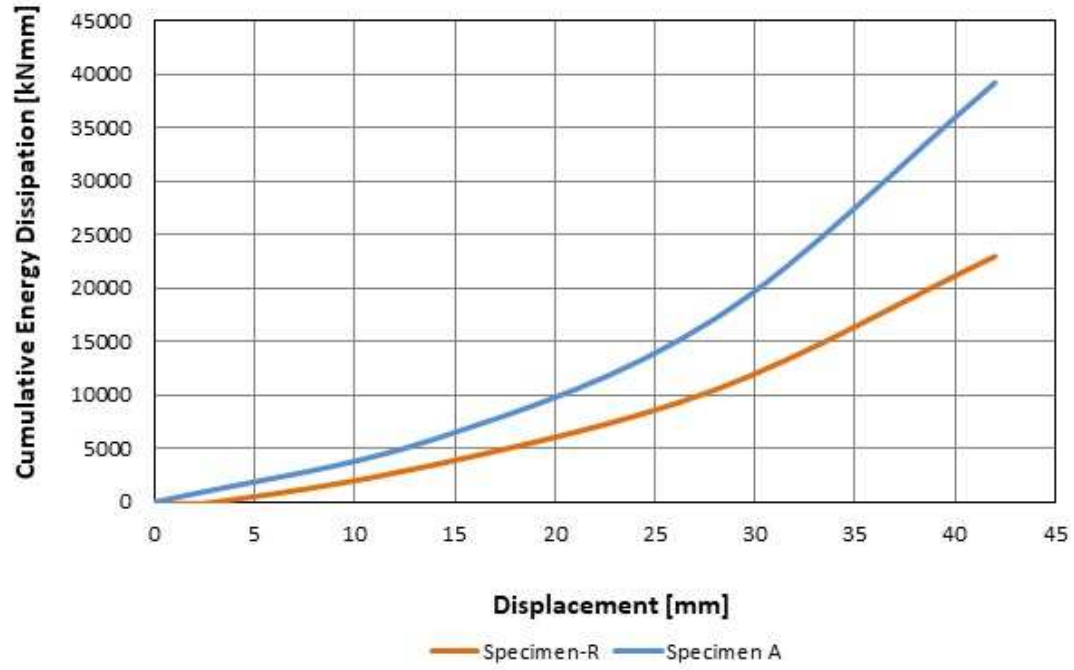

Figure 4.9: Comparison of cumulative energy dissipation capacities of specimen-A and specimen-R

4.2.3 Equivalent Damping Characteristics

In engineering practice, in addition to viscous damping also known as elastic damping model, hysteretic damping model also is utilized to characterize damped dynamic properties of the structures. Viscous damping of a RC structure which is related to critical damping is taken 5% as current TEC [39]suggested and the hysteretic damping which corresponds to the dissipation due to the non-linear (hysteretic) behavior. It is calculated through the hysteresis lateral load-top displacement curves for the specimen. The formula for equivalent damping ratio which is the sum of viscous and hysteretic damping ratios as Priestley at al [40]2007 suggested is given in following equation (4.1):

$$\zeta_{eq} = 0.05 + \zeta_{hysteretic} = 0.05 + (\frac{W_D}{4\pi W_S}) \tag{4.1}$$

As it was mentioned above 0.05 shows viscous damping ratio. W_D and W_S are points out the energy dissipation in one complete cycle which is corresponding a specific displacement level given in Figure 4.10.

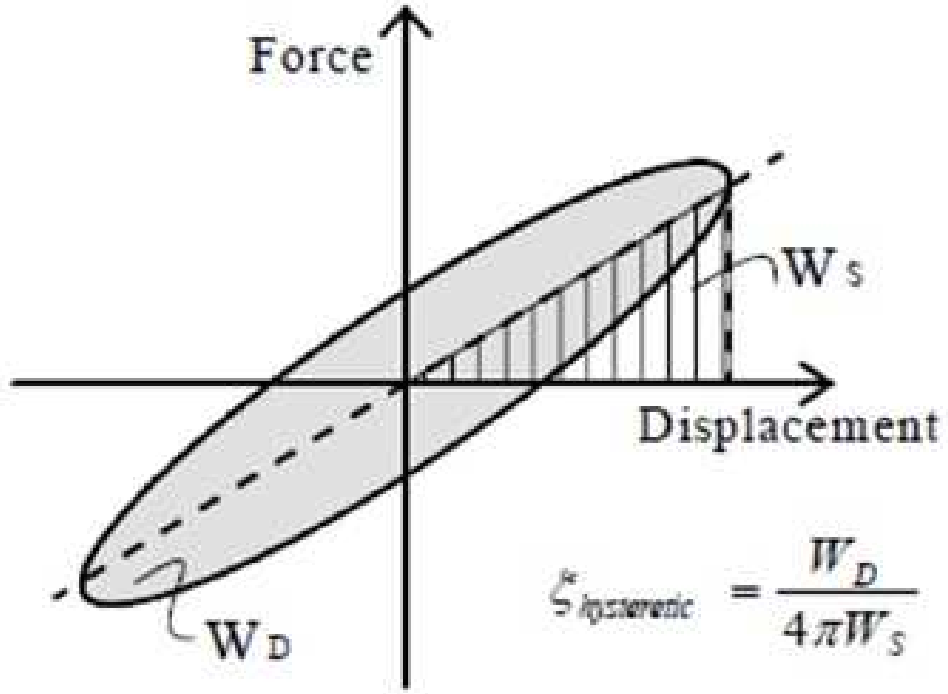

Figure 4.10: Dissipated energy

Comparison of equivalent damping ratios of Specimen-A and Specimen-R is given in Figure 4.11.

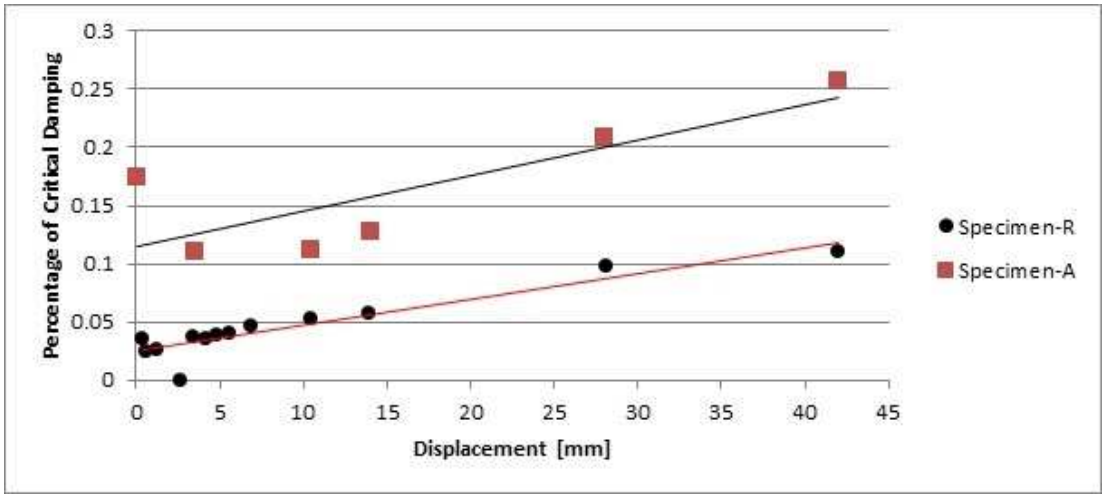

Figure 4.11: Equivalent damping ratios

As it can be seen from Figure 4.11, since the lateral strength and deformation capacity of specimen recently tested is higher than the reference specimen, damping ratio of the Specimen-A is bigger than damping ratio of Specimen-R. In other words, energy dissipation of Specimen-A is greater than energy dissipation of Specimen-R. Besides, as it was pointed out in "PhD thesis of Teymur [38]", damping ratio can be taken as higher than 5% of critical damping as it is suggested by current codes.

4.2.4 Initial Stiffness and Lateral Stiffness

The slope of the line, joining the points of the maximum loads in pull and push cycles which occurred during initial stages of cyclic loading is calculated as the initial stiffness values of the specimens. Initial stiffnesses of the Specimen-A and Specimen-R are given in Table 4.3.

Specimen	**Initial Stiffness**
Specimen-R	22 kN/mm
Specimen-A	28.44 kN/mm

Table 4.3: Initial stiffnesses of the Specimens

As it is seen in Table 4.3, initial stiffness of specimen tested recently 1.3 times higher than the specimen which was tested 9 years ago which means Specimen-A shows more rigid behavior at the initial stages.

The comparison of the lateral stiffness of specimens according to drift ratios are given in Figure 4.12.

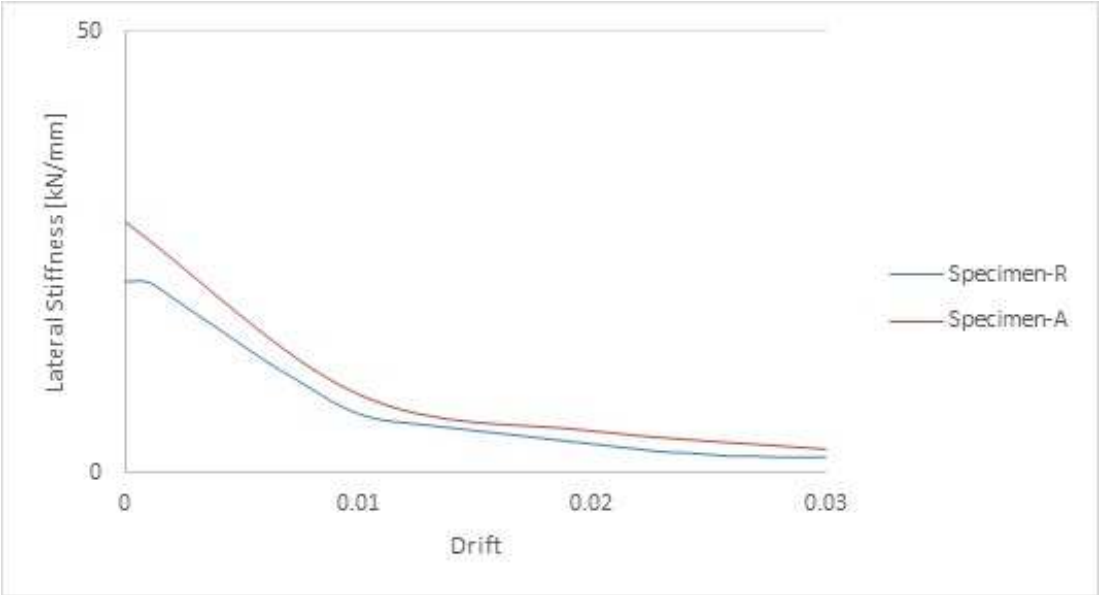

Figure 4.12: Comparison of the lateral stiffness of specimens

As it can be seen from Figure 4.12 after %1 drift ratio, the lateral stiffness almost the same for the specimens.

Chapter 5

ANALYTICAL STUDIES USING THE FINITE ELEMENT METHOD

There are several programs to analyze responses of a structure under static and dynamic loading considering nonlinear analysis. SeismoStruct, SAP2000, ABAQUS, PERFORM-3D are some of these programs. In this study, Seismostruct and SAP2000 are used to analyze nonlinear behavior of single story, single bay existing RC frame and to compare the analytical results with experimental results. For this purpose ;

- **Static Pushover Analysis**
- **Static Time-History Analysis**

techniques were used.

To define the nonlinear behavior of each element;

- **Concentrated**
- **Distributed**

approaches were used.

5.1 Nonlinear Static Analysis Using SeismoStruct

5.1.1 Element Description Of SeismoStruct

SeismoStruct is a finite element program that considers both geometric nonlinearities and material inelasticity, enables prediction of the large displacement behavior of structures under static or dynamic loading. Nonlinear analysis can be done by two formulations: Force based and displacement based. In this study beam and columns are represented as inelastic displacement-based frame element. Fibre modeling approach is adopted in SeismoStruct, separating beam column elements into 200-400 fibers so that material inelasticity is considered to spread along the structural member length and over the cross section, therefore, more accurate evaluation of analysis can be done. There is no need to define moment curvature relationships and cyclic behavior of elements in SeismoStruct, because they are defined by material models that are given Figure 5.1.

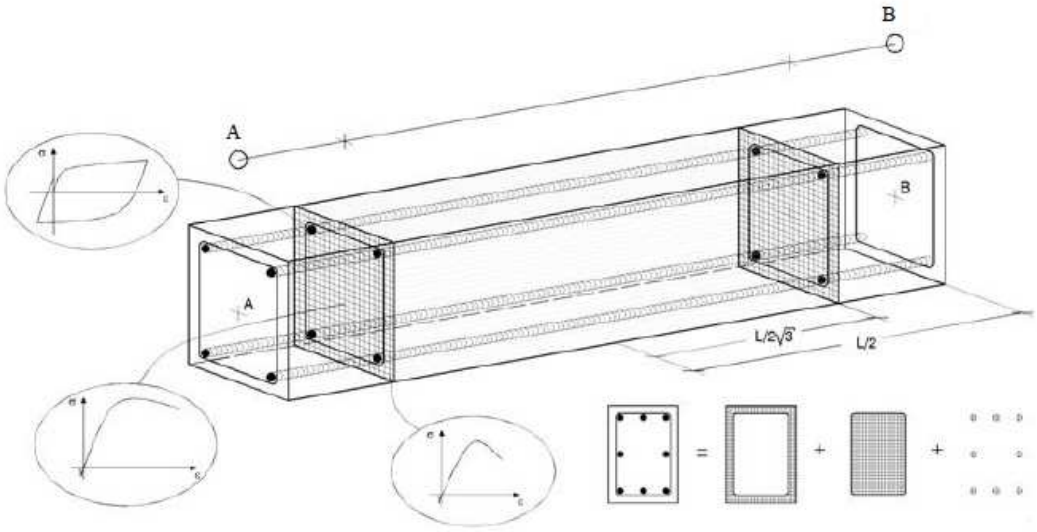

Figure 5.1: Element sections and section fibres

5.1.2 General Description of Structure

One story, one bay existing frame's beam column elements are defined as inelastic displacement-based frame element. Section characteristics, restraints support conditions are introduced in SeismoStruct. Parameters that are introduced in material model are taken from material tests for concrete and reinforcement.

Modulus of elasticity, strain hardening parameter, yield strength for longitudinal bars are taken from material tests result and given in Table 3.6. Other parameters such as transition curve shape calibrating factor, kinematic weighing coefficient etc. are taken as default values of program.

Nonlinear constant confinement concrete model was used for concrete model. In this model confinement effect of transverse reinforcement provided by the rules proposed by Mander et al. (1988) and automatically calculated by the program after giving the program information of lateral reinforcement. Since there are more than one compressive strengths and elasticity modulus for concrete for a better analysis, compressive strength and corresponding elasticity modulus values which are given in Table 3.3 were used. Strain at peak stress was taken from the stress strain relationship graph of concrete as 0.0025; tensile strength was taken as 0.

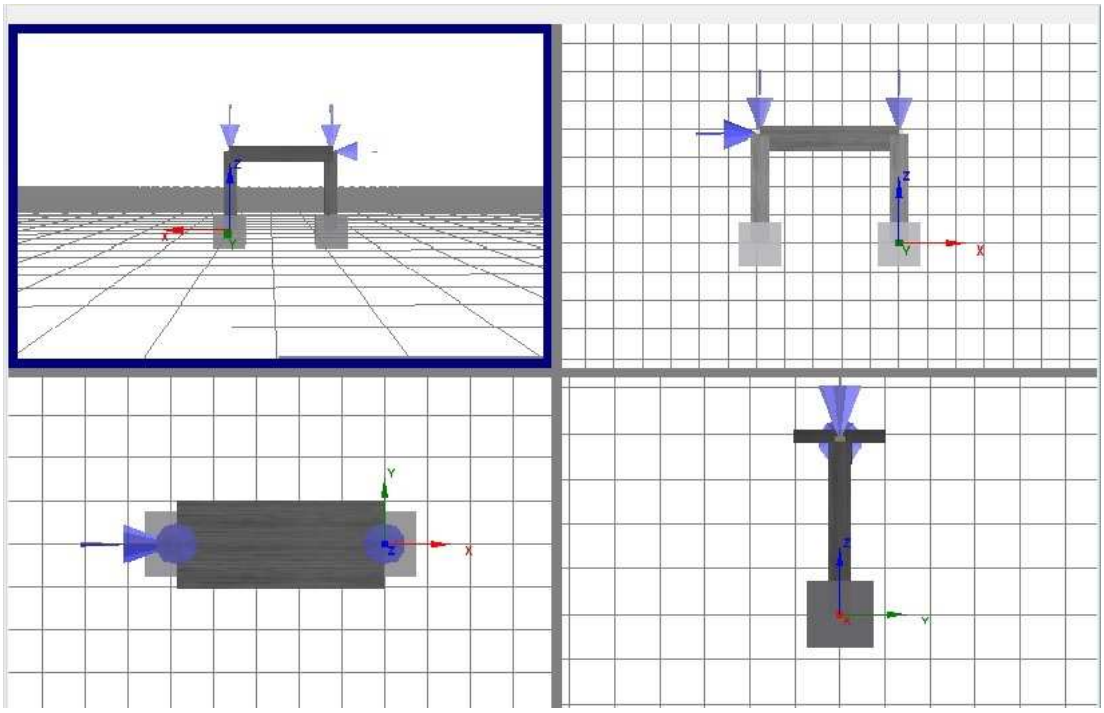

Figure 5.2: View of the frame in SeismoStruct

Same amount of axial force with the experimental axial force value which is 167.5 kN was also applied as the node load. Finally, displacement protocol implemented in the experiment which is shown in Figure 5.3, was applied to the structure given above then static time- history analysis and pushover analysis was done for different compressive strengths and corresponding elasticity modulus of concrete.

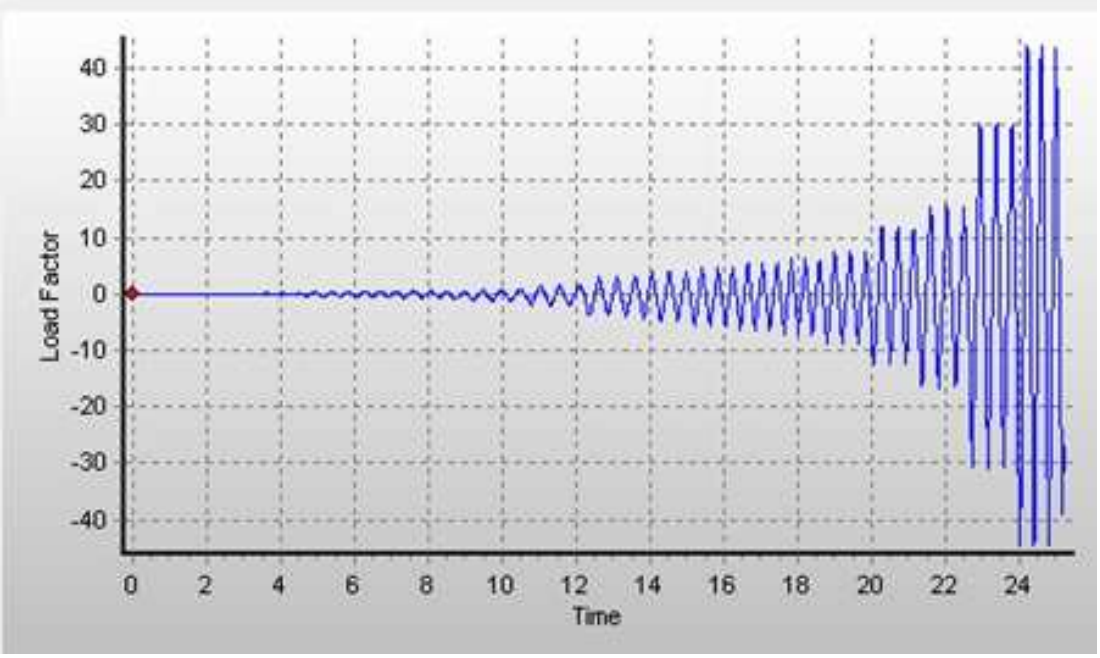

Figure 5.3: Displacement protocol

5.1.3 Analytical Results

The largest displacement applied to specimen was 42 *mm* which corresponds to 4% drift for both pulling and pushing cycles. Graphs (Figures 5.4 and 5.5)presented below are envelops of hysteretic curves for different obtained value of compressive strength of concrete. Elasticity modulus' for each compressive strength value was found according to TS500 proposal and given in Table 3.3.

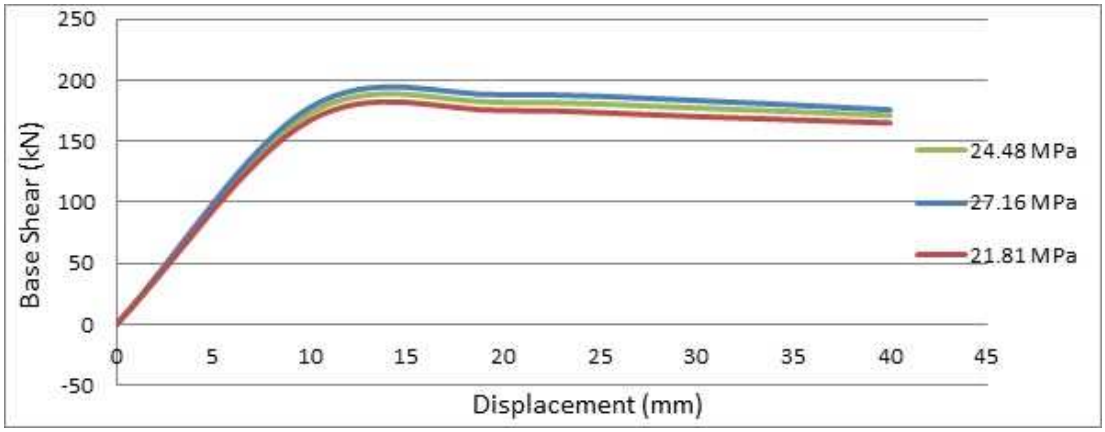

Figure 5.4: Envelope curves for different compressive strength of concrete

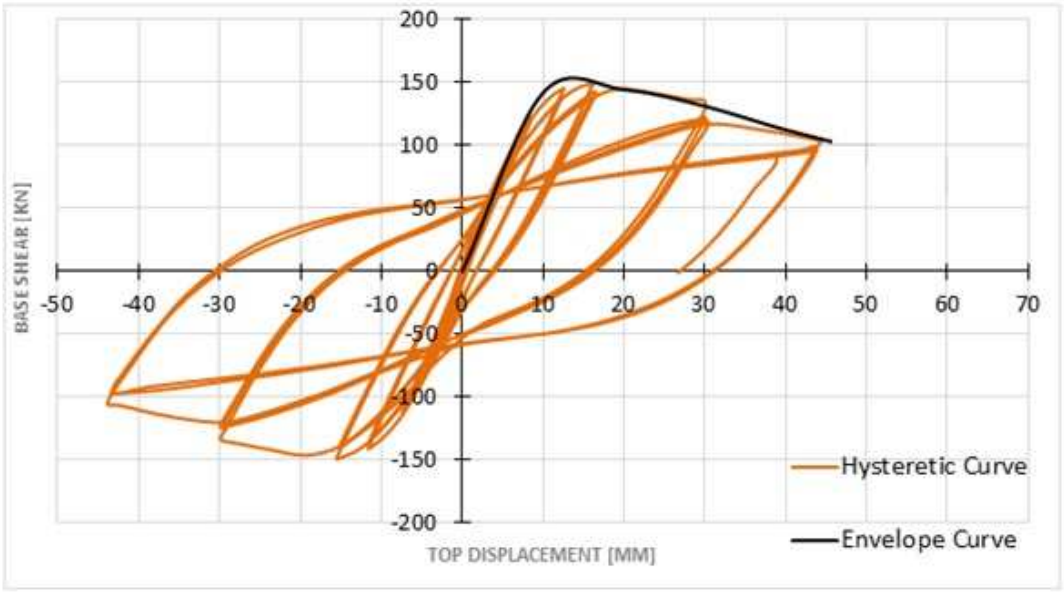

Figure 5.5: Hysteretic and envelope curve for compressive strength of 21.81MPa with different modulus of elasticity of concrete

The Figure 5.5 presented above shows the analytical envelope (capacity) curve and hysteresis loops of the specimen which has the modulus of elasticity of 12500 MPa that is taken from the slope of stress-strain curve.

When the nonlinear cyclic analysis is done, SeismoStruct creates a report about damage states of the members. To represent these damage states for the cyclic loading, strain limits were used according to TEC2007 [41]. Figure 5.7 shows the strain limits to obtain damage states of the frame members according to TEC2007 [41]. Figure 5.6 shows how the frame is divided into smaller elements and how these elements are named as numbers to define damage levels separately.

Figure 5.6: Definition of the frame elements in theoretical model used in SeismoStruct

Damage States in Structural Members	Strain Limit	Place of Deformation
Minimum Damage Limit (MNc)	<- 0.0035	The outer-most fibre of the concrete of the section
Minimum Damage Limit (MNs)	> 0.01	Longitudinal reinforcement
Safety Limit (GVc)	< -0.0085	The outer fibre of the concrete within the transversal reinforcement
Safety Limit (GVs)	> 0.040	Longitudinal reinforcement
Collapse Limit (GCc)	< -0.011	The outer fibre of the concrete within the transversal reinforcement
Collapse Limit (GCs)	> 0.060	Longitudinal reinforcement

c = concrete, s = steel,

compression (-), tension (+) in strain limits

Figure 5.7: Strain limits of the frame members according to TEC2007 [41]

Target Displacement [mm]	**Performance Level**	**Element Name**	**Damage Type**	**Strain**	**Place of Damage**
At the end of the 1st cycle of + 5.6	yield	8	Reinf. Steel	0.00201742	Bottom End
At the end of the 2nd cycle of + 5.6	yield	4	Reinf. Steel	0.00213056	Bottom End
At the end of the 2nd cycle of +7.0	yield	8	Reinf. Steel	0.00200903	Top End
At the end of the 3rd cycle of +7.0	yield	5	Reinf. Steel	0.00221618	Top End
At the end of the 3rd cycle of -7.0	yield	4	Reinf. Steel	0.00222543	Top End
At the end of 1st cycle of +10.5	yield	5	Reinf. Steel	0.00220639	Bottom End
At the end of 1st cycle of +10.5	yield	1	Reinf. Steel	0.00241737	Top End
At the end of 1st cycle of +10.5	MNc	4	Concrete	-0.0036997	Bottom End
At the end of 1st cycle of +10.5	MNc	1	Concrete	-0.00357603	Top End
At the end of 1st cycle of -10.5	yield	1	Reinf. Steel	0.00200505	Bottom End
At the end of 1st cycle of -10.5	MNc	8	Concrete	-0.0038018	Bottom End
At the end of 1st cycle of -14	MNc	5	Concrete	-0.00380482	Top End
At the end of 1st cycle of +28	MNs	8	Reinf. Steel	0.01150613	Bottom End
At the end of 1st cycle of +28	MNs	8	Reinf. Steel	0.01024367	Top End
At the end of 1st cycle of +28	MNs	4	Reinf. Steel	0.01012888	Bottom End
At the end of 1st cycle of +28	GVc	4	Concrete	-0.01023191	Bottom End

Table 5.1 – *Continued on next page*

Table 5.1 – *Continued from previous page*

Target Displacement [mm]	**Performance Level**	**Element Name**	**Damage Type**	**Strain**	**Place of Damage**
At the end of 1st cycle of +28	GVc	1	Concrete	-0.01006005	Top End
At the end of 1st cycle of +28	**GCc**	**4**	**Concrete**	**-0.01318339**	**Bottom End**
At the end of 1st cycle of +28	MNs	5	Reinf. Steel	0.01013222	Top End
At the end of 1st cycle of +28	**GCc**	**1**	**Concrete**	**-0.01120771**	**Top End**
At the end of 1st cycle of -28	GVc	8	Concrete	-0.01027092	Bottom End
At the end of 1st cycle of -28	MNs	4	Reinf. Steel	0.01039486	Top End
At the end of 1st cycle of -28	**GCc**	**8**	**Concrete**	**-0.01322497**	**Bottom End**
At the end of 1st cycle of -28	GVc	5	Concrete	-0.01016471	Top End
At the end of 1st cycle of -28	**GCc**	**5**	**Concrete**	**-0.01113287**	**Top End**
At the end of 1st cycle of -28	MNs	1	Reinf. Steel	0.01010087	Top End
At the end of 1st cycle of +42	MNs	5	Reinf. Steel	0.0117563	Bottom End
At the end of 1st cycle of -42	MNs	1	Reinf. Steel	0.01130615	Bottom End
At the end of 1st cycle of -42	MNc	4	Concrete	-0.03495403	Top End
At the end of 1st cycle of -42	GVc	4	Concrete	-0.03495403	Top End
At the end of 1st cycle of -42	GCc	4	Concrete	-0.03495403	Top End

TABLE 5.1: Damage levels for the specimen

Damage levels during the cyclic loading presented in Figure 5.5, are given in Table

5.1according to strain limits and damage places. Figure 5.8 shows the situation of the frame at the end of the loading history. The collapse limit is reached at the bottom end of the columns and top end of the right column and analysis is stopped by the program.

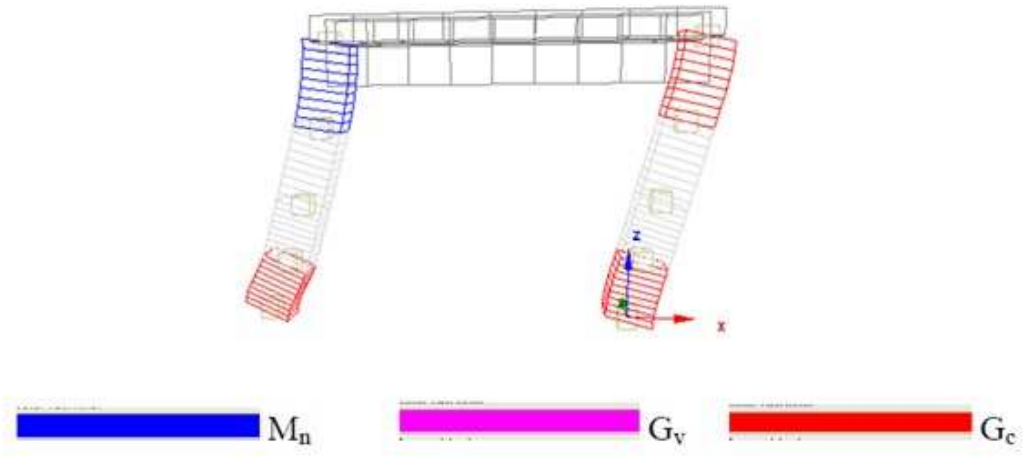

Figure 5.8: Strain limits of the frame members according to TEC 2007 [41]

5.2 Nonlinear Pushover Analysis Using SAP2000

Pushover analysis is a static nonlinear technique to estimate seismic responses and deformations of a structure and also provides an important comprehension of the weak links in seismic performance of a structure. This analysis involves incrementing the magnitude of loading in the horizontal direction of the structure according to a predefined pattern. Therefore, pushing the structure in a certain direction until it reaches collapse state; SAP2000 gives applied displacement and corresponding base shear force at each increment. Besides, since the program assumes that the plastic deformations are concentrated at some certain weak points, it allows users to obtain plastic hinge formations and failure of various structural components.

5.2.1 General Description of the Structure on SAP2000

Beam and column elements of the frame modeled as nonlinear elements with concentrated plasticity by defining plastic hinges at both ends of each element. Frame sections, confinement properties and load cases are defined in accordance with the existing frame as it was analyzed in Seismostruct. Support condition was defined as fixed support at both column ends. Basic material properties of concrete and reinforcing bars were defined again by using the experimental analysis results and given in following Table 5.2.

Longitudinal Steel	**Transverse**	**Concrete**
E_s=210000 MPA (modulus of elasticity of steel)	E_s=210000 MPA	E_c=12500 MPA
f_{sy}=295 MPA (yield stress of steel)	f_{sy}=325 MPA	-
f_{su}=425 MPA	f_{su}=481 MPA	f_c=21.81 MPA
ε_{su}=0.16	ε_{su}=0.35	ε_{cu}=0.0058

Table 5.2: Material properties of 15 years old frame

Beam column joints of the frame is introduced as rigid beam connections due to the fact that the bending rigidity of this part is considerably high.

5.2.1.1 Moment Curvature Relationship of Frame Sections

In order to be able to determine the behavior of a RC structure, its cross sectional behavior should be determined well. Because of the fact that nonlinear properties are defined according to the cross sectional behavior of RC members, the moment-curvature relationship of each member was used to model plastic hinge behavior of reinforced concrete members under flexure. All the cross section and reinforcement details given in Chapter 3 and material properties are

given in Table 5.2 were used to obtained moment-curvature curve of each frame element. Axial force is also considered for columns' moment curvature analysis only. Since columns have two different cross sectional property due to the number and place of longitudinal reinforcing bars at each end, two different moment curvature relationships were obtain for columns. Moment curvature relationship for each member were obtained by XTRACT which is a moment curvature analysis program.

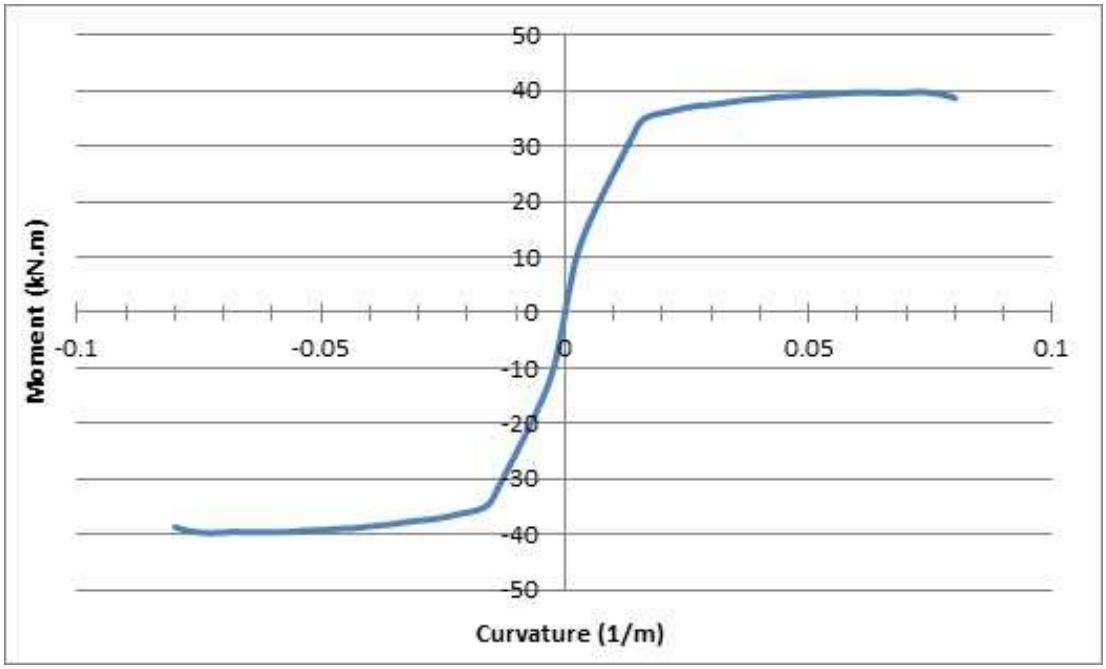

Figure 5.9: Moment-curvature relationship for bottom section of column

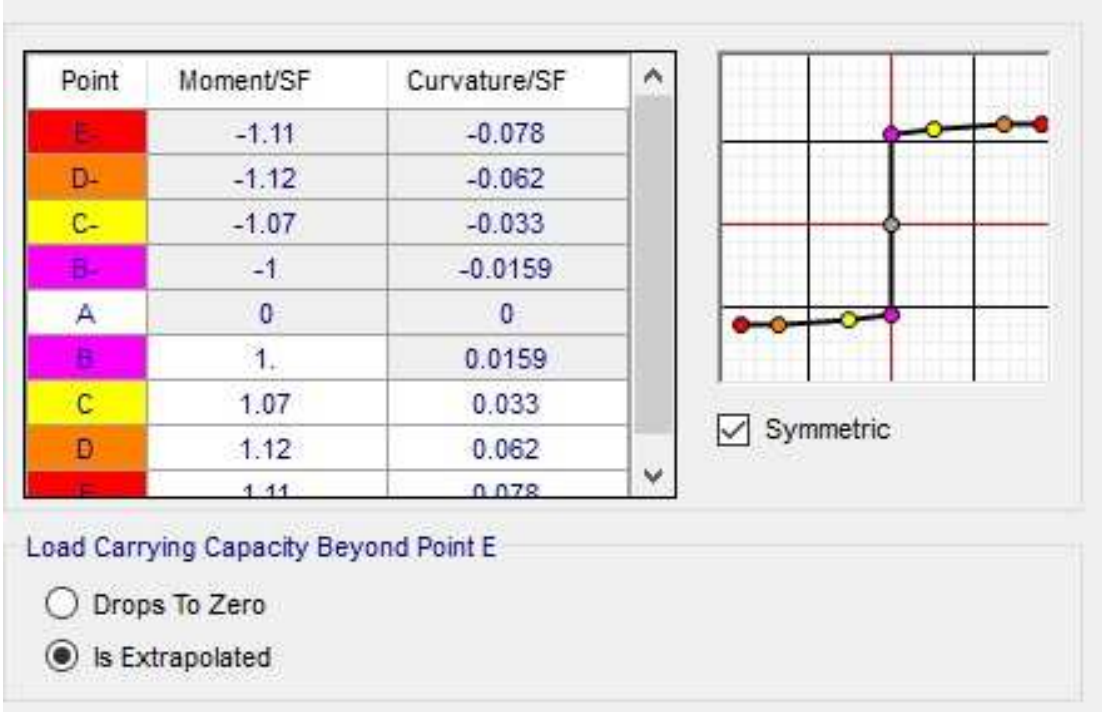

Figure 5.10: Moment-curvature relationship for bottom section of column in SAP2000

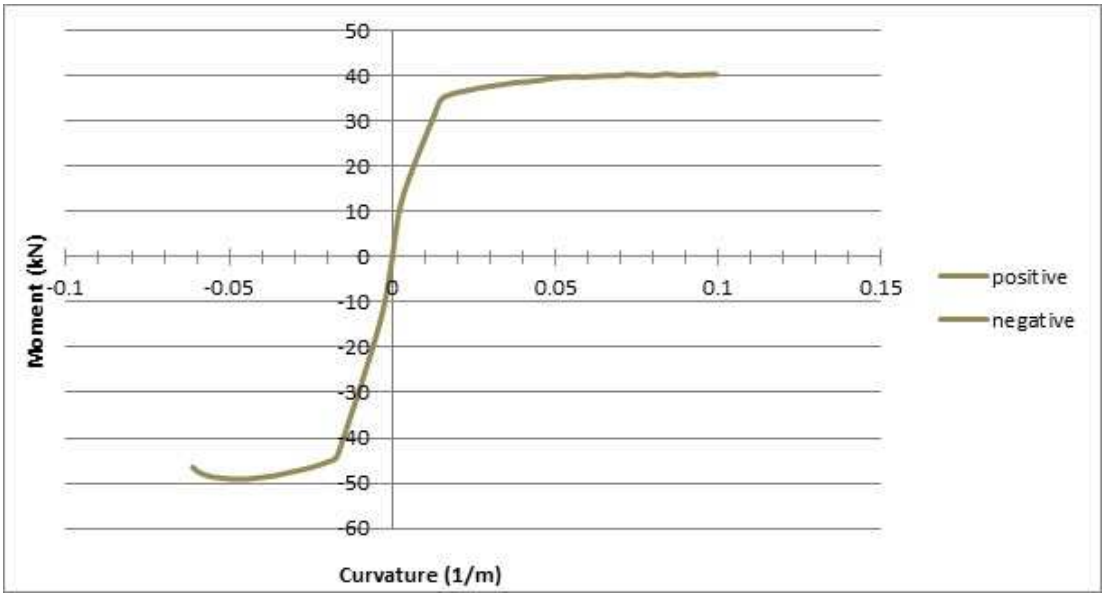

Figure 5.11: Moment curvature relationship of top section of column

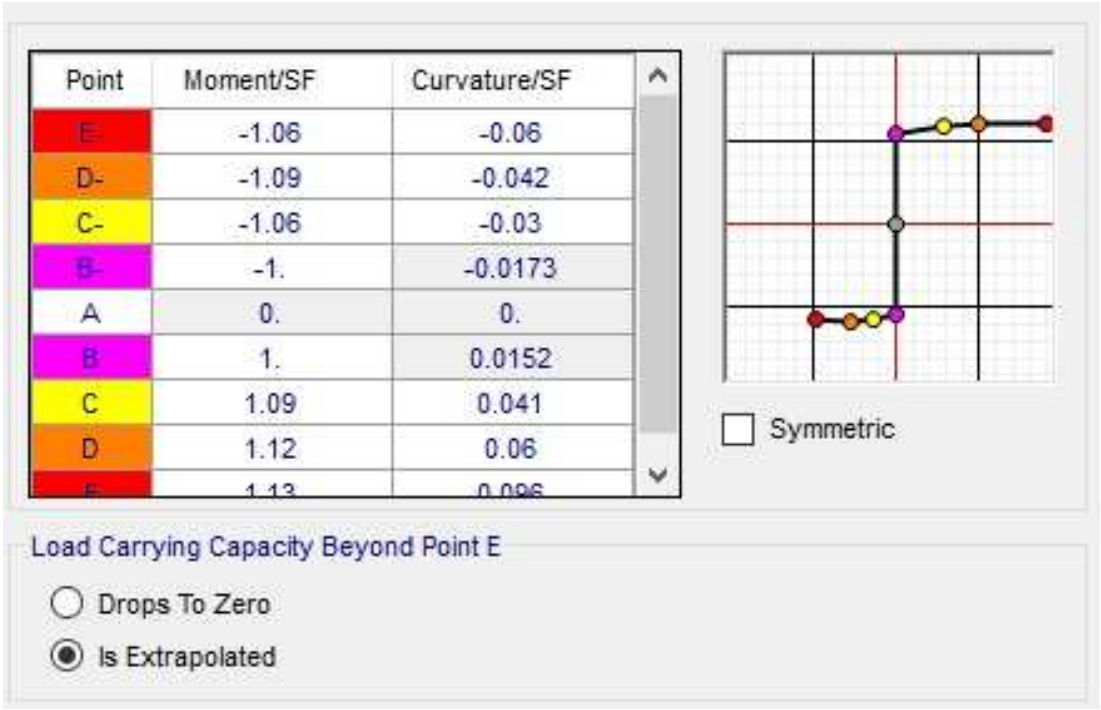

Figure 5.12: Moment curvature relationship of top section of column in SAP2000

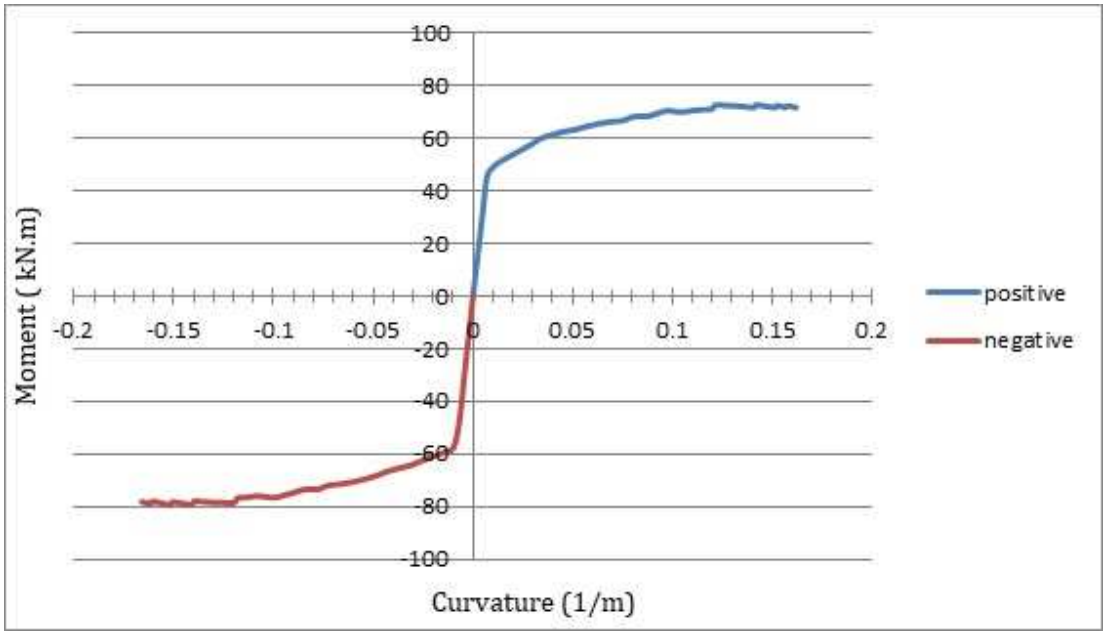

Figure 5.13: Moment-curvature relationship for both end section of beam element

These moment curvature relationships were used to define plastic hinge properties of each element on SAP2000. Plastic hinge length is assumed to be h/2 as proposed by TEC2016 [39], where h indicates the effective depth of cross section

of column in bending. SAP2000 implements plastic hinge properties described in FEMA-356 (or ATC-40). As shown in below figure a five points labeled as A, B, C, D, and E define the force-deformation behavior of a plastic hinge.

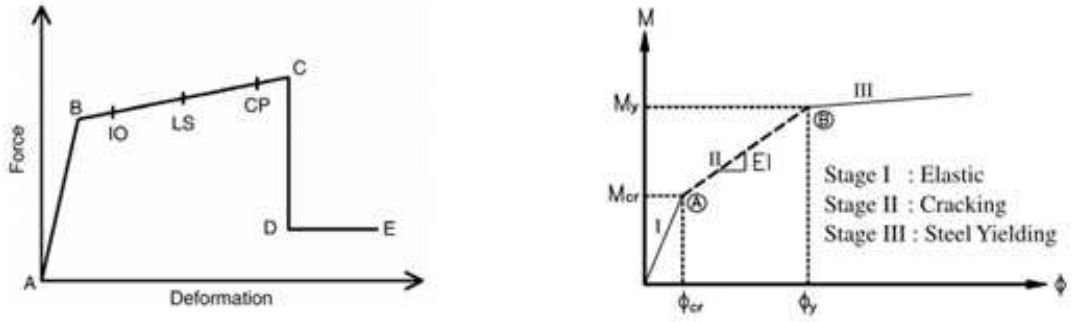

Figure 5.14: a)Force-deformation relationship of a typical plastic hinge. b)Idealized moment curvature relationship

IO, LS and CP points stand for Immediate Occupancy, Life Safety and Collapse Prevention respectively and these points were assumed as 10 %,50 % and 80% of plastic hinge deformation capacity, respectively. As it is stated in TEC2016 [39] part 15.4.11, for elements that are subjected to bending, effective bending rigidity is taken as the bending rigidity of cracked section. As it is proposed in TEC2016 [39], moment-curvature relationships of sections were utilized to determine $EI_{cracked}$ of each section by obtaining the tangent of the later defined line from zero point to the yielding point of the curve. Effective bending rigidities are given in following table, since beams was not damaged during the experimental analysis, bending rigidity for beam is taken as the initial bending rigidity.

Right Top Section of Column	EI_c=2500 $kN.m^2$	$0.76EI_0$
Left Top Section of Column	EI_c=1888.88 $kN.m^2$	$0.58EI_0$
Bottom Section of Column	EI_c=2333.33 $kN.m^2$	$0.71EI_0$

Table 5.3: Effective bending rigidities of frame elements

5.2.1.2 Pushover Analysis Results

After defining sections, materials and plastic hinges pushover analysis was done by displacement control defining a small lateral displacement at beam column joint as it can be seen in Figure **??** and frame was pushed till it reached target displacement.

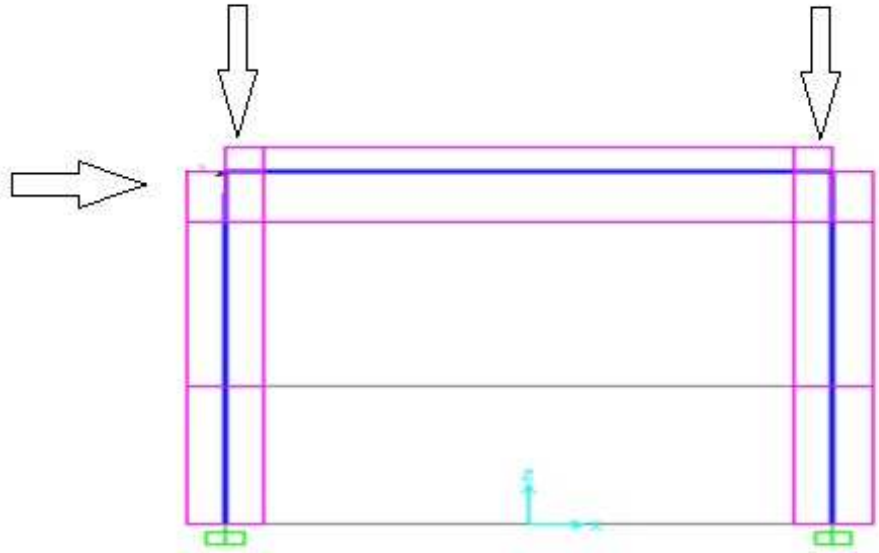

Figure 5.15: Frame model in Sap2000

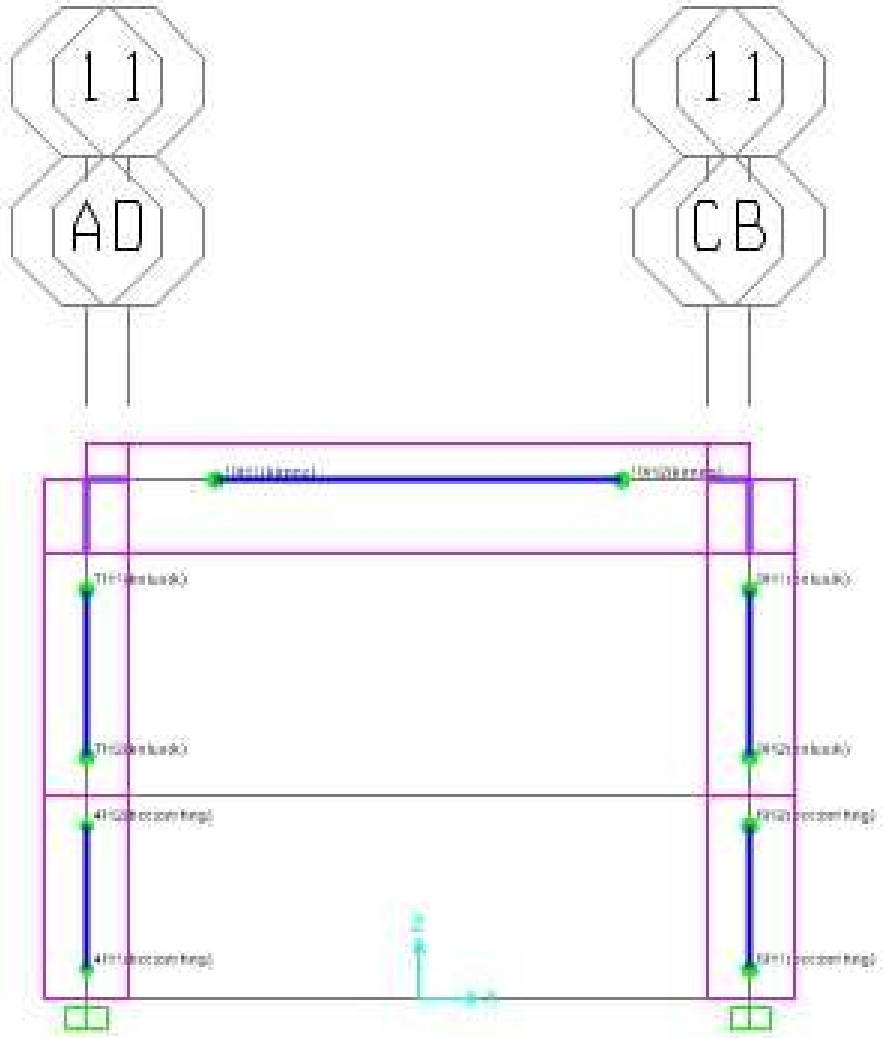

Figure 5.16: Definition of hinges in SAP2000

Static pushover curve is given in below (Figure 5.17):

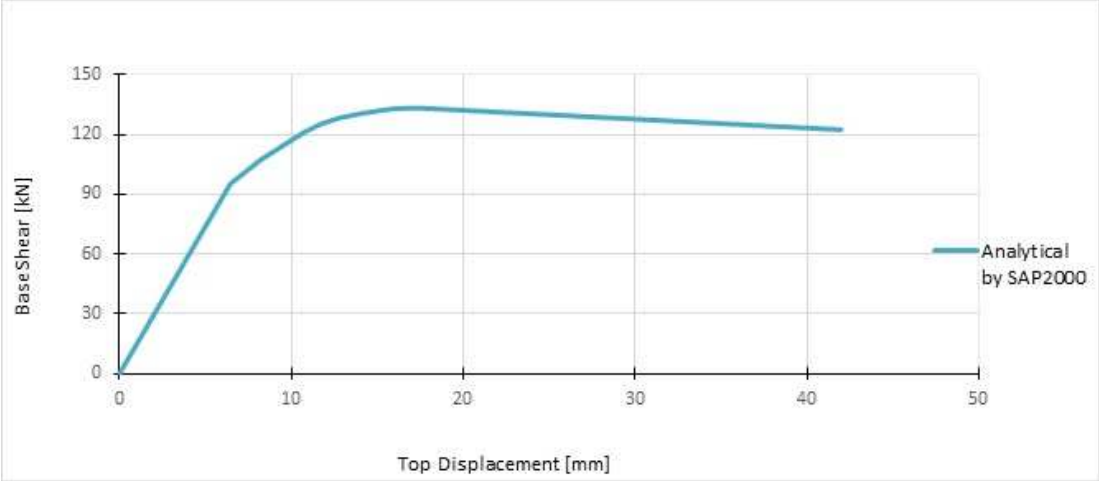

Figure 5.17: Pushover curve of the frame

Hinge formation of the frame during pushover analysis is given as follows (Figure 5.18). Hinges have colors according to predefined plastic hinge performance (damage) levels that were mentioned in this chapter.

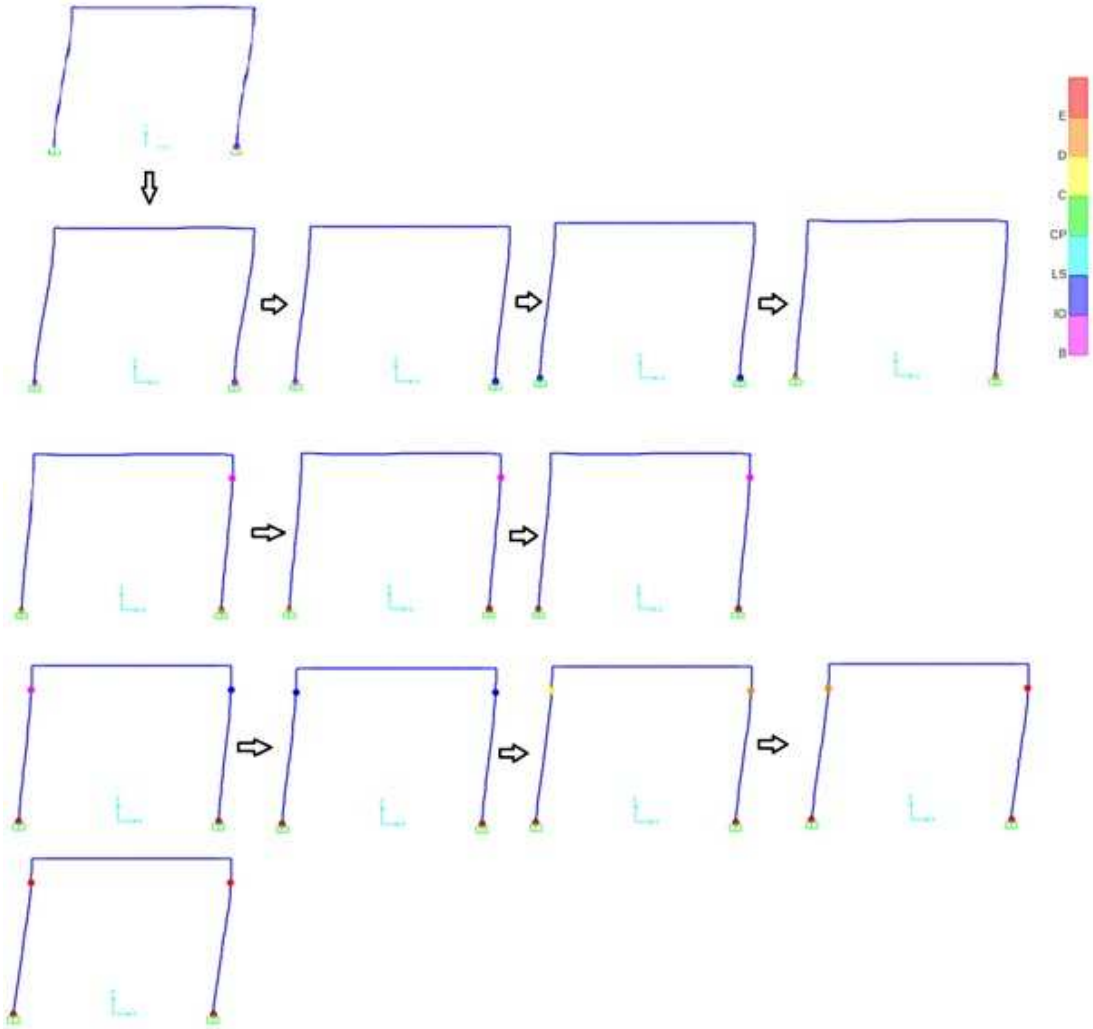

Figure 5.18: Plastic hinge formation for the frame

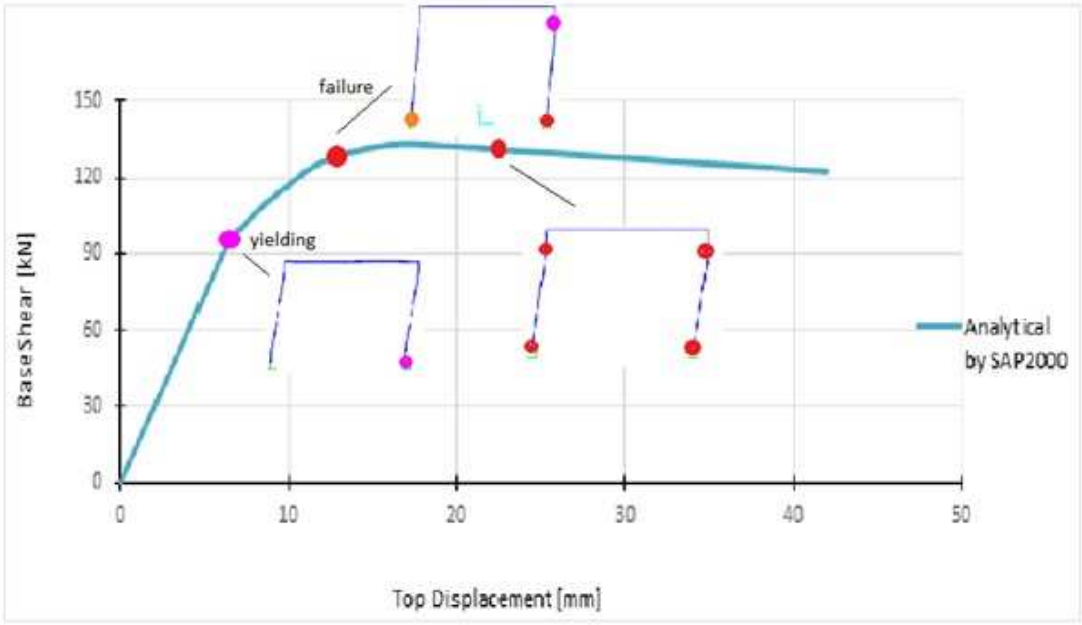

Figure 5.19: Damage states obtained at displacement levels of the frame

5.3 Comparison of the Analytical Results with the Experimental Results

The tested specimen was modeled in SAP2000 and SeismoStruct programs for the comparison of the analytical results with the experimental results .For both programs, reinforcement and concrete properties were defined by the use of material test results that were obtained by experiments.167.5 kN constant axial load was defined for columns and the fixed support condition was provided. The main difference of the programs was the modeling approach. SeismoStruct has fibre modeling approach, which means plasticity is distributed along the members on the other hand SAP2000 has concentrated plasticity approach which means the plasticity occurs in some weak expected sections, therefore, it is needed to assign plastic hinges to the structure. In this section, experimental results are compared with the analytical results that are obtained by SAP2000 and SeismoStruct.

Figure 5.20 presented below shows the comparison of base shear top displacement curves of the specimen that were obtained by SeismoStruct for different compressive strengths and elasticity modulus' that are given in Table 3.3. The elasticity modulus for these compressive strength of concrete values are taken from TS500.

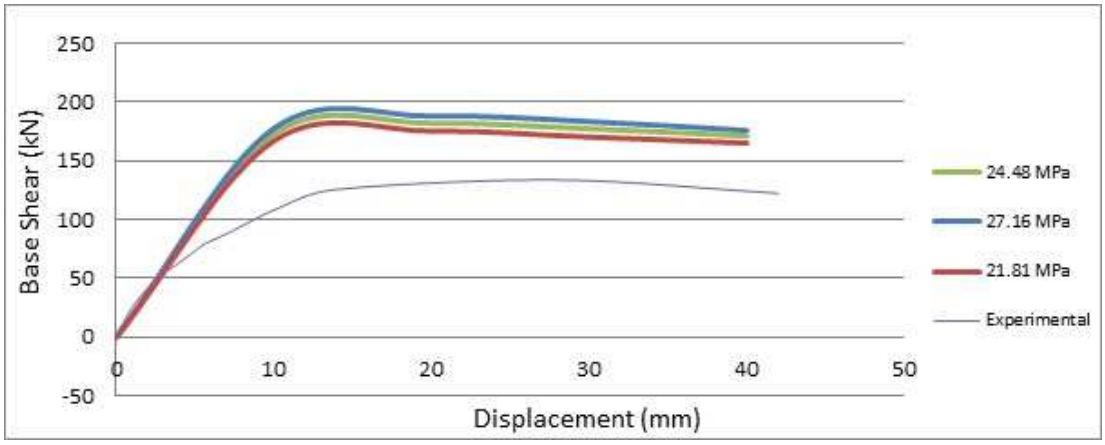

Figure 5.20: Comparison of experimental and analytical base shear top displacement curves for different compressive strength of concrete obtained by SeismoStruct

It can be seen from the Figure 5.20, for different compressive strength values of concrete obtaining the elasticity modulus' from TS500 has different envelop curves. None of them is close to the experimental behavior. Increasing and descending branch of envelopes of analytical hysteretic curves are steeper than experimental curve. The initial stiffness for three curves which is determined by slope of initial displacement cycles are greater than the experimental value due to steeper curves.

Analytical hysteretic curve presented in Figure 5.21 below was obtained for the 21.81 MPa compressive strength of concrete and the concrete modulus of elasticity of 12500 MPa which was taken into account as the slope of increasing branch of stress-strain relationship of the concrete that was obtained by material test.

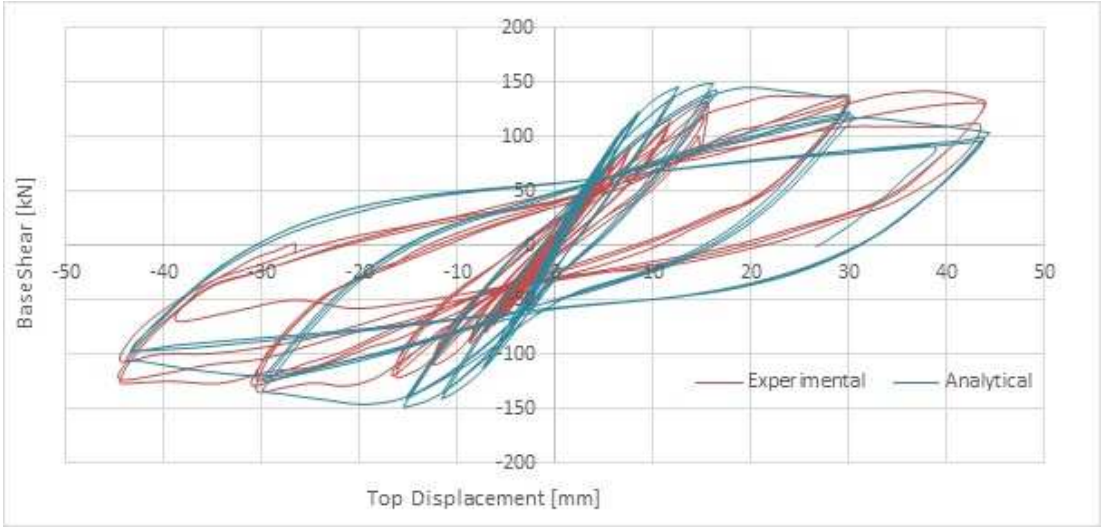

Figure 5.21: Comparison of experimental hysteretic curve and analytical hysteretic curve for compressive strength of $21.81MPa$ of concrete obtained by SeismoStruct

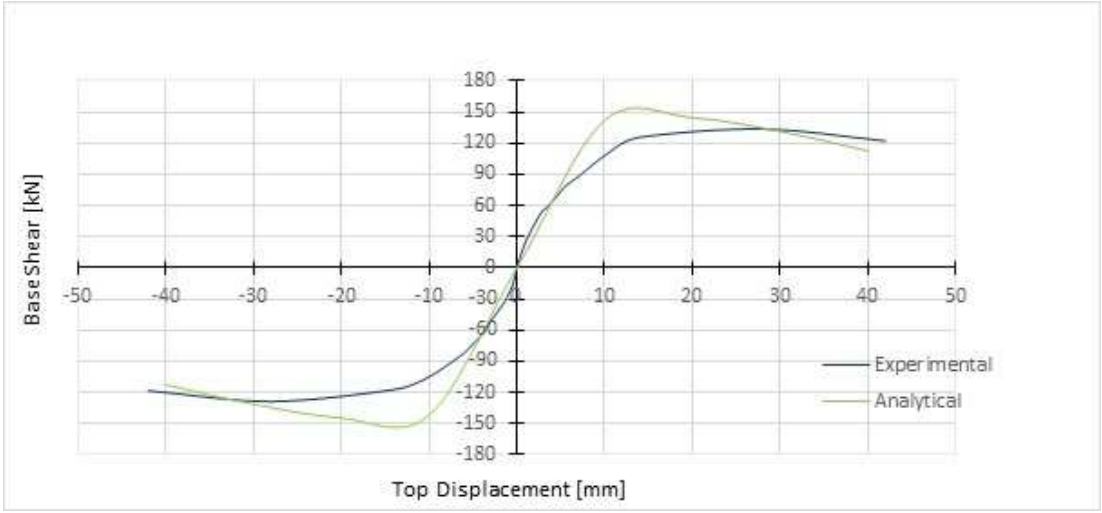

Figure 5.22: Comparison of experimental and analytical base shear top displacement curve for compressive strength of $21.81MPa$ of concrete obtained by SeismoStruct

The closest analytical hysteretic behavior can be seen from Figure 5.21. When comparing the hysteretic behaviors that were presented in Figure 5.20, especially initial stiffness is closer to analytical value with respect to initial cycle slopes which can be seen also in comparison of capacity curves in Figure 5.22. Moreover, slopes of the descending and increasing branches are closer to the experimental

hysteretic branches. The maximum strength values presented in Figure 5.21) for push and pull cycles also closer to experimental values when comparing to maximum strength values that can be seen in Figure 5.20 However, SeismoStruct still overestimates the strength values for the initial displacement cycles and underestimates latest pull and push displacement cycles given in Figure 5.21).

Comparison of the experimental base shear top displacement curve and the analytical curve obtained by SAP2000 is shown in Figure 5.23.

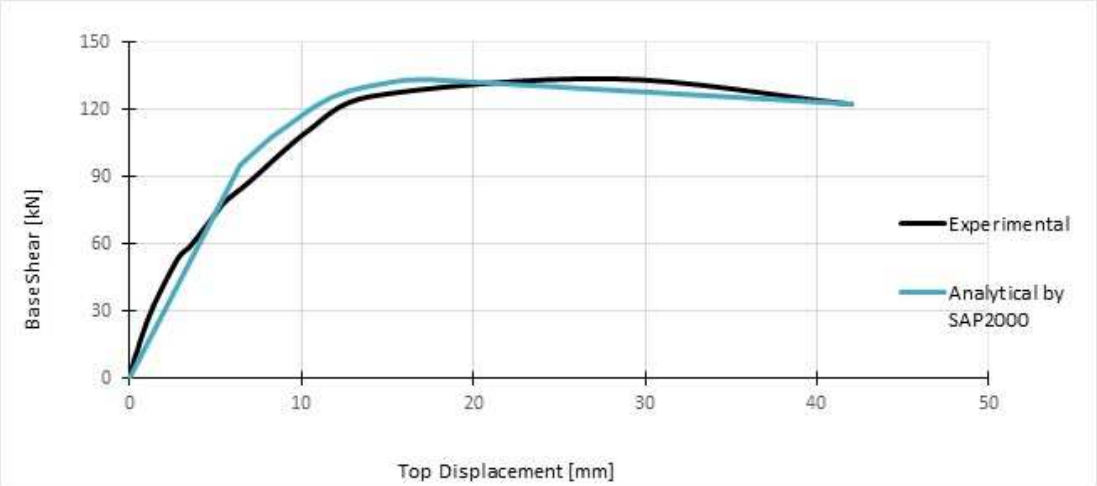

Figure 5.23: Comparison of the experimental base shear top displacement curve and the analytical curve obtained by SAP2000

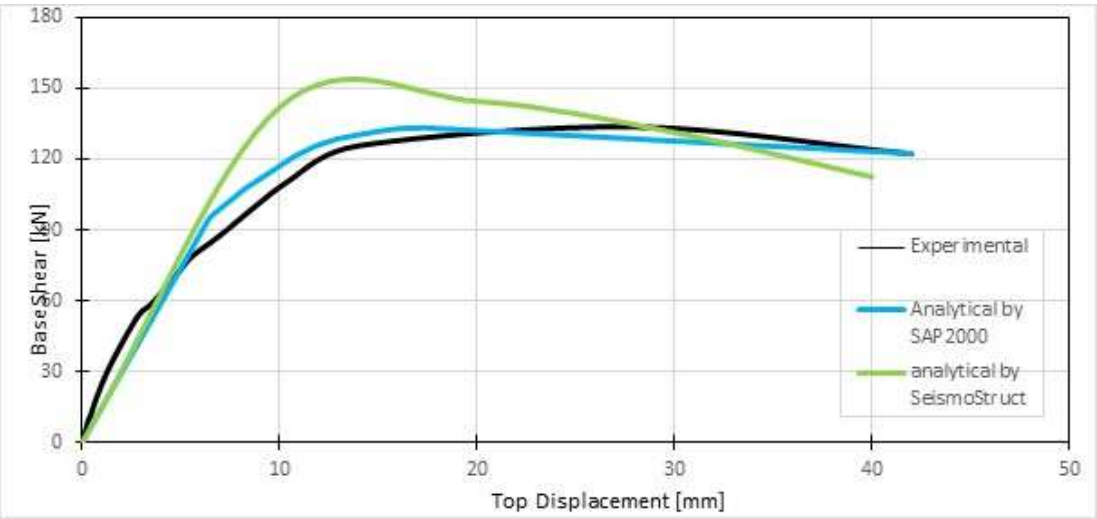

Figure 5.24: Comparison of the experimental base shear top displacement curve and the analytical pushover curves of the specimen

As seen from Figure 5.23 the capacity curves are quite close when comparing to SeismoStruct results. Maximum lateral load carried by the frame is 132.50 kN according to analytical study in SAP2000 and maximum load carried by the frame during the experiment was 133.65 kN. As it is seen from Figure 5.24 maximum lateral strength of the frame obtained by SeismoStruct is far beyond the experimental and therotical value of SAP2000.

Damage states after the analysis is done in SeismoStruct are given in Table 5.1 The bold lines in the table are matching the damage levels obtained during the experiments. These specified damage levels and places of damages are almost same as it was observed during the experiment.

It was shown in Figure 5.18, first plastic hinges occurred at column bottom ends as it was in the experiment. Then the plastic hinges occurred in column top end and in the experiment one of the column's top and bottom ends outer part totally crushed. During the experiment, weak column strong beam mechanism occurred as it is the case in the plastic hinge formation of analytical study given in previous parts.

Chapter 6

PARAMETRIC STUDIES

6.1 Retrofitting of Columns of the Frame by RC Jacketing

TEC2016 [39] part 7.3.5 states the weak beam stronger column principle as "In a load bearing system consisting of only frameworks or a combination of partitions and frameworks, the total bearing capacity moments of the columns integrating at each column-beam node point must be at least 20% more than the total of the bearing capacity moments in cross sections of the column surfaces of beams integrated at that node point". The formula is stated as:

$$(M_{ra} + M_{ru}) \geq 1.2(M_{ri} + M_{rj}) \tag{6.1}$$

Figure 6.1 shows the bearing capacity moments of the beam column elements acting on the node.

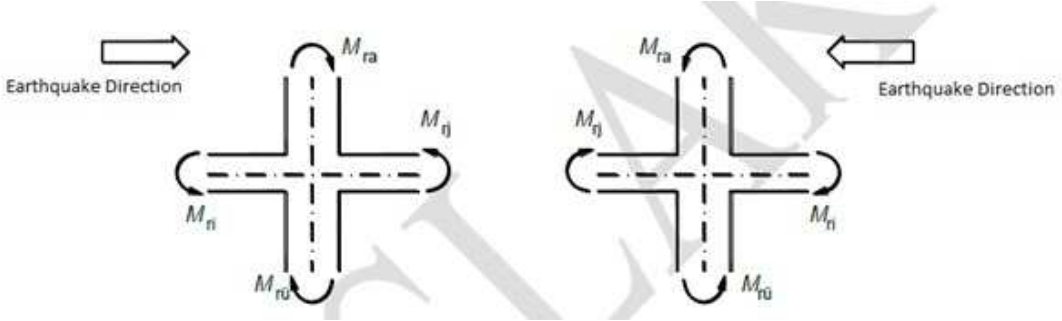

Figure 6.1: Bearing capacity moments acting the node point (TEC2016 [39])

The Idea of strong column-weak beam concept is having a strong column with more stiffness as compared to beams to prevent total collapse of the structure while resisting the lateral loads especially the earthquake loads. If the moment capacity of reinforced concrete beam is more than the reinforced concrete column, beam reaches its ultimate moment capacity before the columns, plastic hinges form at the ends of the beam and it results in partial collapse and the energy dissipation occurs in the plastic hinge at the ends of the beam. However if the columns are designed to be weaker than beams, the columns will reach its ultimate bearing capacity before the beam and thereby it will result in loss of stability and total collapse. In other words stronger column -weak beam failure give local failure, so the sign of failure can be seen and precautions can be taken. On the other hand, strong beam and weak column gives global failure that does not give sign of failure and structure collapses suddenly.

Since the experimental and analytical studies have shown that the structure has weak columns and stronger beam due to no damage on beam and plastic hinges that formed at the column ends, retrofitting techniques can be utilized to increase the load carrying capacity and ductility of columns against the lateral load. Retrofitting by reinforced concrete jacketing is handled in the following part of the study.

There are several techniques of jacketing of damaged structural members. Reinforced concrete jacketing technique is the most preferred method of retrofitting used both in practical and experimental purposes as it was mentioned in Chapter 1.

In this part of the study, application of RC jacketing to columns and its results are investigated analytically. Assumptions that were considered for analysis are as follows:

- LaFarge- Agilia brand of C30 concrete is considered for concrete. Agilia has some features: it is self-placing and self-leveling and it requires no vibration

- Confined Mander Model is considered for concrete and reinforcement with strain hardening considered for steel bars
- Minimum 1% of the sectional area is taken as amount of longitudinal reinforcement in the jacket. In some cases it has been increased to see how important the contribution of reinforcement in compression part of the section on the sectional ductility.
- To calculate elasticity modulus, TS500 is used.
- To obtain the changes in strength and curvature ductility, different jacketing options for columns are examined such as:
    1. Inner part of the jacketed column section (actual frame section) totally neglected and only jacketing is considered.
    2. The thicknesses of jacketing considered are 4 cm, and 6 cm and $\phi 6$ is used as transverse reinforcement for both case.
    3. 6 cm jacketing is considered and in order to increase volumetric ratio of stirrups, $\phi 10$ has been used as transverse reinforcement instead of $\phi 6$.
- Tension strength of concrete is taken as zero.
- Cross sectional analysis is done by the XTRACT program for each specified section.

6.1.1 Cross Sectional Analysis

Cross sectional analysis is required to have insight of the advantages and disadvantages of jacketing. Xtract provides the ability to work on different composite sections by considering the small fibers with the number of approximately 200-400 therefore, in this part of the study, jacketed cross-sections with different characteristics are considered and analyzed by Xtract.

6.1.1.1 Cross Sectional Analysis of Existing Frame

For the actual frame materials, average experimental stress strain relationship of longitudinal reinforcing bar is given in Table 3.6 .Material models to analyze the recently tested frame sections are given as follows:

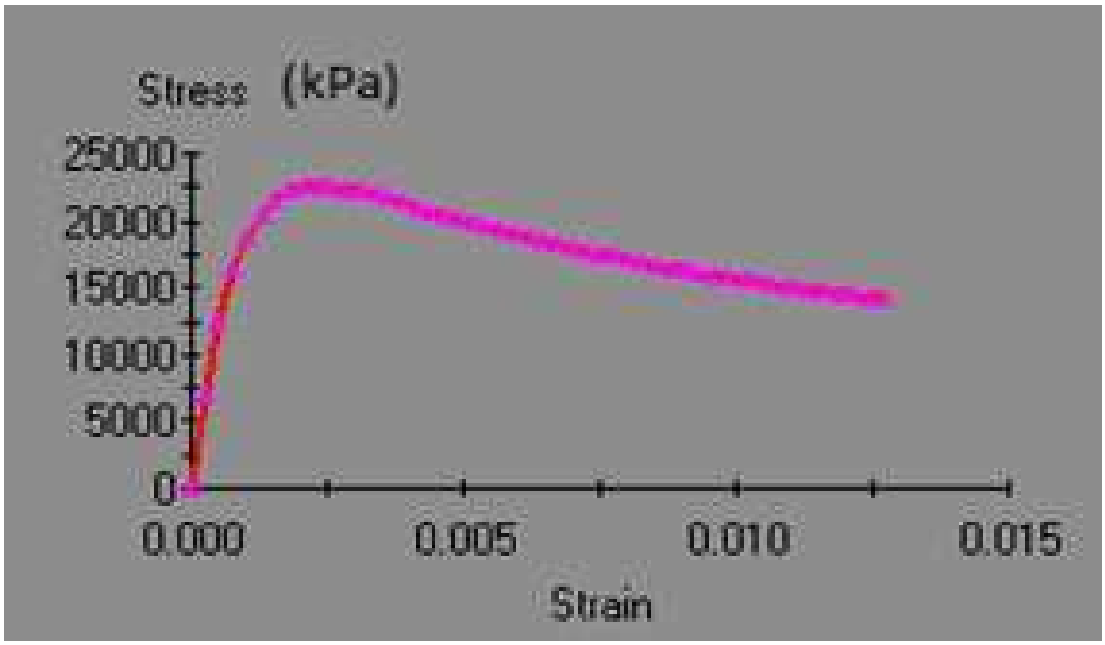

Figure 6.2: Stress-strain relationship of confined concrete

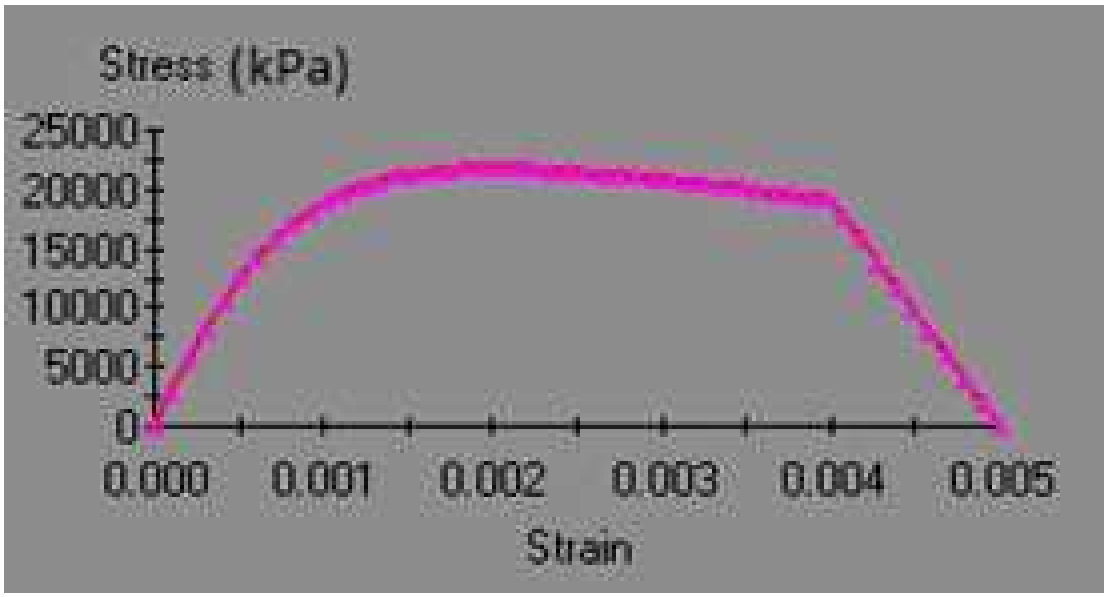

Figure 6.3: Stress-strain relationship of unconfined concrete

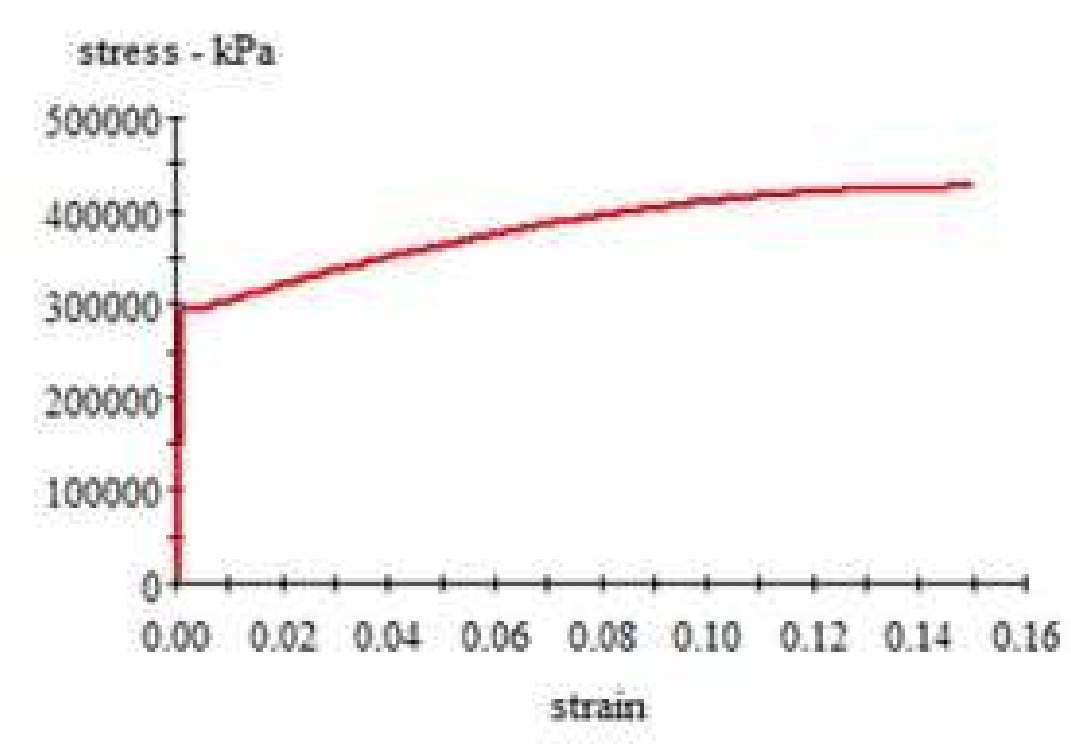

Figure 6.4: Stress-Strain relationship for steel

Moment curvature analysis for each section of actual frame was done using the above stress-strain relationship of materials and the results of the analysis are given below.

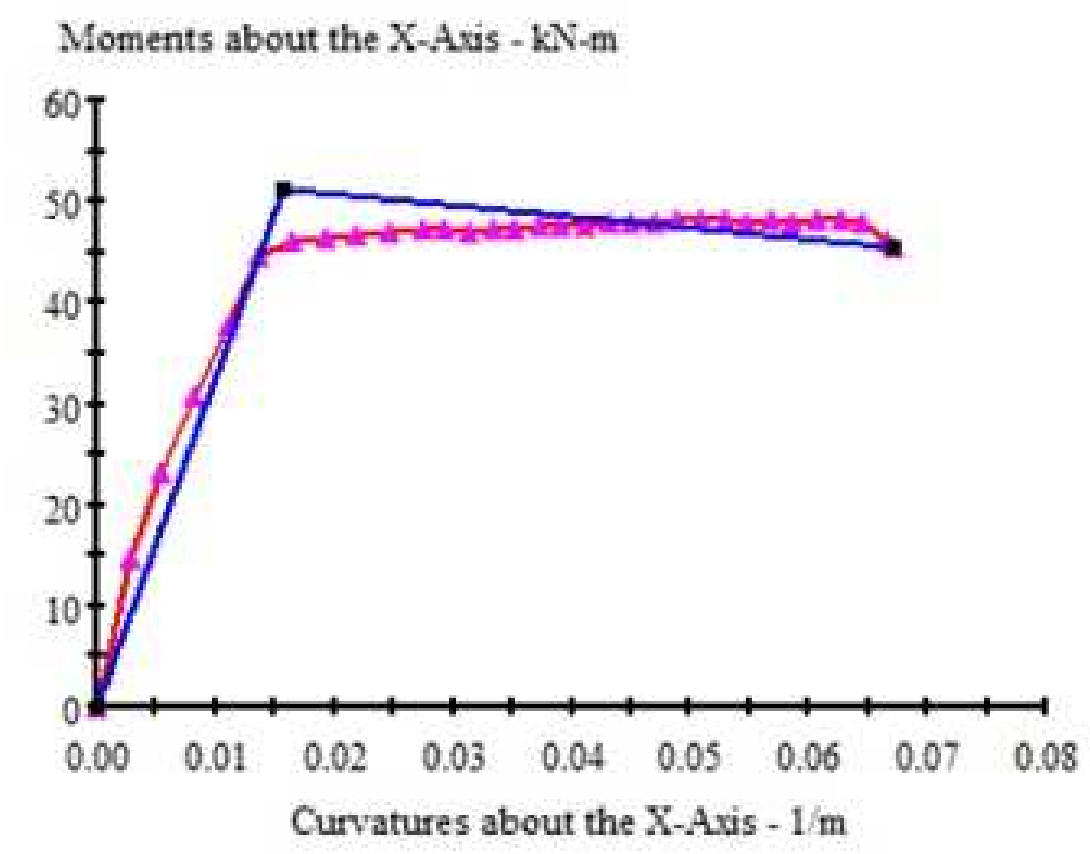

Figure 6.5: Negative moment-curvature relation of asymmetrically reinforced section (top section)

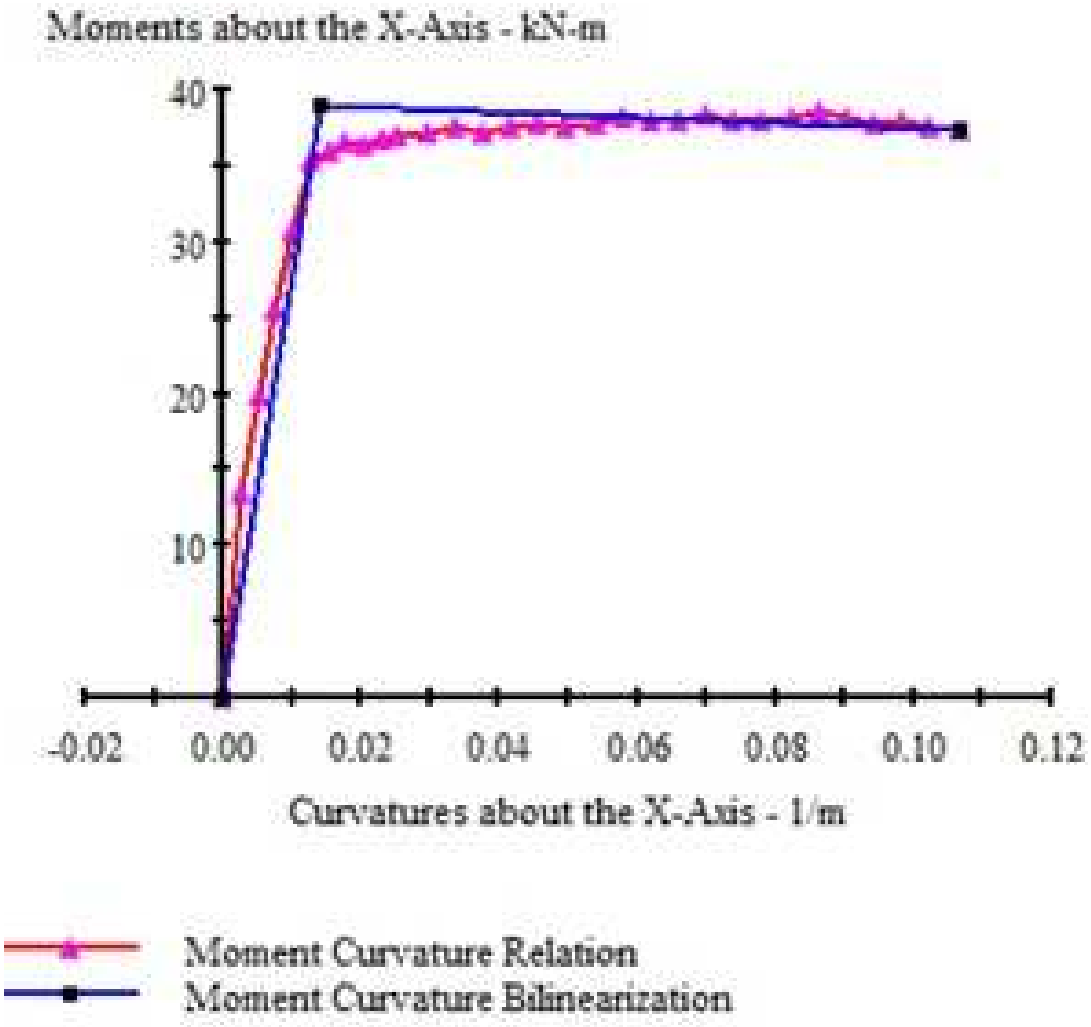

Figure 6.6: Positive moment-curvature relation of asymmetrically reinforced section (top section)

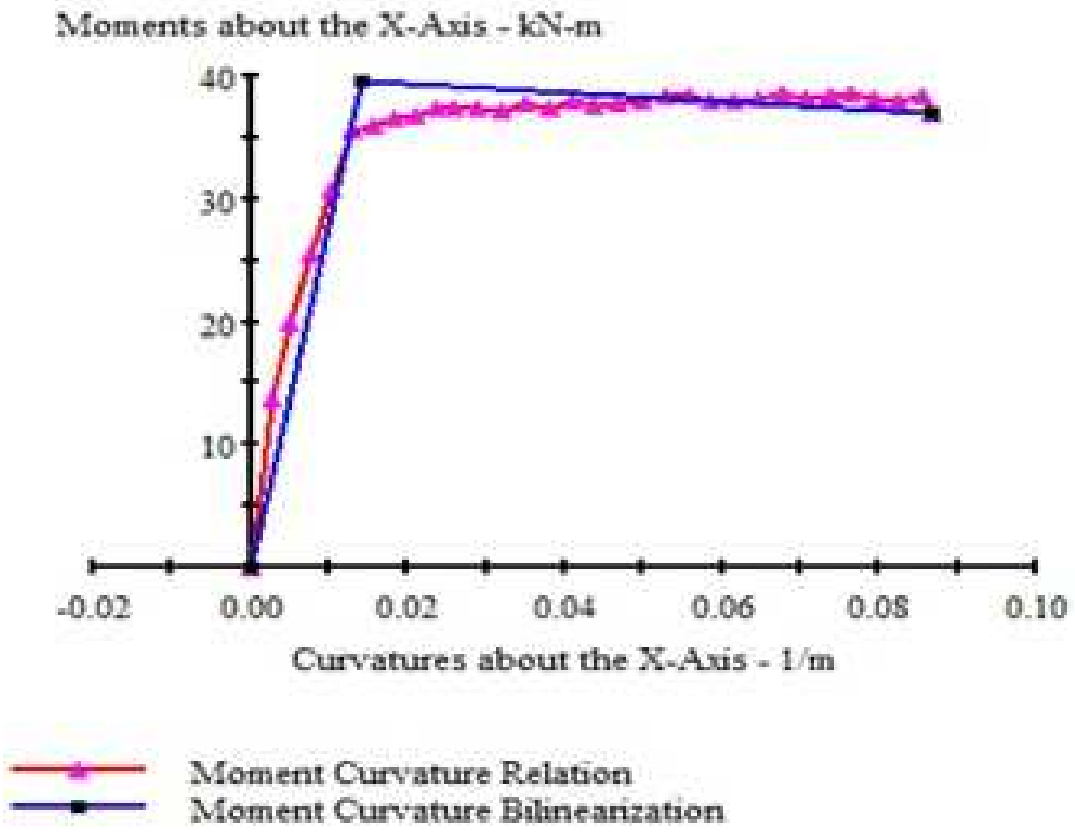

Figure 6.7: Positive and negative moment-curvature relation of symmetrically reinforced section (bottom section)

Curvature ductility is found as 7.640 for positive moment, 4.248 for negative moment for the top section of the column and for bottom section it is found as 6.10.

6.1.1.2 Cross Sectional Analysis of Jacketed Sections

In Figure 6.8 "section a" shows the top section and "section b" shows the bottom section of column element. For Retroffitted sections they are considered separately.

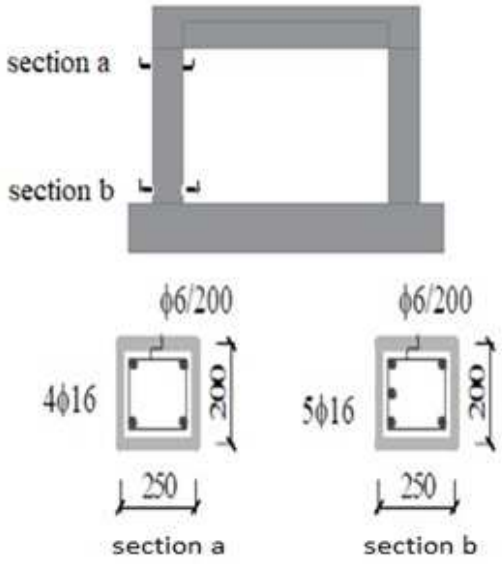

Figure 6.8: Column Sections

Confined concrete strenght and strain values are calculated automatically by XRACT program according to Mander model and confined Stress-strain model for concrete and reinforcement model with strain-hardening were considered. There are 3 confined and one unconfined stress-strain relationship for each retrofit assumption,except for the first assumption.In the case of concrete jacketing of 4 cm and transverse reinforcement of, $\phi 6$, material characteristics for concrete and steel that were considered are given as follows;

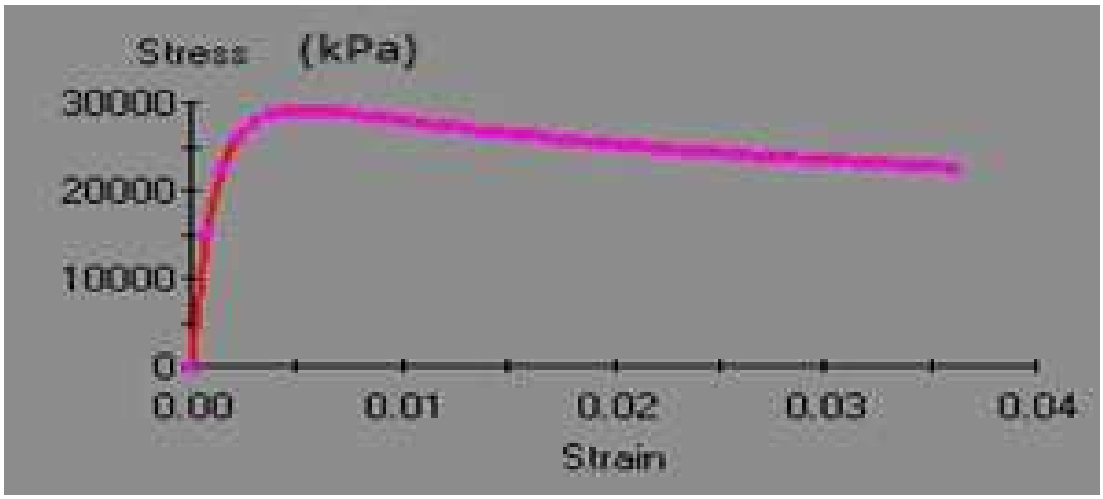

Figure 6.9: Stress-strain relationship of actual frame's concrete after jacketing

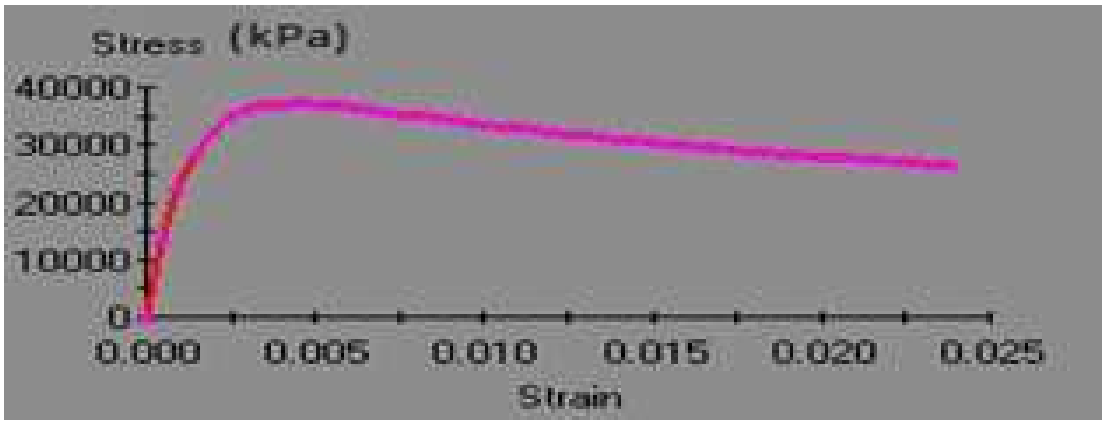

Figure 6.10: Stress-strain relationship of confined jacketed part (C30)

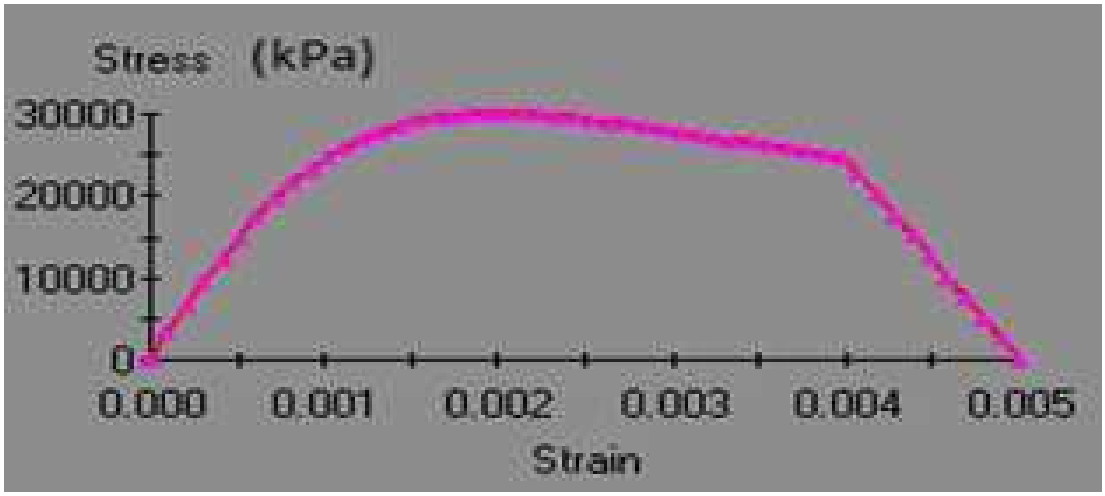

Figure 6.11: Stress-strain relationship of unconfined part of the section (C30)

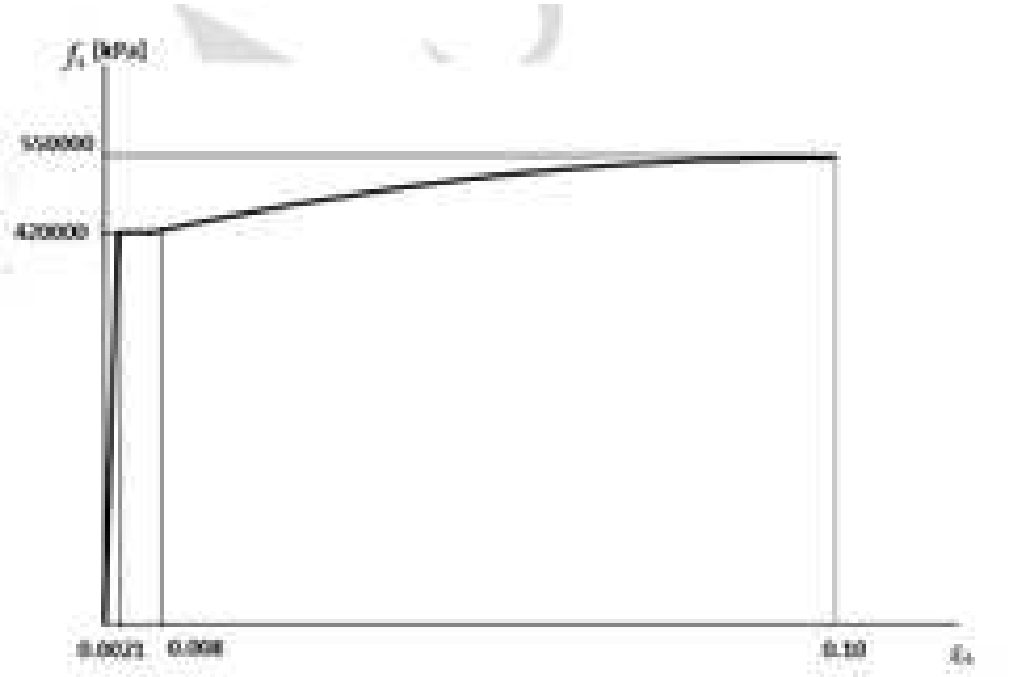

Figure 6.12: Stress-strain relationship for steel- S420 (TEC2016 [39])

Considering constant 167.5 kN of axial load, using material properties mentioned above, cross sectional analysis, under bending moment in x-x direction was done for several sections to obtain moment curvature relationship. Cross-sections that are considered and their analysis results are given in next part of this section. Material color states that are obtained after cross-sectional analysis are given in Figure 6.13.

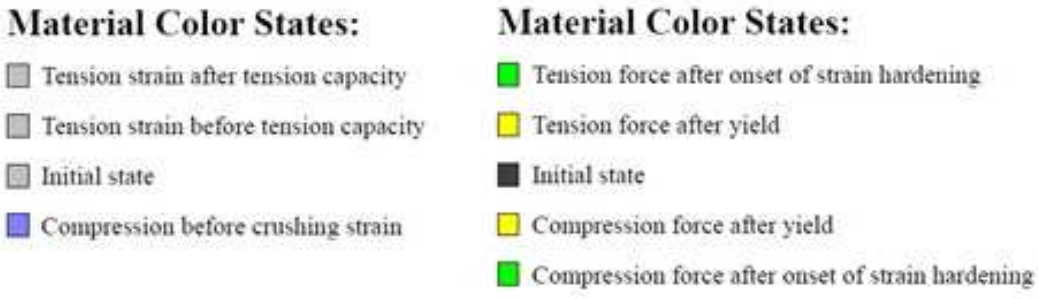

Figure 6.13: Materials color states

a. Cross Sectional Analysis of the 4 cm Jacketing with Neglected Inner Part

First assumption is neglecting inner part of the jacketed section, in other words actual frame's section is not taken into consideration. View of the section in XTRACT is given in Figure 6.14. Pink colored part is the clear cover of RC jacketing and the grey part is confined section.

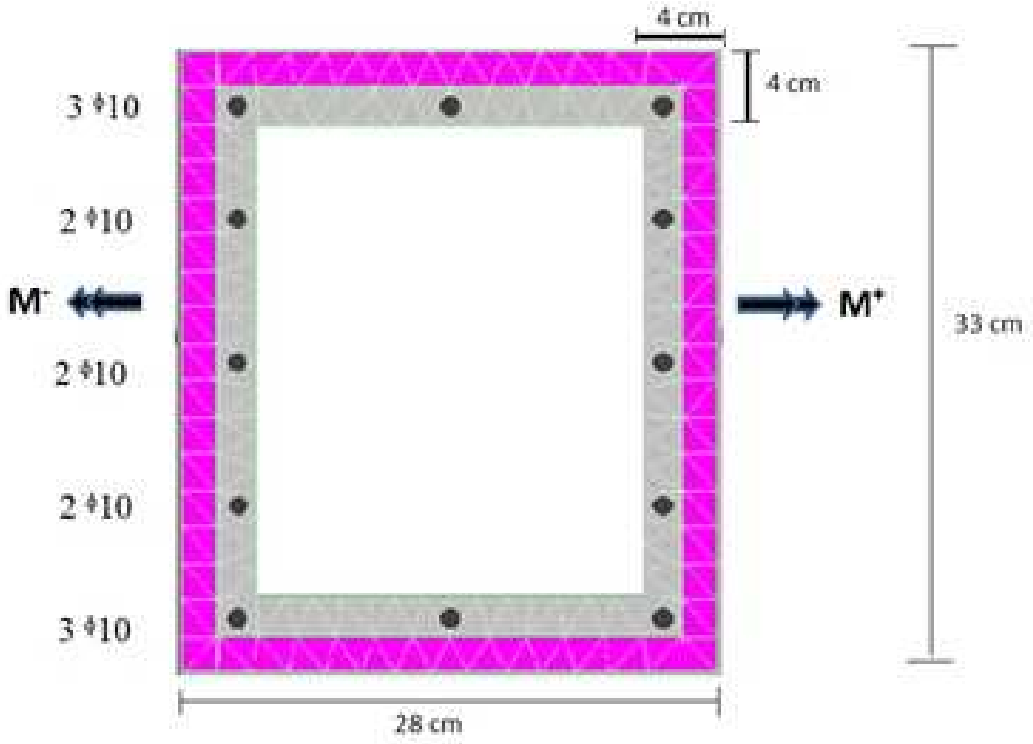

Figure 6.14: View of the section

Reinforcement characteristics of the section is presented in the Table 6.1

Reinforcement in jacketing	$12\phi10$
Transverse Reinforcement	$\phi6$
Transverse Reinforcement Volumetric Ratio	0.01018
Transverse Reinforcement spacing	0.05 m
Clear Cover	0.02 m

Table 6.1: Reinforcement characteristics of the section

Analyzing the section by XTRACT program moment curvature graph of the section under bending moment in x-x direction was obtained. Moment curvature graph and the curvature ductility is found as 5.66. The situation of the section at the end of the analysis is given in Figure 6.15 and moment curvature relationship of the section is given in Figure 6.15. Color states that indicate the states like yielding, crushing, spalling etc. also given in the Figure 6.13.

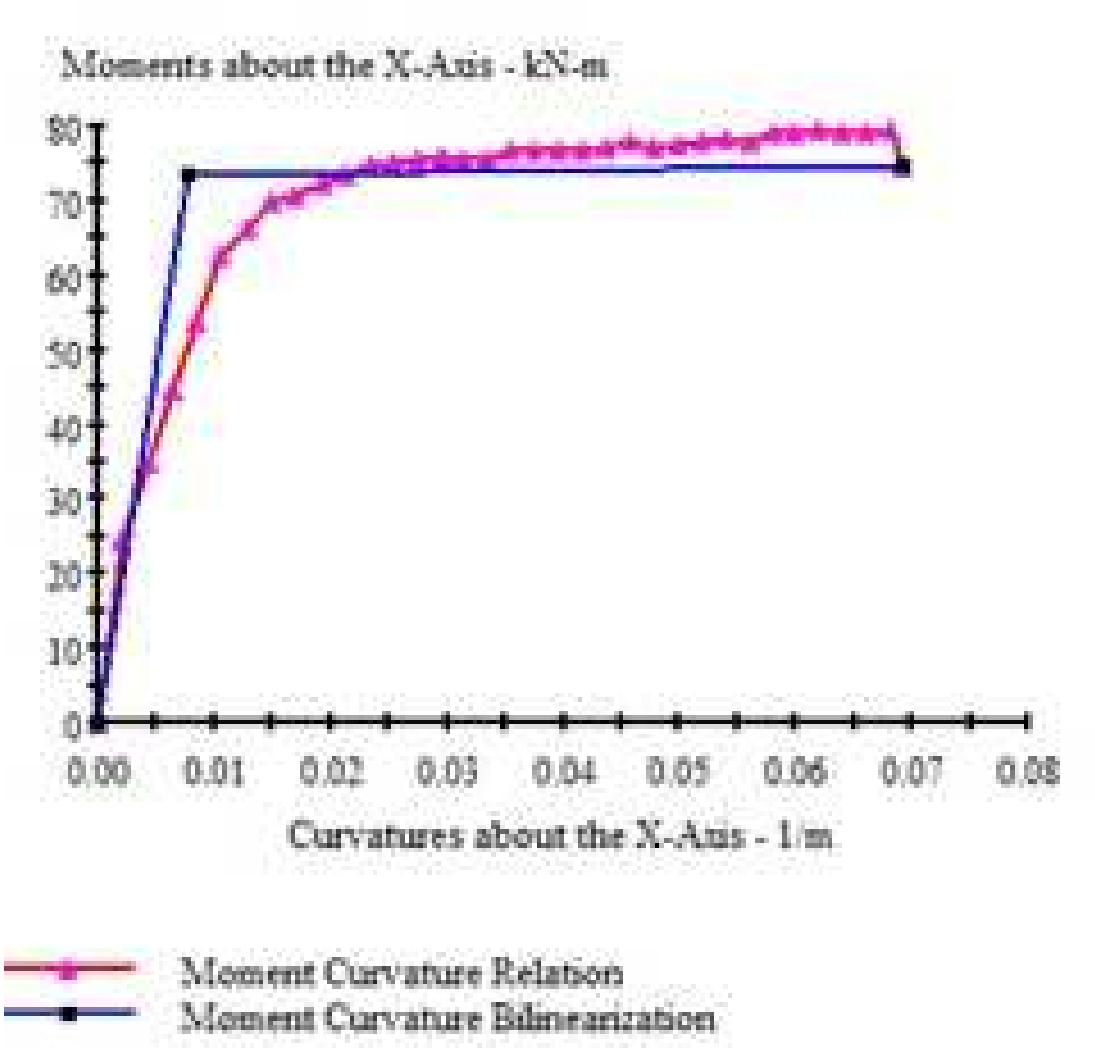

Figure 6.15: Moment curvature relationship of the section 1

Since it is has same and symmetric reinforcement with respect to bending axis x-x, positive and negative moment curvature relationship of the section is the same.

Figure 6.16: State of the section after loading

b. Cross Sectional Analysis of 4 cm Jacketing

One of the assumptions is the reinforced concrete jacketing of 4 cm. View of the section in XTRACT is given in Figure 6.17. Grey colored part is the confined part of the section, pink colored part is clear cover of jacketing. Reinforcement characteristics of the section is given in Table 6.2. It should be note that it is not allowed in TS500 to design a column with longitudinal reinforcing bars smaller

than 14 mm of diameter, however since this is a theoretical study, it can be acceptable.

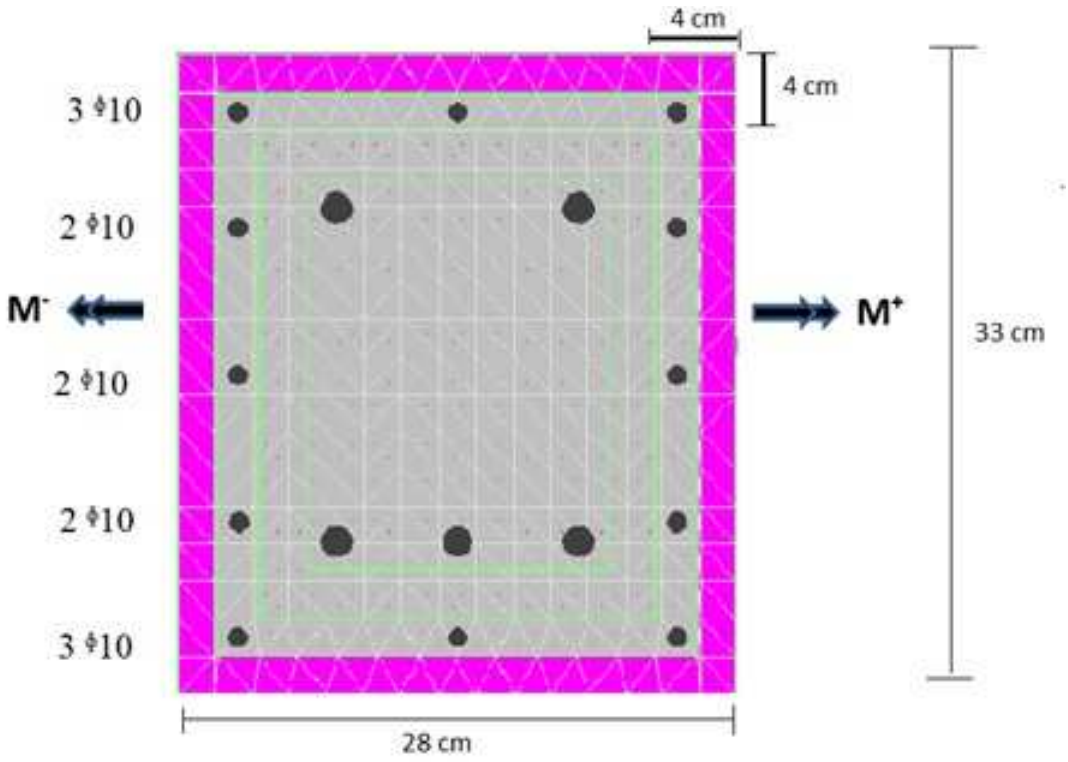

Figure 6.17: View of the cross section in Xtract

Reinforcement in jacketing	$12\phi10$
Transverse Reinforcement	$\phi6$
Transverse Reinforcement Volumetric Ratio	0.01288
Transverse Reinforcement spacing	0.05 m
Clear Cover	0.02 m

Table 6.2: Reinforcement characteristics of the section 2

Curvature ductility is found as 6.424 for positive moment, 6.280 for negative moment for the top section of the column and for bottom section it is found as 7.380. Failure occur at compression part of unconfined concrete. Positive and negative moment curvature relationship and bilinearization of the curves and last state of the sections under negative and positive bending moment has shown below.

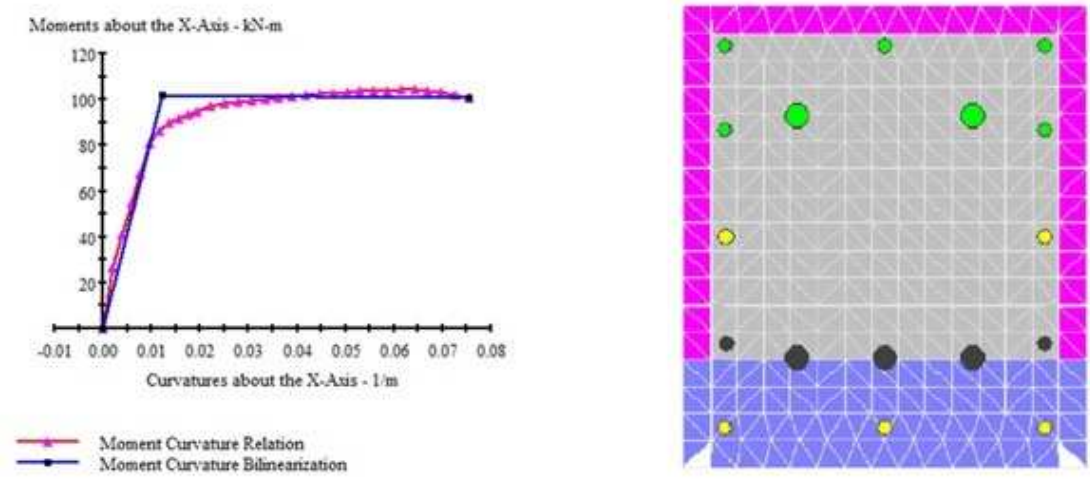

Figure 6.18: Positive moment-curvature relationship of asymmetrically reinforced section and the section after analysis

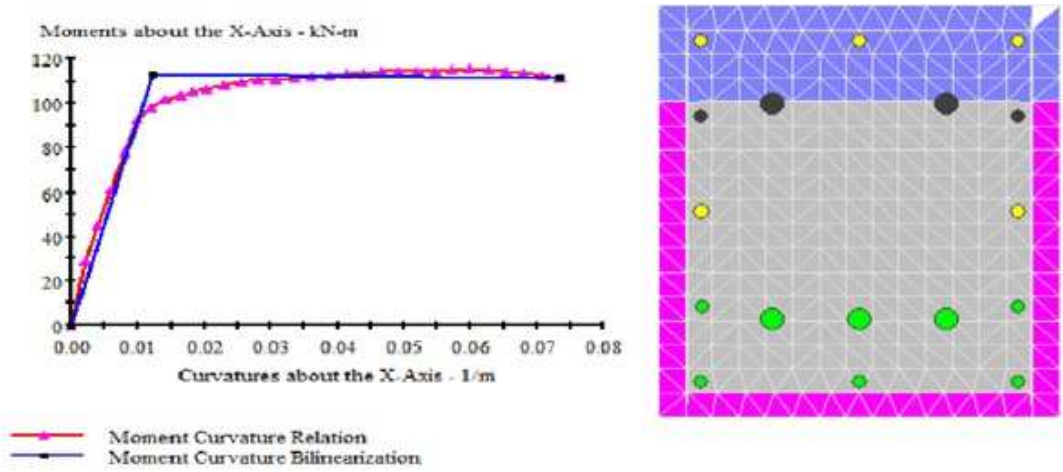

Figure 6.19: Negative moment-curvature relationship of asymmetrically reinforced section and the section after analysis

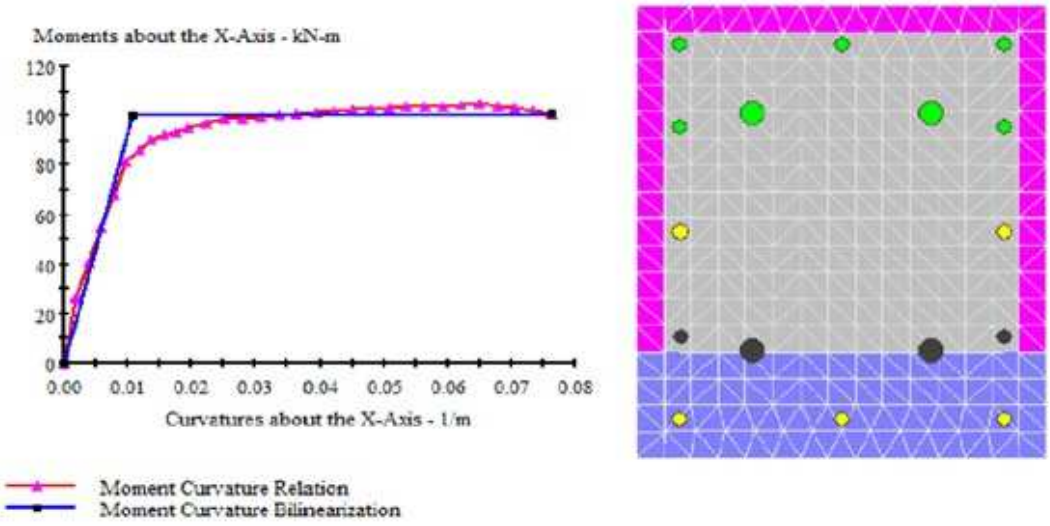

Figure 6.20: Negative and positive moment-curvature relationship of symmetrically reinforced section and the view of the section after analysis

Positive and negative moment curvature relationship of the bottom section of the column is same, since it is has same and symmetric reinforcement with respect to bending axis x-x.

c. Cross Sectional Analysis with 6 cm Jacketing

Third section model considered is the section with 6 *cm* of reinforced concrete jacketing. View of the section in XTRACT is given in Figure 6.21. Grey colored part is the confined part of the section, purple colored part is clear cover of jacketing. Reinforcement characteristics of the section are given in Table 6.3.

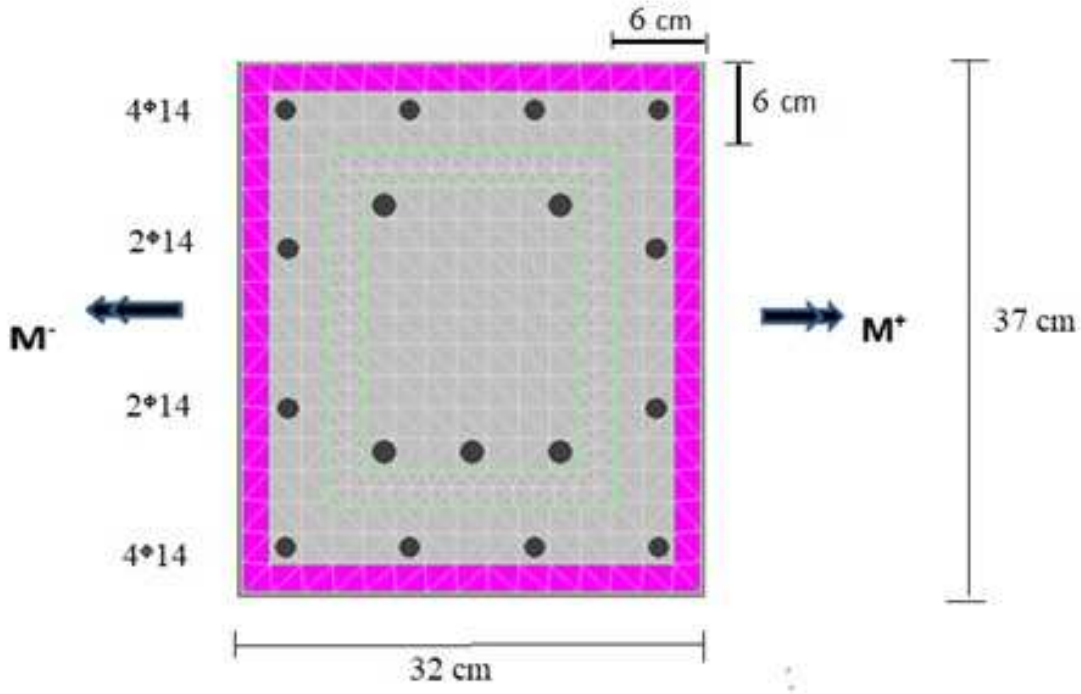

Figure 6.21: View of the cross section in Xtract

Reinforcement in jacketing	$12\phi14$
Transverse Reinforcement	$\phi6$
Transverse Reinforcement Volumetric Ratio	0.009135
Transverse Reinforcement spacing	0.05 m
Clear Cover	0.02 m

Table 6.3: Reinforcement characteristics of the section 3

Curvature ductility is found as 5.735 for positive moment, 5.629 for negative moment for the top section of the column and for bottom section it is found as 5.874. Failure occurs at compression part of unconfined concrete. Positive and negative moment curvature relationship and bilinearization of the curves and last state of the sections under negative and positive bending moment has shown below.

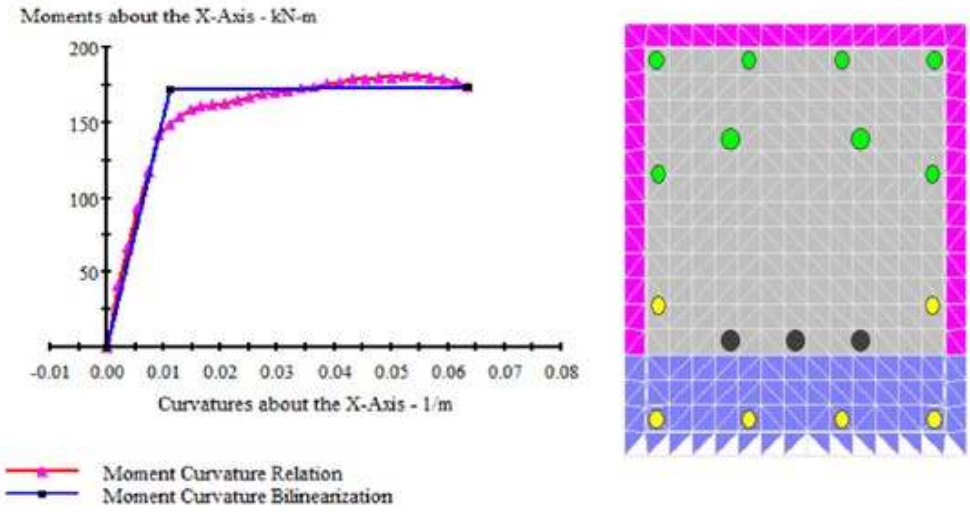

Figure 6.22: Positive moment-curvature relationship of asymmetrically reinforced section and the section after analysis

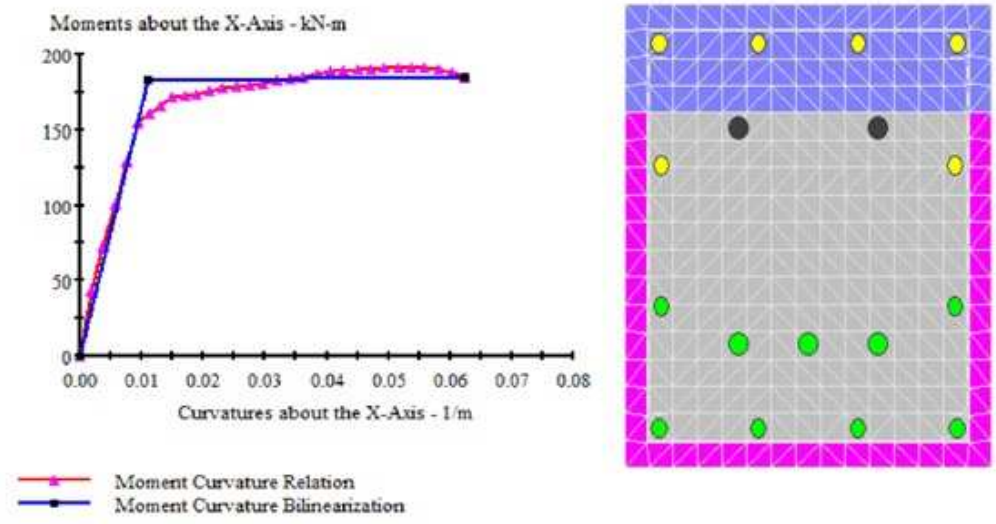

Figure 6.23: Negative moment-curvature relationship of asymmetrically reinforced section and the section after analysis

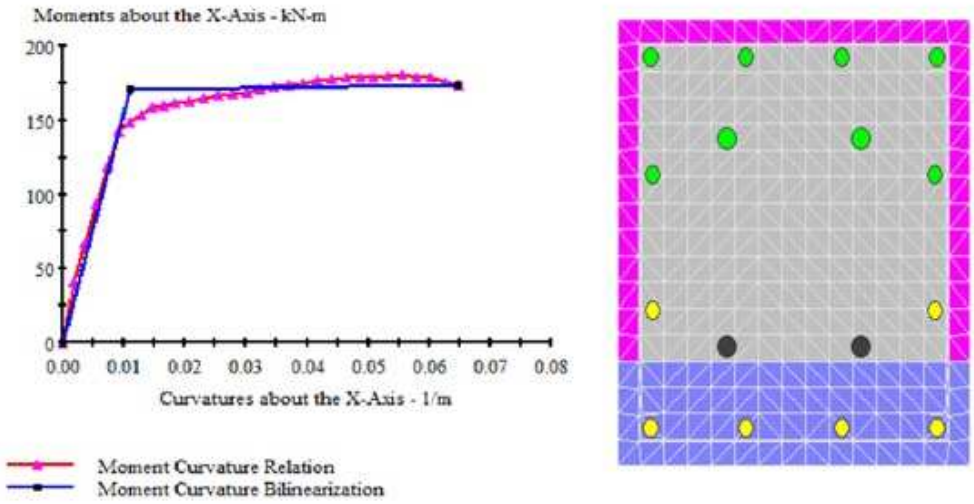

Figure 6.24: Positive and negative moment-curvature relationship of symmetrically reinforced section and the view of the section after analysis

Positive and negative moment curvature relationship of the bottom section of the column is same, since it is has same and symmetric reinforcement with respect to bending axis x-x.

d. Cross Sectional Analysis with 6 cm Jacketing with Higher Volumetric Ratio of Transverse Reinforcement

Again, 6 *cm* jacket is considered having higher transverse reinforcement ratio when comparing to other sections that were mentioned in this chapter. View of the section in XTRACT is given in Figure 6.25. Grey colored part is the confined part of the section, purple colored part is clear cover of jacketed section. Reinforcement characteristics of the section are given in Table 6.4.

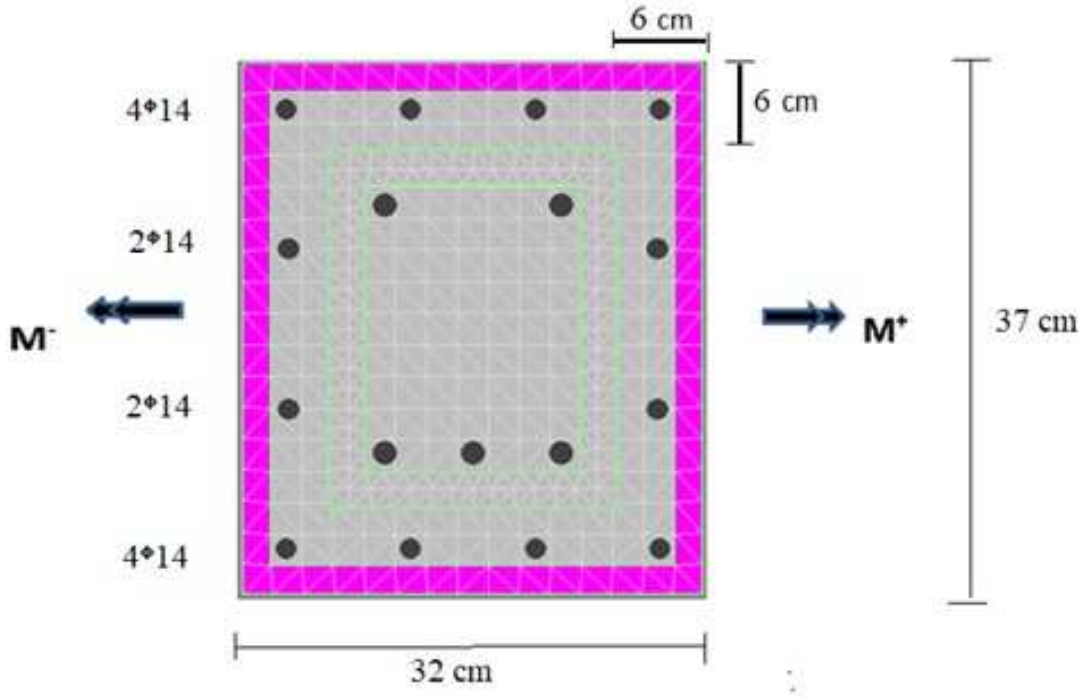

Figure 6.25: View of the cross section in Xtract

Reinforcement in jacketing	$12\phi14$
Transverse Reinforcement	$\phi10$
Transverse Reinforcement Volumetric Ratio	0.018
Transverse Reinforcement spacing	0.05 m
Clear Cover	0.02 m

Table 6.4: Reinforcement characteristics of the section 4

Curvature ductility is found as 5.893 for positive moment, 5.779 for negative moment for the top section of the column and for bottom section it is found as 6.026. Failure occurs at compression part of unconfined concrete. Positive and negative moment curvature relationship and bilinearization of the curves and the last state of the sections under negative and positive bending moment has shown below.

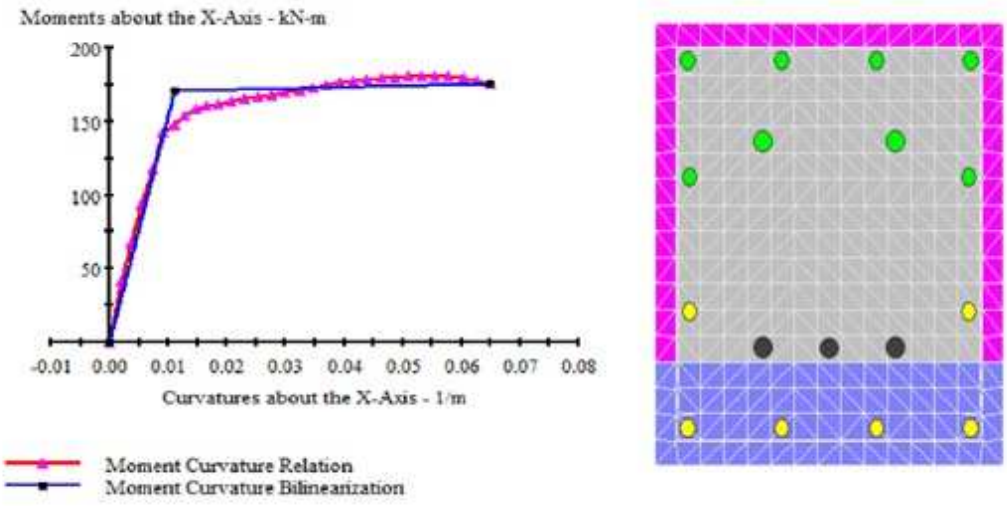

Figure 6.26: Positive moment-curvature relationship of asymmetrically reinforced section and the view of the section after analysis

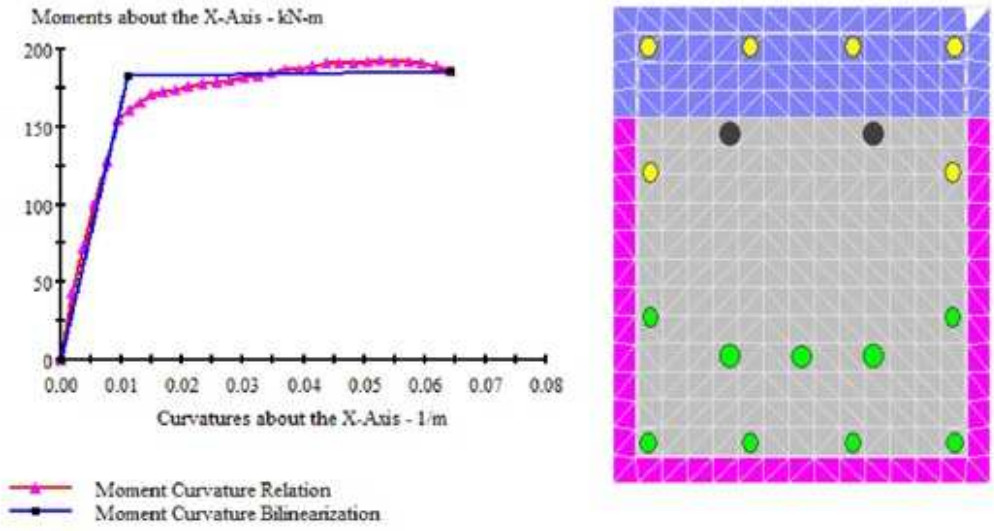

Figure 6.27: Negative moment-curvature relationship of asymmetrically reinforced section and the view of the section after analysis

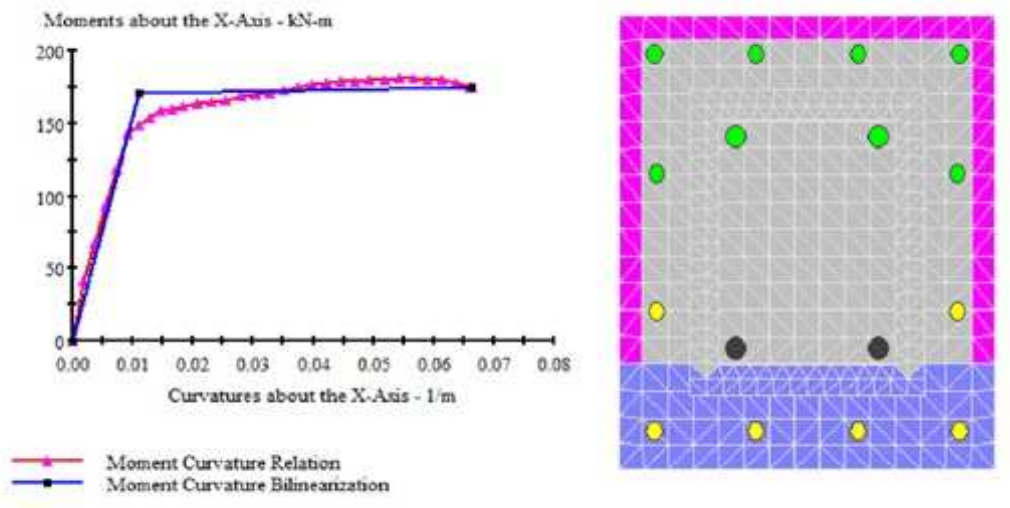

Figure 6.28: Positive and negative moment-curvature relationship of symmetrically reinforced section and the view of the section after analysis

Comparisons of moment curvature relationships of the retrofitted sections are given in Figures 6.29 and 6.30.

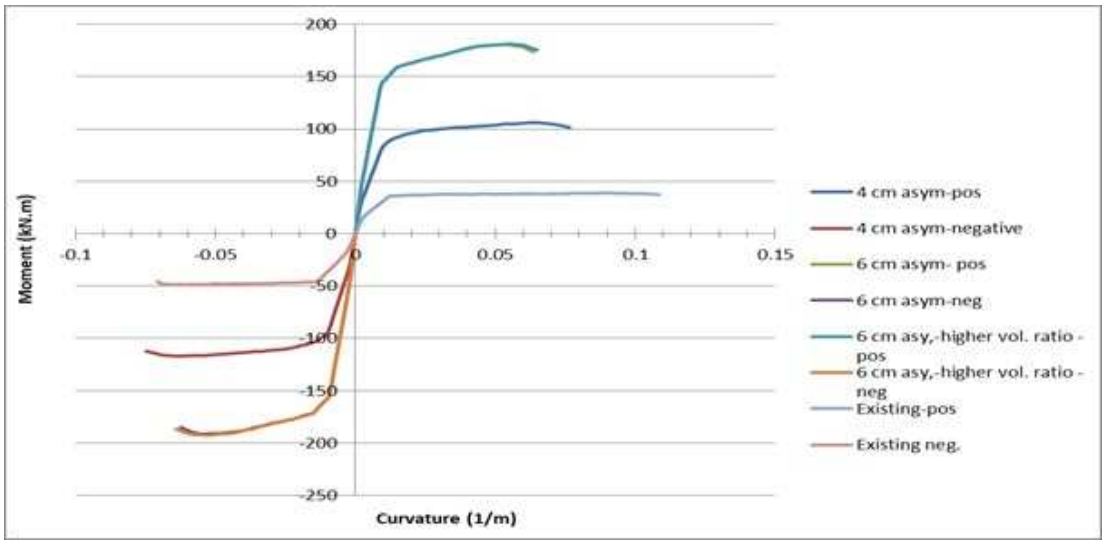

Figure 6.29: Comparison of moment curvature relationship for top section

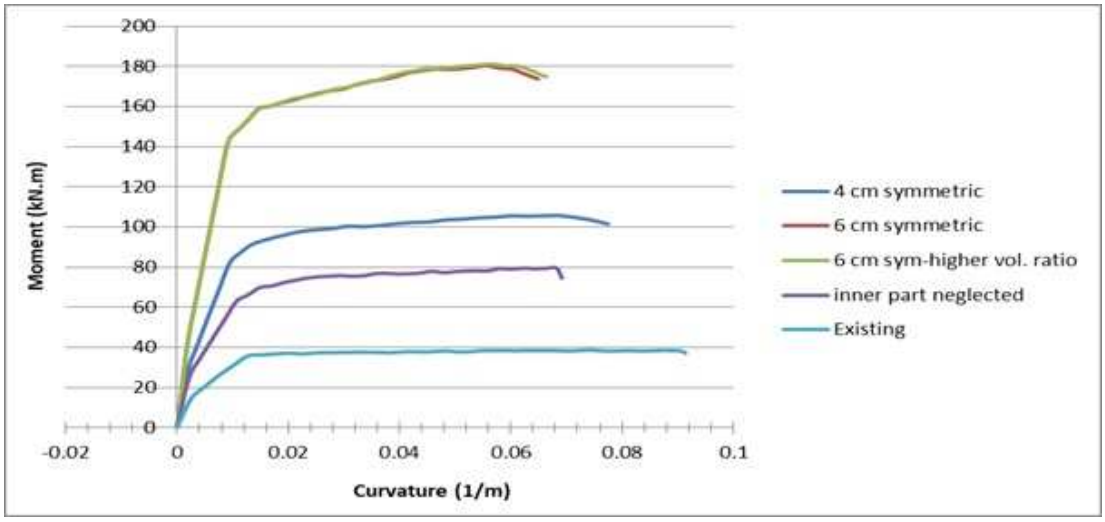

Figure 6.30: Comparison of moment curvature relationship for bottom section

6.1.2 Pushover Analysis with Jacketed Column Cross Sections

Cross sections mentioned in previous part of this chapter were analyzed in SAP2000. Changing moment curvature relationship of existing frame in SAP2000 program, pushover analysis was done for each cross section mentioned in previous part. Formation of plastic hinges and base shear-top displacement curves were obtained for each situation. Also natural period and the period after each plastic hinge formation of the frame for each retrofitting assumption and the corresponding base shear forces are given in Table 6.5. T1, F1 stands for natural period and corresponding base shear respectively. The other periods are found according to plastic hinge formations. As it is expected, when the frame is retrofitted, rigidity of the structure increases, therefore period of the frame decreases.

Period(sec)& Base Shear Force(kN)	**Existing Frame**	**4 cm Retrofitted**	**6 cm retrofitted**
T1	0.112	0.068	0.057
F1	33.34	34.09	34.36
T2	0.143	0.088	0.075
F2	33.19	33.9	34.12
T3	0.226	0.141	0.124
F3	33.13	33.4	33.64
T4	0.341	0.235	0.214
F4	33.13	33.36	33.51

Table 6.5: Periods and corresponding shear forces

1. First assumption was neglecting inner part of the jacketed section, in other words actual frame's section is not taken into consideration. Base shear vs top displacement curve for this state is given in Figure 6.31.When comparing to existing frame, lateral force that is carried by frame that is bigger.

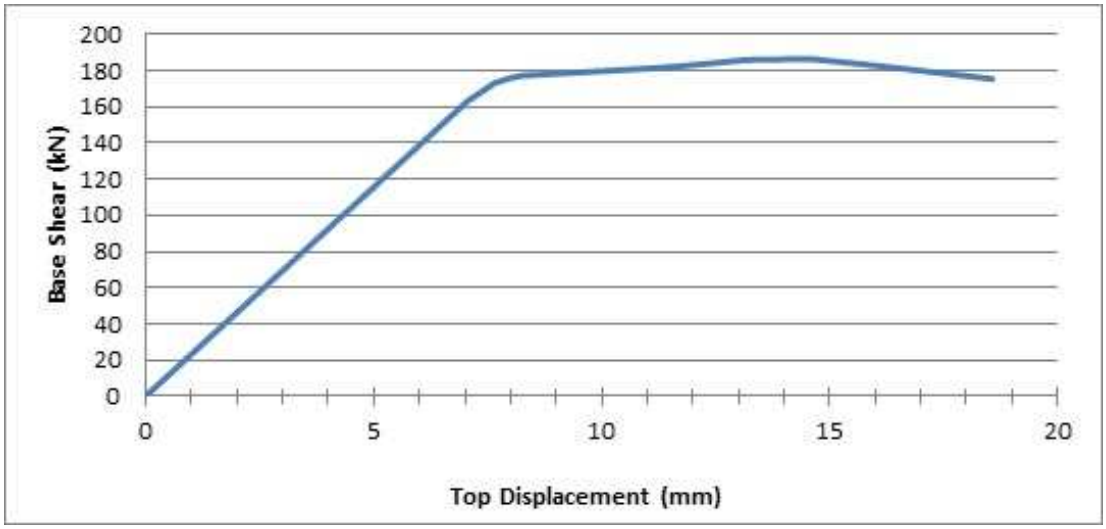

Figure 6.31: Base shear top displacement curve

2. One of the assumptions is the 4 cm reinforced jacketed column sections. Base shear vs top displacement curve for this assumption is given in Figure 6.32.

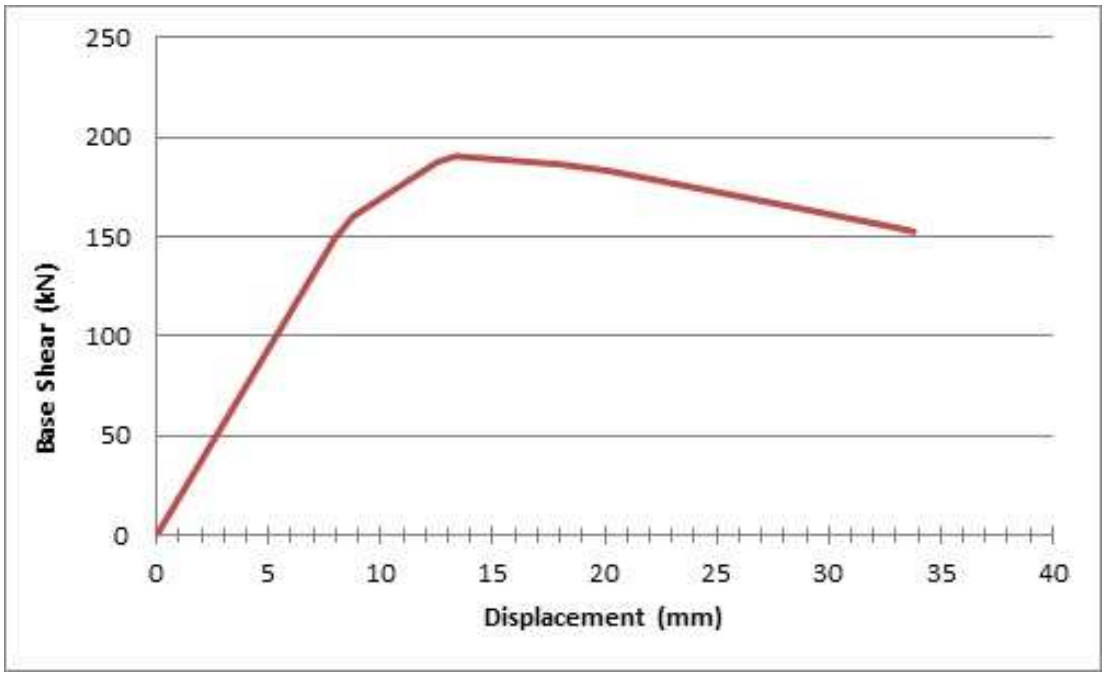

Figure 6.32: Base shear top displacement curve

3. Third section model considered is the section 6 cm reinforced concrete jacketing. Base shear vs top displacement curve for this state is given in Figure 6.33.

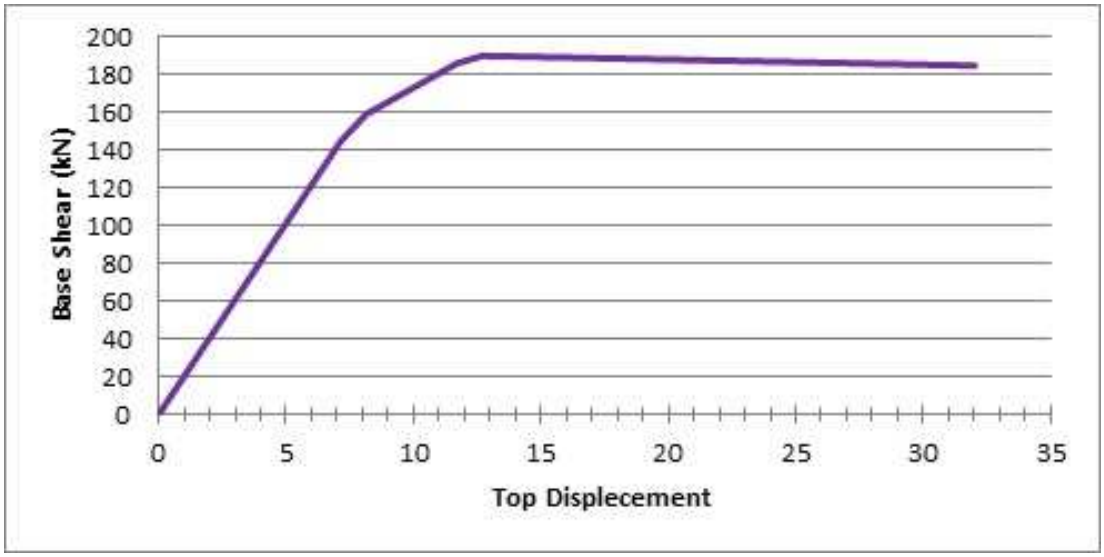

Figure 6.33: Base shear top displacement curve

4.Lastly, a section which has 6 *cm* RC jacket having higher transverse reinforcement ratio when comparing to other sections, was analyzed by using XTRACT. Base shear vs top displacement curve for this state is given in Figure 6.34.

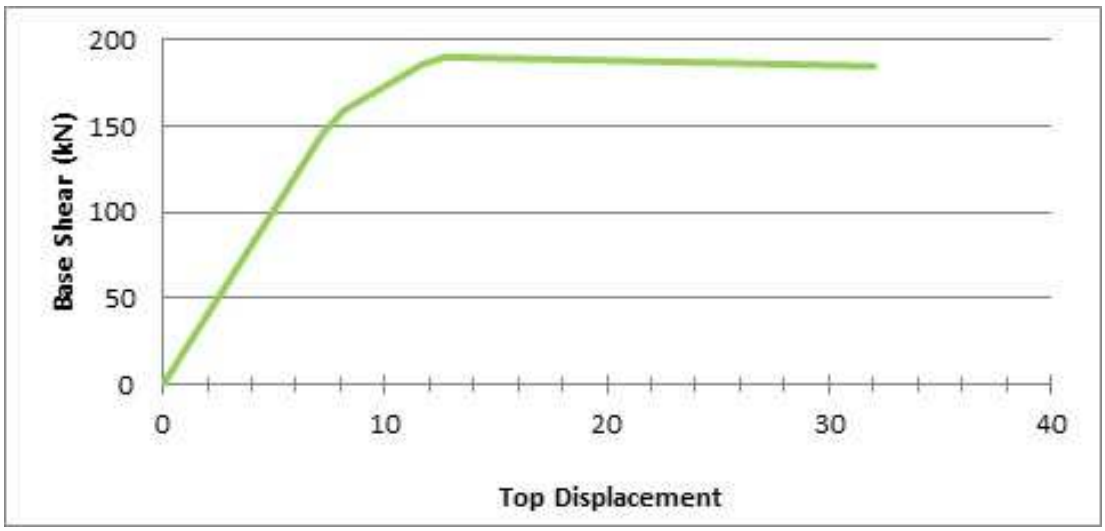

Figure 6.34: Base shear top displacement curve

The comparison for the capacity curves of the retrofitting approaches and existing frame is given in Figure 6.35.

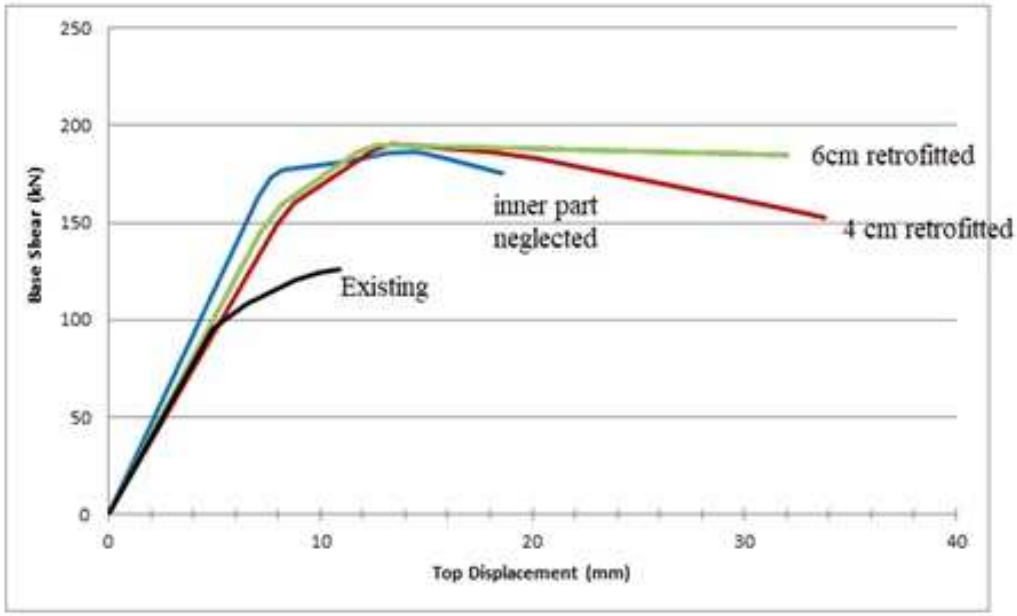

Figure 6.35: Comparison of the capacity curves

Displacement ductilies for existing frame and retrofitted frames are given in below table. Due to increase in sectional strength and ductility, as it can be seen from Table 6.6 displacement ductility of retrofitted frames are almost 2 times of reference frame which is not retrofitted.

Frame	Displacement Ductility
Existing frame	2.35
4 cm retrofitted	4.19
Inner part neglected	2.66
6 cm retrofitted	4.43
6 cm retrofitted with higher vol. ratio of steel	4.5

Table 6.6: Displacement ductilities of retrofitted frames

6.2 Effect of Corrosion Amount on Seismic Behavior

In order to investigate effect of corrosion amount of column reinforcement on seismic behavior, different corrosion amounts for longitudinal reinforcements are considered and frame is subjected to pushover analysis in this part for each corrosion case. The corrosion amounts that are considered at left column's specific sections can be seen in Figure 6.37. There are several assumptions for corrosion rates. Firstly 2% and 10%, then 2%, 10%, 50% corrosion in certain column sections are studied. Lastly, whole column reinforcements are assumed to be corroded by the amounts of 2%, 10% and 50%, separately. Amount of reinforcement corrosion is considered as the loss in diameter of longitudinal reinforcement and moment curvature relationships of each section are found according to the sectional properties and pushover analysis procedure applied similarly as it is mentioned in previous parts.

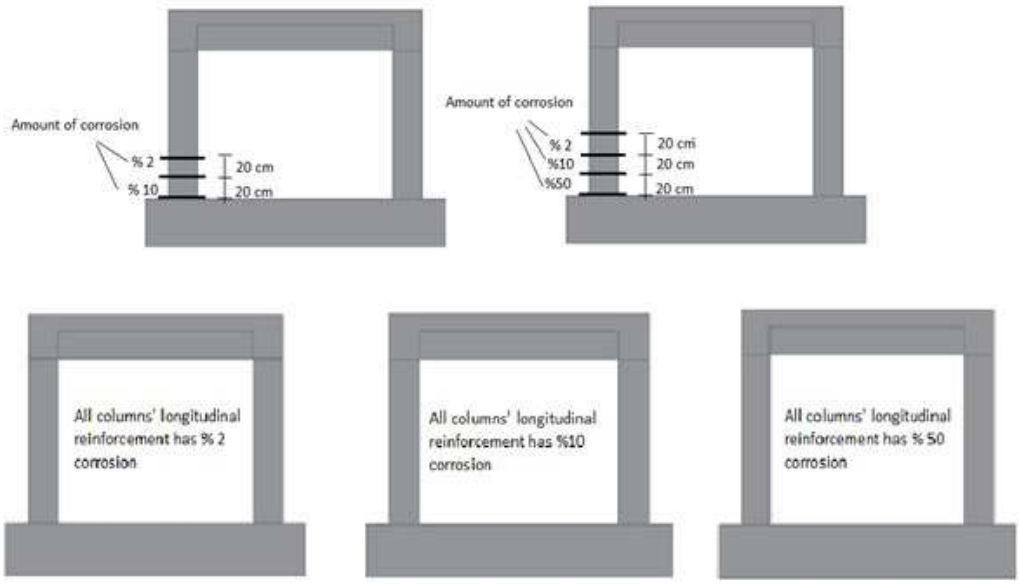

Figure 6.36: Different corrosion amounts of the column sections

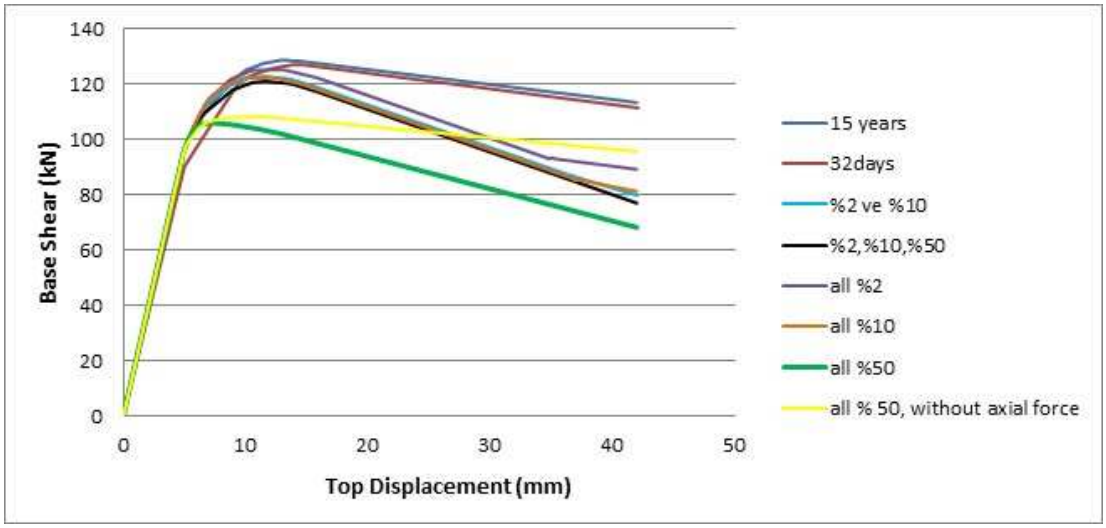

Figure 6.37: Comparison of pushover curves of different amount of corrosion in column reinforcement

The concrete properties and reinforcement properties such as strength and unit deformations are the same which is taken from experimental investigations and shown in Table 5.2. For all assumptions the only difference is amount of corrosion at specified sections which is indicated by diameter loss in longitudinal reinforcement.

The failure of these frames, under these assumptions, occurred at column ends. Again, strong beam weak column case is valid here. In order to see the difference, pushover curve of 15 years old frame which has a little amount of corrosion and the pushover curve when the concrete is 32 days old are also presented in the graph. Since the compressive strength of the frame concrete did not show significant increase in 15 years and the frame did not have an important amount of corrosion, capacity curves of 15 years old frame and the curve when concrete is 32 days old quite close.

As it can be seen from Figure 6.37, as the corrosion amount increases, lateral strength of the structure decreases. Also displacement ductilies which are presented in Table 6.7 have shown that,increase in corrosion rate results in decrease in displacement ductility of the frame.

Moreover, if we neglect the axial force for the assumption of 50% corrosion rate of all column reinforcement, descending part of the curve which is steep becomes upward. It is obvious that second order effect of axial forces are quite important significant here.

Corrosion Rate	Displacement Ductility
All % 2	1.85
All % 10	1.62
All % 50	1.31
%2 and %10	1.72
%2,%10,%50	1.55
Existing Frame	2.35

Table 6.7: Displacement ductility of the frame according to corrosion rate

Chapter 7

CONCLUSION

Within the scope of this thesis, experimental and theoretical studies on the effect of reinforcement corrosion on seismic behavior of the naturally corroded, single storey, single bay 15 years old RC frame is examined. The specimen was constructed using low strength concrete made of sea sand and mild reinforcing bars having inadequate seismic details, represents the existing relatively old structures built without complying the existing design codes. The specimen was exposed to outdoor conditions for 15 years without having any plaster on it. After 15 years, specimen has been subjected to displacement reversals which represents more or less seismic loading. The test ended when the failure occurred and after having removed the concrete, a little amount of corrosion was observed on the reinforcement which can be related to high compressive strength of the frame concrete and hence high tensile strength of it that slows down the corrosion process.

The aim of this study is to investigate seismic behavior of a 15 years old structure experimentally and theoretically and to obtain a solution for the rehabilitation of corroded structures which are going to be subjected to seismic loads. The performance of this RC frame under earthquake loads were studied through its strength, deformation capacity, displacement capacity, moment-curvature relationships of critical sections, energy dissipation capacity and failure mode characteristics. The following observations and results are important to mention and it is important

to be careful while generalizing the result since they are based on limited amount of experiment.

1-Comparison of the experimental results of the reference frame and the frame tested is given in Section 4.2. As failure modes, both of them has firstly bending type and then shear type cracks at column ends. Since it has insufficient amount of transverse reinforcement and large spacing of it, shear cracks occurred. The specimen tested recently, did not have any damage on the beam element. Crack patterns and the places of cracks of the actual specimen and the reference specimen after the tests are more or less similar. Due to the fact that specimen tested recently has a bigger compressive strength of concrete and had increase in compressive strength after 15 years it revealed greater amount of energy dissipation when comparing to reference specimen and also had bigger initial stiffness and higher load capacity.

2-In order to investigate the effect of time and outdoor conditions on the RC frame, capacity curve of the frame was obtained by pushover analysis when the concrete is 32 days old. Because of the fact that compressive strength of the concrete of frame increased in small amount and the frame had low amount of corrosion by that time, base shear top displacement curves of 32 days old and 15 years old frames are quite close.

3- Comparisons of the analytical and experimental results of the recently tested specimen is given in Section 5.3. Comparisons have shown that when it is assumed that plasticity is distributed along the member of the structure, in this case it was provided by SeismiStruct, the experimental and analytical hysteretic curves and the capacity curves differ. Assumption of considering plasticity concentrated at critical sections of the structure which is provided by SAP2000 has shown a quite closer result when compared to distributed plasticity. Analytically formation of plastic hinges for the RC specimen under simulated earthquake loads are in good agreement with the experimental result which indicates the strong beam and weak column case.

4- The 15 years old frame has insufficient seismic details such as; large spacing of stirrups, no use of 135° seismic hoops and insufficient confinement in beam column connections. Because of those reasons it failed having bending and shear cracks at column ends under reversed cyclic loading. Therefore, in the scope of this thesis, effect of reinforced concrete jacketing of the columns on the strength and ductility of the structure was also examined analytically. Moment curvature relationship of each critical sections, curvature ductility and base shear - top displacement curves of the structure were obtained for each jacketing assumptions. This study consist of 4 *cm* and 6 *cm* jacketing assumptions which correspond 8 *cm* and 12 *cm* for a full scale frame can be considered as thin jacketing. Using self-placing, self-vibrating concrete and without obtaining dramatic increase in lateral stiffness since the abrupt changes in the stiffnesses cause increase in lateral earthquake forces imparted to the structures, it is important to achieve economic and effective solution. Results show that RC jacketing is an effective method in order to retrofit the structures and it can be utilized to enhance displacement ductility, strength, deformation and lateral load carrying capacity of the structure. As it is expected, for the frame tested, natural period obtained as 0.112 sec and when the columns are retrofitted by RC jacketing it decreased to 0.068 sec and 0.057 sec for 4 *cm* and 6 *cm* jacketing assumptions respectively and higher displacement ductility of jacketed frame has led higher load reduction factor R_a. Also with this retrofitting technique, it has been achieved strong column weak beam concept which is proposed by newly adopted TEC.

5- In order to obtain the effect of variable corrosion rates of reinforcement on seismic behavior of the frame, a parametric study has been carried out. Considering the assumptions given in Chapter 6 as the corrosion rate of reinforcing steel of columns increases, lateral strength and ductility of the frame structure decreases as it is expected.

References

[1] S. Ahmad, "Reinforcement corrosion in concrete structures, its monitoring and service life prdiction-a review," *Cement and Concrete Composites*, vol. 25, no. 1, pp. 459–471, 2003.

[2] M. Dogan, "Corrosion failure in concrete rainforcement to damage during seismic," *Engineering Failure Analysis*, vol. 56, no. 1, pp. 275–287, 2015.

[3] S. Dhawan, S. Bhalla, and B. Bhattacharjee, "Reinforcement corrosion in concrete structures and service life predictions- a review," *9th Internatinal Symposium on Advanced Science and Technology in Experimental Mechanics*, vol. 108, 2012.

[4] A. Almusallam, "Effect of degree of corrosion on the properties of reinforcing steel bars," *Construction and Building Materials*, vol. 15, no. 1, pp. 361–368, 2001.

[5] C. Andrade, C. Alonso, D. Garcia, and J. Rodriquez, "Remaining lifetime of reinforced concrete structures: Effect of corrosion on the mechanical properties of the steel," *2nd Meeting, Life prediction of corrodible structures, 1994, Cambridge*, vol. 2, pp. 546–557, 1994.

[6] S. Yang, X. Song, H. Jia, X. Chen, and X. Liu, "Experimental research on hysteric behaviors of corroded reinforced concrete column with different maximum amounts of corrosion of rebar," *Construction and Building Materials*, vol. 121, no. 1, pp. 319–327, 2016.

[7] G. Malumbela, P. Moyo, and M. Alexander, "Behaviour of rc beams corroded under sustained service loads," *Construction and Building Materials*, vol. 23, no. 11, pp. 3346–3351, 2009.

[8] V. Dang and R. Francois, "Influence of long-term corrosion in chloride environment on mechanical behaviour of rc beam," *Engineering Structures*, vol. 48, pp. 558–568, 2013.

[9] C. Apostolopoulos and D. Michalopoulos, "Effect of corrosion on mass loss, and high and low cycle fatigue of reinforcing steel," *Journal of Materials Engineering and Performance*, vol. 15, pp. 742–749, 2006.

[10] R. Zhang, A. Castel, and R. Francois, "Concrete cover cracking with reinforcement corrosion of rc beam during chloride-induced corrosion process," *Cement and Concrete Research*, vol. 40, pp. 415–425, 2010.

[11] T. Vidal, A. Castel, and R. Francois, "Analysing crack width to predict corrosion in reinforced concrete," *Cement and Concrete Research*, vol. 34, pp. 165–174, 2004.

[12] ——, "Corrosion process and structural performance of a 17 year old reinforced concrete beam stored in cloride environment," *Cement and Concrete Research*, vol. 37, pp. 1551–1561, 2007.

[13] T. Ali, "Flexural behavior of reinforced beams reinforced with corrosive rebar," *International Journal of Civil and Structural Engineering*, vol. 5, no. 1, pp. 64–72, 2014.

[14] H. Lee, T. Kage, T. Noguchi, and F. Tomosawa, "An experimental study on the retrofitting effects of reinforced concrete columns demaged by rebar corrosion strengthened with carbon fiber sheets," *Cement and Concrete Research*, vol. 33, no. 4, pp. 563–570, 2003.

[15] A. Meda, S. Mostosi, Z. Rinaldi, and P. Riva, "Experimental evaluation of the corrosion influence on the cyclic behavior of rc columns," *Engineering Structures*, vol. 76, pp. 112–123, 2014.

[16] M. Decoster, F. Buyle-Bodin, O. Maurel, and Y. Delmas, "Modelling of the flexural behaviour of rc beams subjected to localised and unifor corrosion," *Engineering Structures*, vol. 25, pp. 1333–1341, 2003.

[17] C. Fang, K. Gylltoft, K. Lundgren, and M. Plos, "Effect of corrosion on bond in reinforced concrete under cyclic loading," *Cement and Concrete Research*, vol. 36, pp. 548–555, 2006.

[18] V. Carbone, G. Mancini, and F. Tondolo, "Structural behavior with reinforcement corrosion," *International Fib Symposium*, 2008.

[19] J. Moehle, "State of research on seismic retrofit of concrete building structures in the us," *US-Japan Symposium and Workshop on Seismic Retrofit of Concrete Structures*, 2000.

[20] T. Ucar, S. Toumatari, and Y. Ertutar, "Çerçeve düzlemi içinde eklenen perdelerin betonarme binaların yapısal özelliklerine etkilerinin incelenmesi," *Journal of Advanced Technology Sciences*, vol. 3, no. 1, pp. 56–68, 2014.

[21] H. Kaplan and S. Yilmaz, "Seismic strengthening of reinforced concrete buildings," *Earthquake-Resistant Structures - Design, Assessment and Rehabilitation*, 2012.

[22] Y. Alashkar, S. Nazar, and M. Ahmed, "A comparative study of seismic strengthening of rc buildings by steel bracings and concrete shear walls," *International Journal of Civil and Structural Engineering Research*, vol. 2, no. 2, pp. 24–34, 2015.

[23] "Imo," http://www.imo.org.tr/resimler/ekutuphane/pdf/250.pdf, accessed: 2018-05-21.

[24] A. Benavent-Climent, A. Ramirez-Marquez, and S. Pujol, "Seismic strengthening of low-rise reinforced concrete frame structures with masonry infill walls: shaking-table test," *Engineering Structures*, vol. 165, pp. 142–151, 2018.

[25] A. Dautaj, Q. Kadiri, and N. Kabashi, "Experimental study on the contribution of masonry infill in the behavior of rc frame under seismic loading," *Engineering Structures*, vol. 165, pp. 27–37, 2018.

[26] M. Sassu, M. Puppio, and E. Mannari, "Seismic reinforcement of a r.c. school structure with strength irregularities throughout external bracing walls," *Buildings*, vol. 7, no. 58, 2017.

[27] M. Fardis, "Seismic assessment and retrofit of reinforced concrete buildings," in *Seismic Assessment and Retrofit of Reinforced Concrete Buildings*, Case Postale 88, CH-1015 Lausanne, Switzerland, 2003.

[28] M. Ferraioli and A. Mandara, "Base isolation for seismic retrofitting of a multiple building structure: design, construction, and assessment," *Mathematical Problems in Engineering*, vol. 2017, 2017.

[29] G. Thermou and A. Elnashai, "Seismic retrofit schemes for rc structures and local-global consequences," *Progress in Structural Engineering and Materials*, vol. 8, no. 1, pp. 1–15, 2006.

[30] M. Valente and G. Milani, "An under-designed rc frame: seismic assessment through displacement based approach and possible refurbishment with frp strips and rc jacketing," *AIP Conference Proceedings*, vol. 1863, 2017.

[31] C. Baciu, P. Murzea, and V. Cucu, "The retrofitting of reinforced concrete columns," *De Gruyter*, vol. 21, no. 3, 2015.

[32] H. Elbakry and A. Tarabia, "Factors affecting bond strength of rc column jackets," *Alexandria Engineering Journal*, vol. 55, pp. 57–67, 2016.

[33] T. Sheikh, M. Khan, and T. Izhar, "A review on strenghtening of rcc square columns with reinforced concrete jacketing," *International Research Journal of Engineering and Tecnology*, vol. 04, no. 03, pp. 1797–1799, 2017.

[34] V. Rawat and S. Narain, "Increasing yhe strenght of existing building using retrofitting techniques," *International Journal of Engineering Tecnology Science and Research*, vol. 4, no. 6, pp. 513–521, 2017.

[35] H. Nahavandi, "Master of science in civil and environmental engineering," in *Pushover Analysis of Retrofitted Reinforced Concreate Buildings*, Portland State University, hamid2@pdx.edu, 2015.

[36] A. Hemy, "The effect of retrofitting technique on the structural behaviour of rc columns," *Sustainable Vital Technologies in Engineering and Informatics*, 2016.

[37] A. He, J. Cai, Q. Chen, X. Liu, P. Huang, and X. Tang, "Seismic behaviour of steel-jacket retrofitted reinforced concrete columns with recycled aggregate concrete," *Construction and Building Materials*, vol. 158, pp. 624–639, 2018.

[38] P. Teymur, "Phd thesis of p. teymur," in *Retrofitting of Valnurable Reinforced Concrete Frames with Shotcrete Walls*, Istanbul Technical Univercity - Institute of Science and Technology, 2009.

[39] TEC, "Tec," in *Turkish Code for Earthquake Resistant Design*, Ministary of Public Works and Settlement, Ankara, 2016.

[40] M. Priestly, G. Calvi, and M. Cowalsky, "Displacement-based seismic design of structures," in *Displacement-Based Seismic Design of Structures*, IUSS PRESS, Pavia, ITALY, 2007.

[41] TEC, "Tec," in *Turkish Code for Earthquake Resistant Design*, Ministary of Public Works and Settlement, Ankara, 2007.